



(Imported for this occasion)

HST **mid-UV** and **near-IR** Imaging of Nearby Galaxies: Tools to Understand High-Redshift Galaxy Morphology

Rogier A. Windhorst (ASU)

+ the HST mid-UV Team:

V. Taylor, R. Jansen, & S. Cohen (ASU)

S. Odewahn (U. Texas)

C. Conselice (Caltech), R. de Grijs (Sheffield)

R. S. de Jong (STScI), J. MacKenty (STScI)

P. Eskridge (Minnesota), J. Frogel (OSU)

J. Gallagher, (U. Wis), L. Matthews (Harvard CfA)

J. Hibbard (NRAO), R. O'Connell (U. Virginia)

Sponsored by NASA/STScI

www.asu.edu/clas/hst/www/midUV.html

hubblesite.org/newscenter/archive/2001/04/

hubblesite.org/newscenter/archive/2001/37/

Talk to the 2004 Bars Conference, June 10, 2004, Bakubung, South Africa

Outline

- (1) Scientific Background
- (2) Scientific Goals
- (3) Experimental Design of the HST mid-UV Survey
- (4) Results for Early, Mid- and Late-type galaxies
- (5) Results from Near-IR images and Ground-based Light-profiles
- (6) Predict Galaxy Appearance for JWST at $z \simeq 1-15$
- (7) Summary — Consequences of More Reliable Galaxy Classifications

(1) Scientific Background

- At $\lesssim 1990$: Little known about UV morphology/structure of galaxies.
- Early 1990's: ASTRO/UIT imaging of nearby galaxies at 150 (& some at 250) nm (Bohlin et al. 1992; Hill et al. 1992).

\implies Galaxies often appear of later Hubble type at shorter $\lambda_{rest} \implies$ significant “Morphological K-correction” (K_{morph}).

- Mid 1990's: Faint high redshift galaxies are observed by HST in the rest-frame mid-UV (0.2-0.3 μm).
- These resemble nearby late-type galaxies (*e.g.*, Driver et al. 1995, Odewahn et al. 1996), but are they really physically similar classes of objects, or are they due to the K_{morph} in earlier types?

Imaging nearby galaxies at 250–290 nm is critical because:

- (1) Largest HST samples, best sampling & FOV available in the **red**.
- (2) At $I \simeq 26$ mag, median sizes are $r_e \simeq 0''.25 \Rightarrow$ need $\lambda_{obs} \lesssim 800$ nm.
- (3) Morphology available today for $\gtrsim 10^5$ HST galaxies with $I \lesssim 26$ –27. Fewer galaxies have both z_{spect} and spatially resolved spectra ($I \lesssim 24$).

$N(m, T)$ & $N(z_{phot}, T)$ constrain galaxy evolution, if T-types reliable.

- (4) Median redshift at $I \lesssim 26$ mag is “only” $z_{med} \simeq 1$ –2.

\implies Need local benchmark at $\lambda_{rest} \simeq 250$ –400 nm to reliably classify high-z galaxies in **I_{814}** .

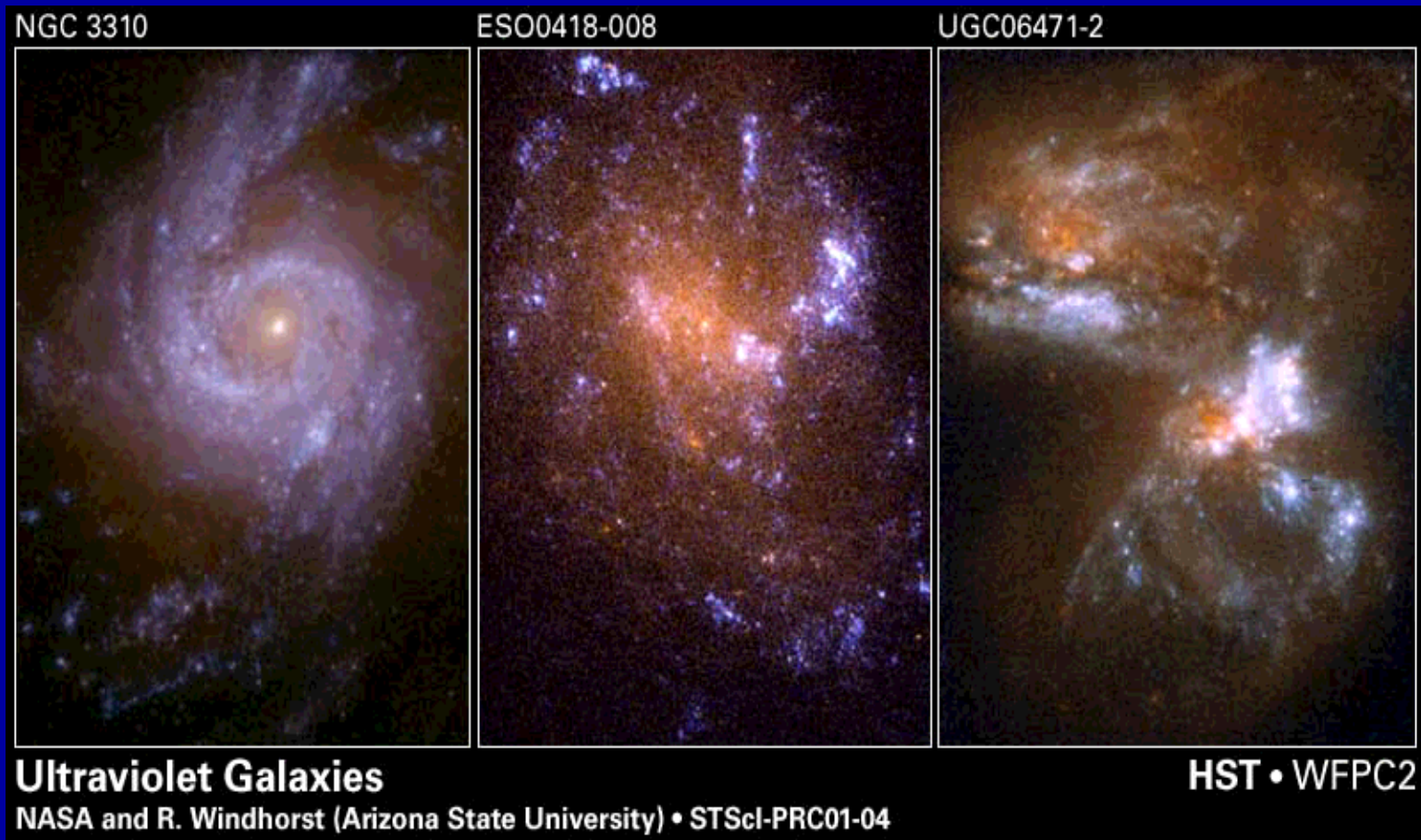
(2) Scientific Goals of our HST Cycle 9, 10, 12 projects:

1. Provide local benchmark that we can redshift to $z \approx 1 \rightarrow 20$ for quantitative comparison of structural properties of high- z galaxies.
2. Consistently classify structure and photometric properties of galaxies from $0.2\text{-}2\mu$ (using Artificial Neural Networks; S. Odewahn's talk), and reliably determine $N(m, \text{Type})$ for $AB=15\text{--}27$ mag.
3. Map the dust as function of type, inclination, and radius.
4. Map the spatial distribution, luminosities, sizes of SF regions responsible for the UV morphology, and relate these to global galaxy properties.

- Main Science Goal: Understanding the Faint Blue Galaxies



One of the remarkable HST discoveries was how numerous and small faint galaxies are: the building blocks of the giant galaxies seen today?!

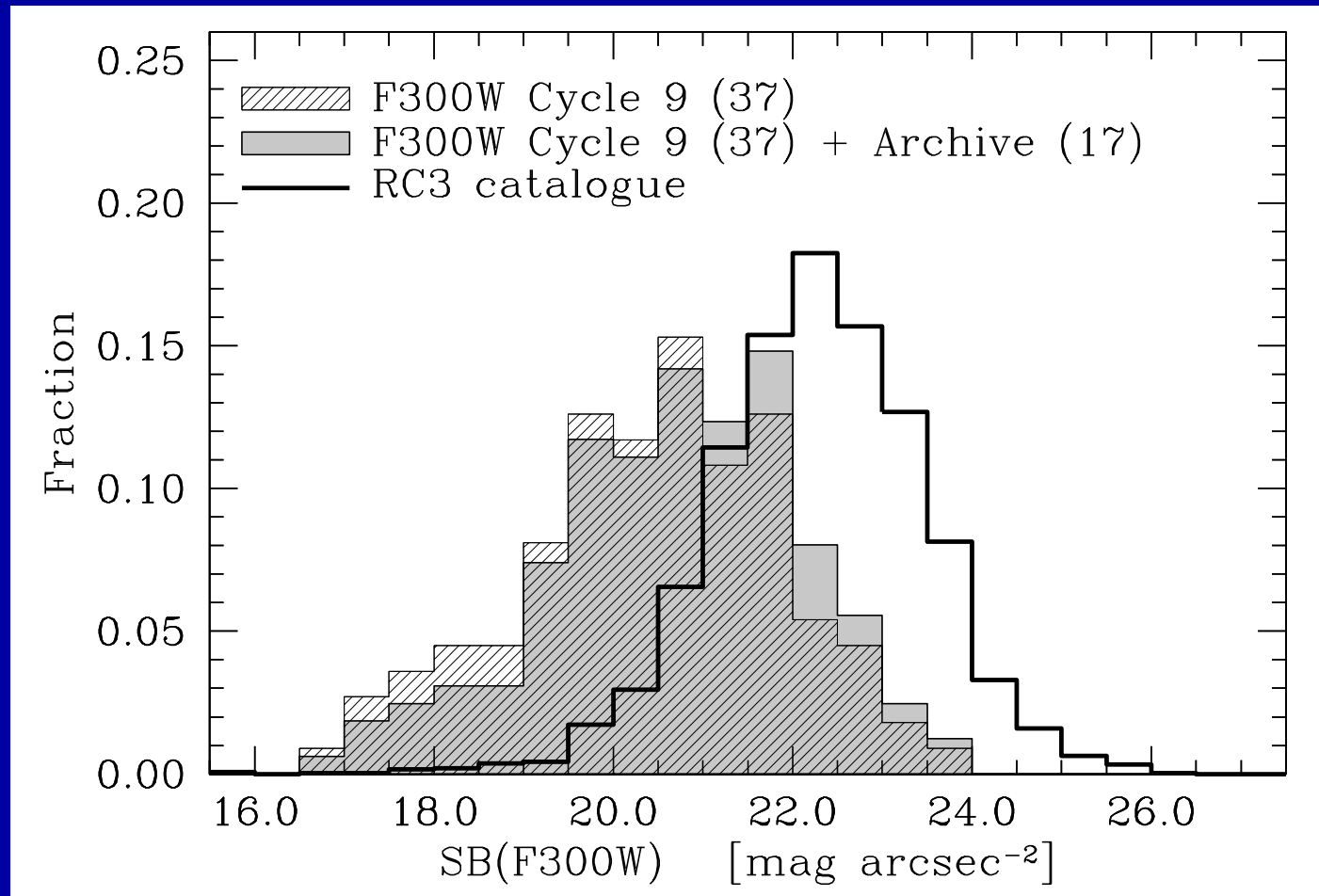


- The uncertain rest-frame UV-morphology of galaxies is dominated by young and hot stars, with often significant dust superimposed.
- This complicates comparison with high redshift galaxies seen by HST, but with good images a quantitative analysis of the restframe- λ dependent morphology and structure can be made (Odewahn et al. 2002; talk here).

(3) Experimental Design of the HST Survey

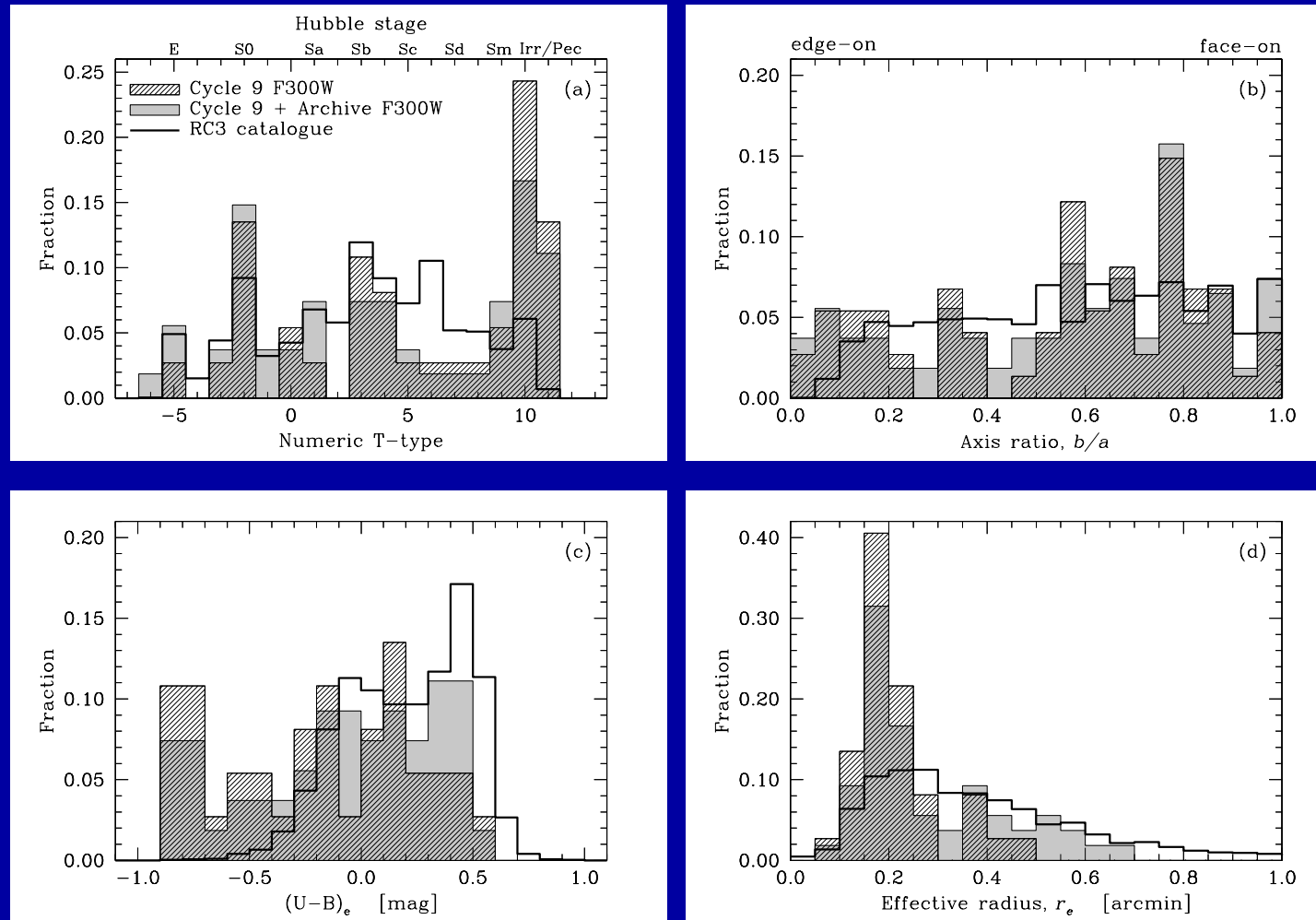
- ~ 100 nearby galaxies with WFPC2 in mid-UV: F300W & F255W (Windhorst et al. 2002, ApJS, 143, 113; Taylor et al. 2005, ApJ, 630, 784; Taylor et al. 2007, ApJ, 659, 162).
- Short F814W exposures for old stellar pops and red-leak removal.
- NIC3: $\gtrsim 12$ have F160W images to study old stellar pops and dust.
- Carefully select sample for size and surface brightness:
 $r_e \lesssim 1'$ and $SB(290 \text{ nm}) \lesssim 23.0 \text{ mag arcsec}^{-2}$
- Representative range of Hubble types and inclinations.
- Ground-based UBVR+(IJHK) images (Taylor et al. 2005).
Some also have ACS H- α images (see R. Jansen's talk here).
- Include 15 galaxies with far-UV UIT images at 150 nm.

Distribution of mid-UV SB out to r_e



- Predicted average mid-UV surface brightness (SB) out to r_e for HST Cycle 9 and Archival sample is ~ 1.5 mag brighter than that of RC3.
- For high redshift comparisons, this deliberate bias is acceptable:
The cosmological $(1+z)^4$ SB-dimming at high redshift is much worse.

Distribution over Type, b/a , $(U-B)$, half-light radius r_e



- Sample all types: (a) Emphasize late-types \iff High-z FBG connection.
- Axis ratio representative of RC3 and HDF: View SF+dust at all angles.
- Sample all colors: Emphasize nearby blue gxys \iff High-z FBG's.
- Sample r_e range as in RC3: Emphasize smaller galaxies.

(4) Results for Early-type Galaxies

(1) EARLY-TYPE GALAXIES show a significant change in SB from the mid-UV to the red, reflecting the lack of young stellar population in general.

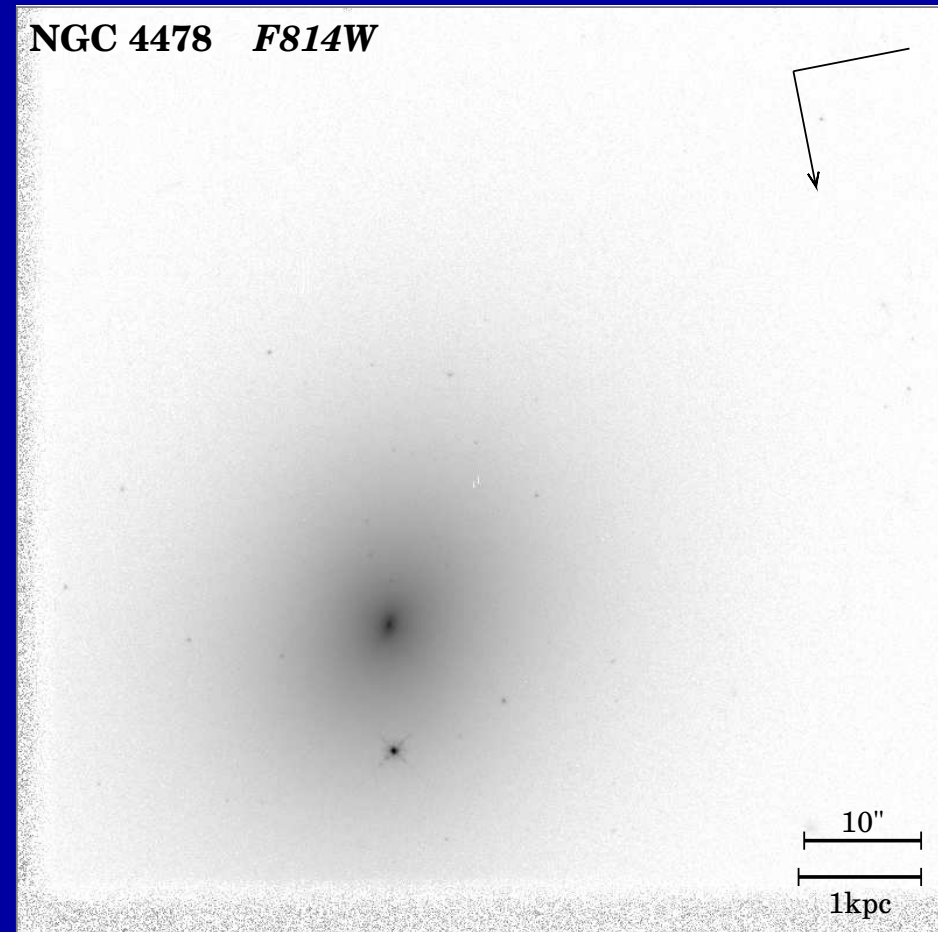
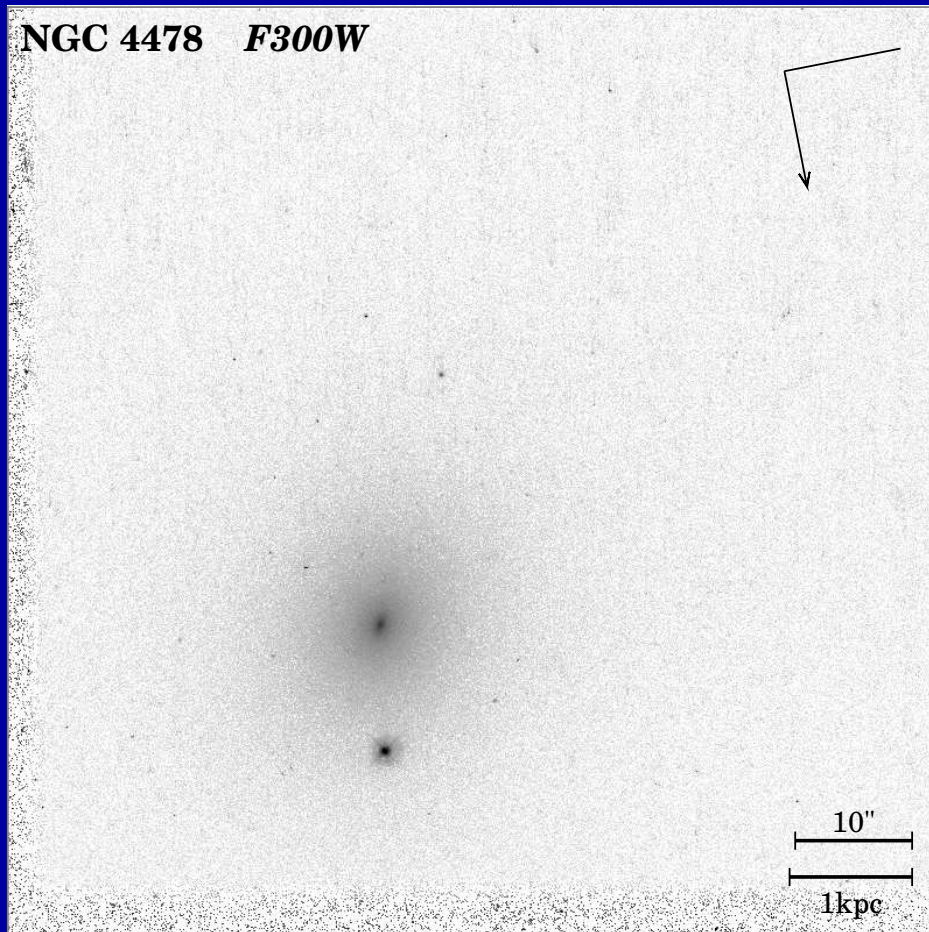
- Faint mid-UV bulges \Leftarrow Older stellar populations.
 - Some nuclear disks and/or significant dust disks.
 - Others are merger remnants, dusty in the mid-UV.
 - Several of the selected ellipticals become dominated by point sources in the mid-UV (weak AGN, Seyferts, LINER's).
- $\Rightarrow K_{morph}$ may cause (part of) the cosmological evolution of (weak) AGN in early-type galaxies.

HST/WFPC2 images of:

NGC 4478

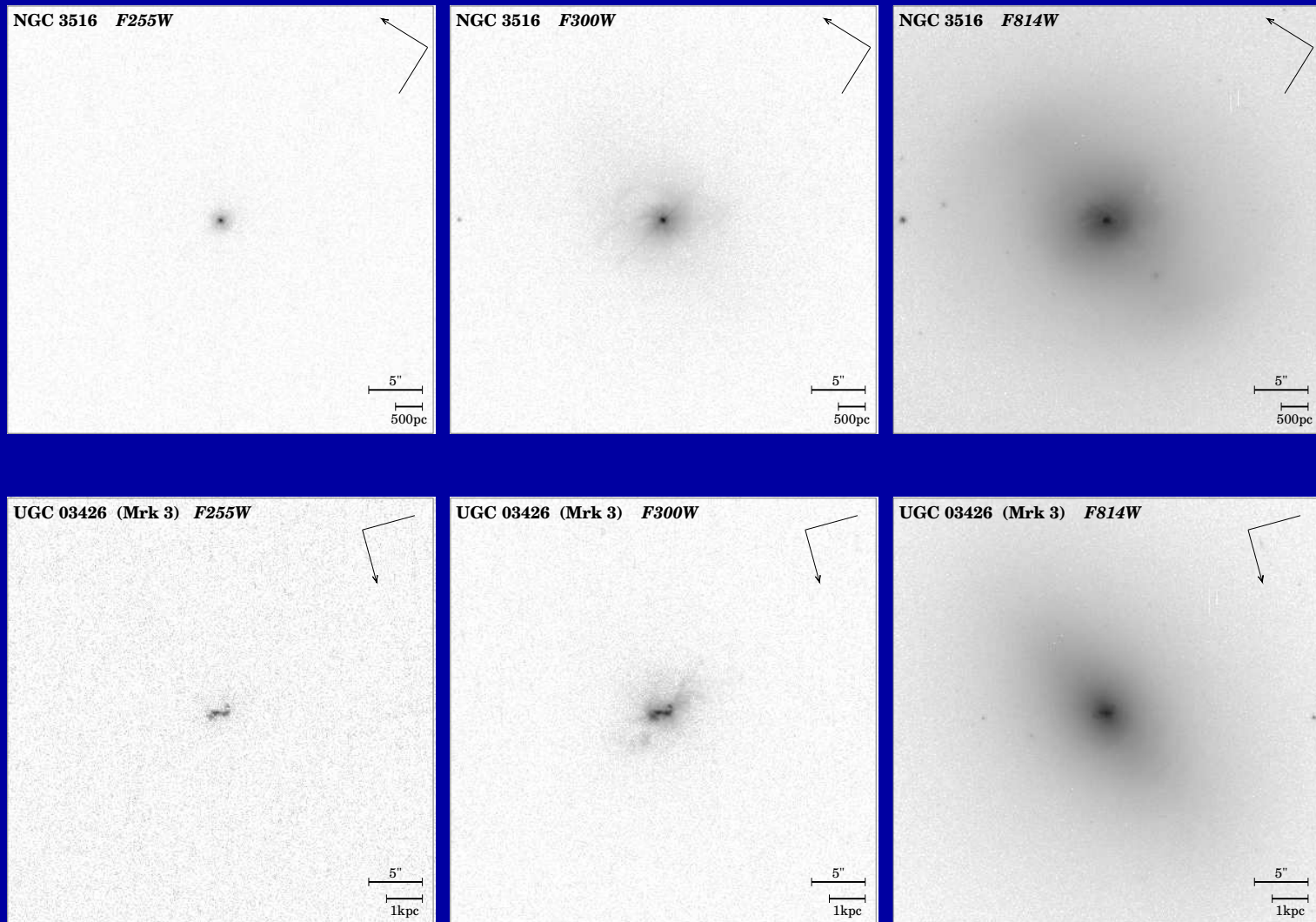
F300W

F814W



- Ordinary ellipticals are dim and dull in the UV, but ...

HST/WFPC2 images of: NGC 3516 and UGC 03426 (Mrk 3)
F255W F300W F814W



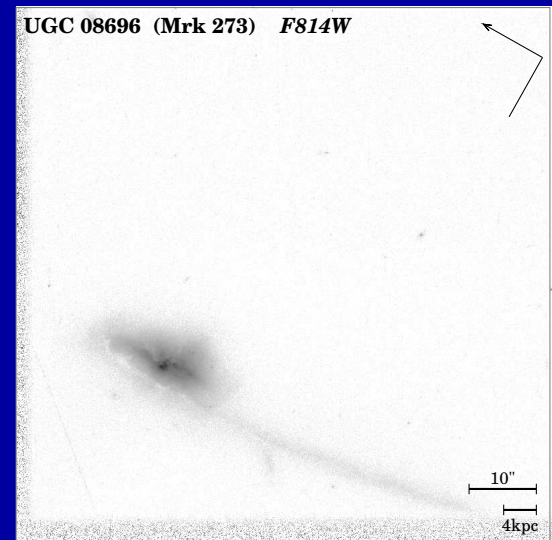
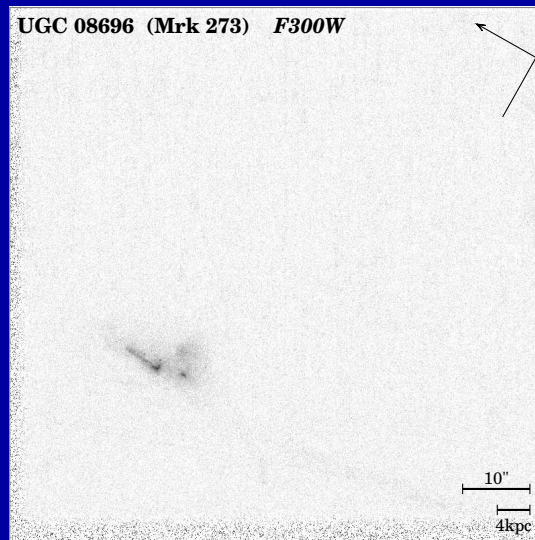
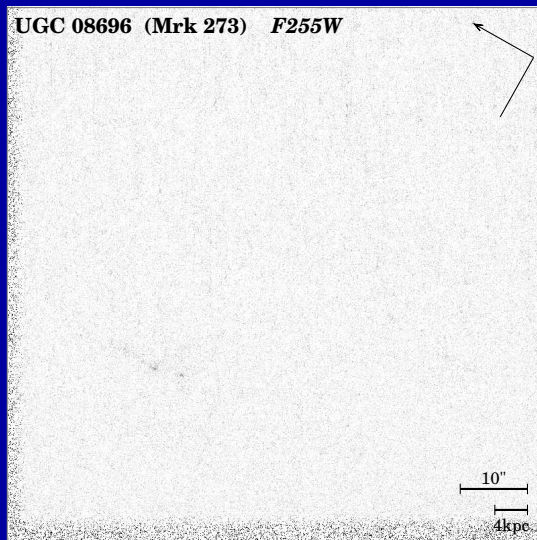
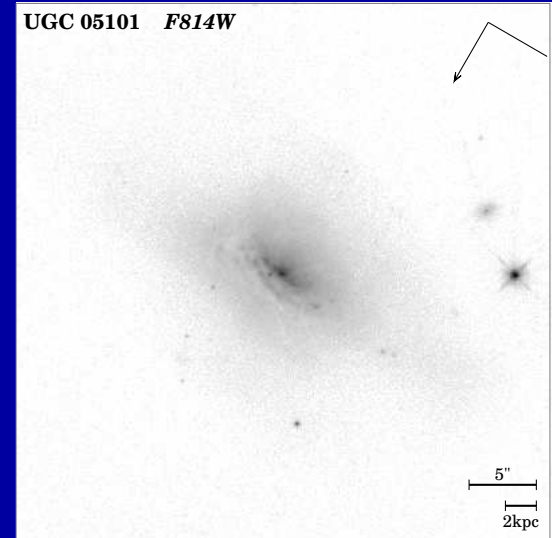
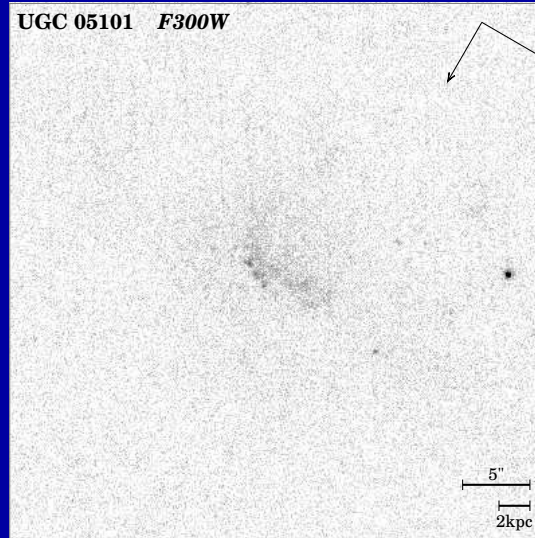
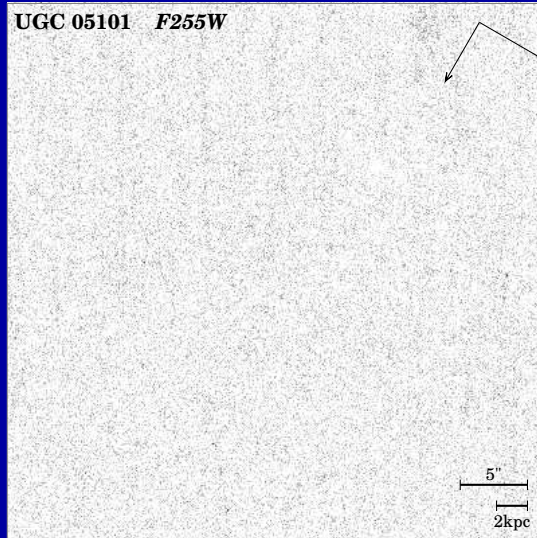
- But some turn into point sources in the mid-UV (NGC 3516).
- Others have blue nuclear disks or bipolar outflow (UGC 03426).

HST/WFPC2 images of: UGC 05101 and UGC 08698 (Mrk 273)

F255W

F300W

F814W



- Early-type galaxies that are merger remnants: dusty and dim in UV.

4. Results for Mid-type Galaxies

(2) MID-TYPE SPIRALS can appear as later/different types in the mid-UV. But most ($\gtrsim 70\%$) appear similar from mid-UV to optical ($\Delta T \lesssim 1-2$).

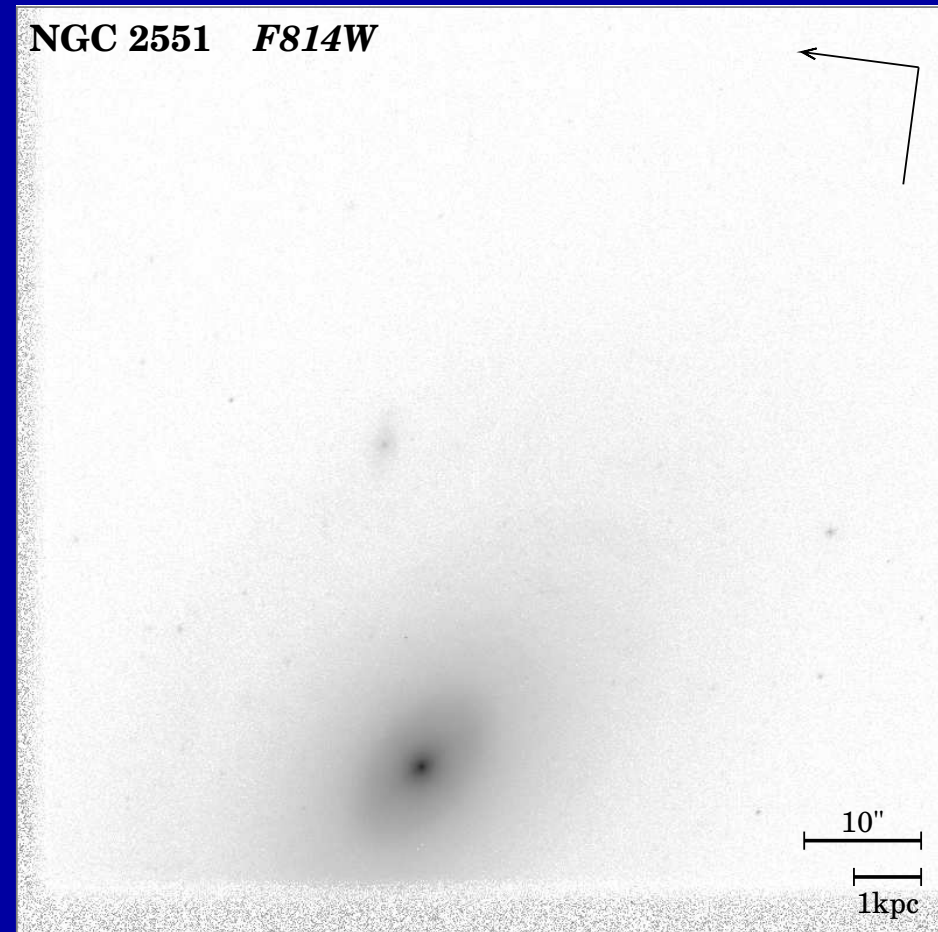
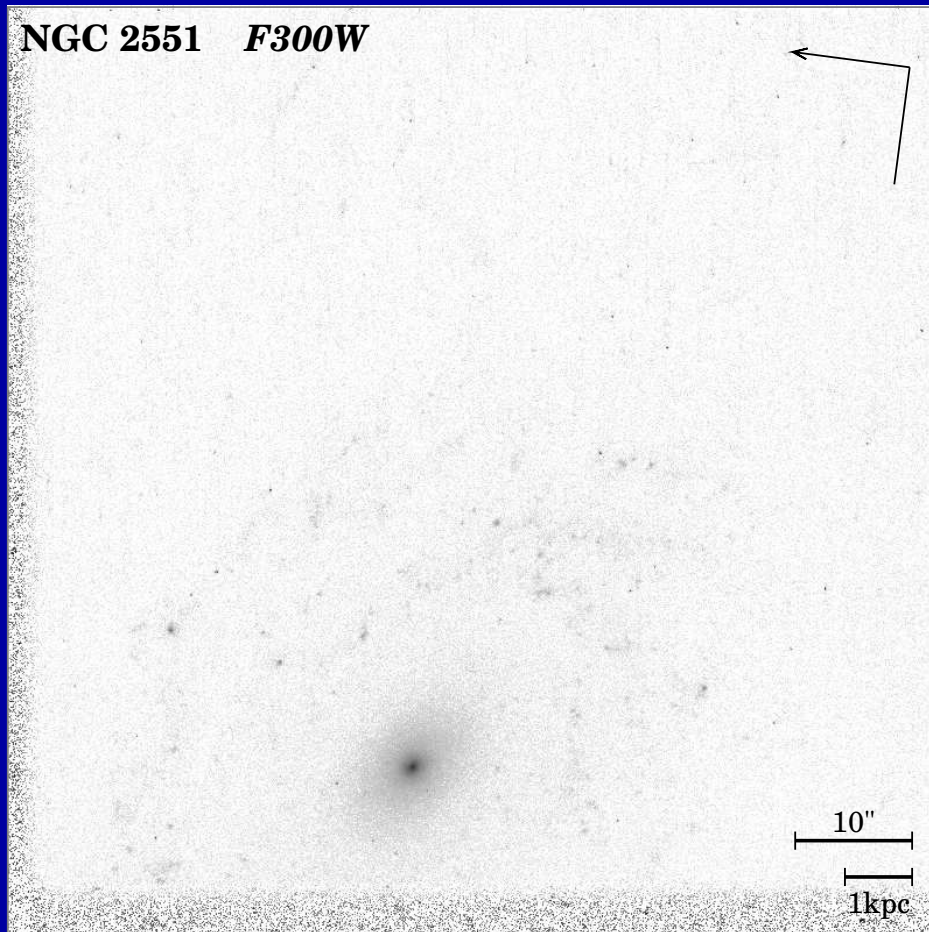
- Some show drastic changes in type, since spiral arms more pronounced in mid-UV. One shows a spectacular resonance ring of young stars.
- Dust lanes are well traceable comparing mid-UV to I_{814} . Visible dust is in lanes (following spiral arms), patches, pockets, or bubbles (?).
- Most spirals show nuclear dust lanes emerging from a small bulge.
- Many edge-on's are nearly opaque in the mid-UV, some have UV-sources in front of the dust. Most show $F300W/I_{814}$ increasing from inside out (decreasing dust content or stellar population age?).

HST/WFPC2 images of:

NGC 2551

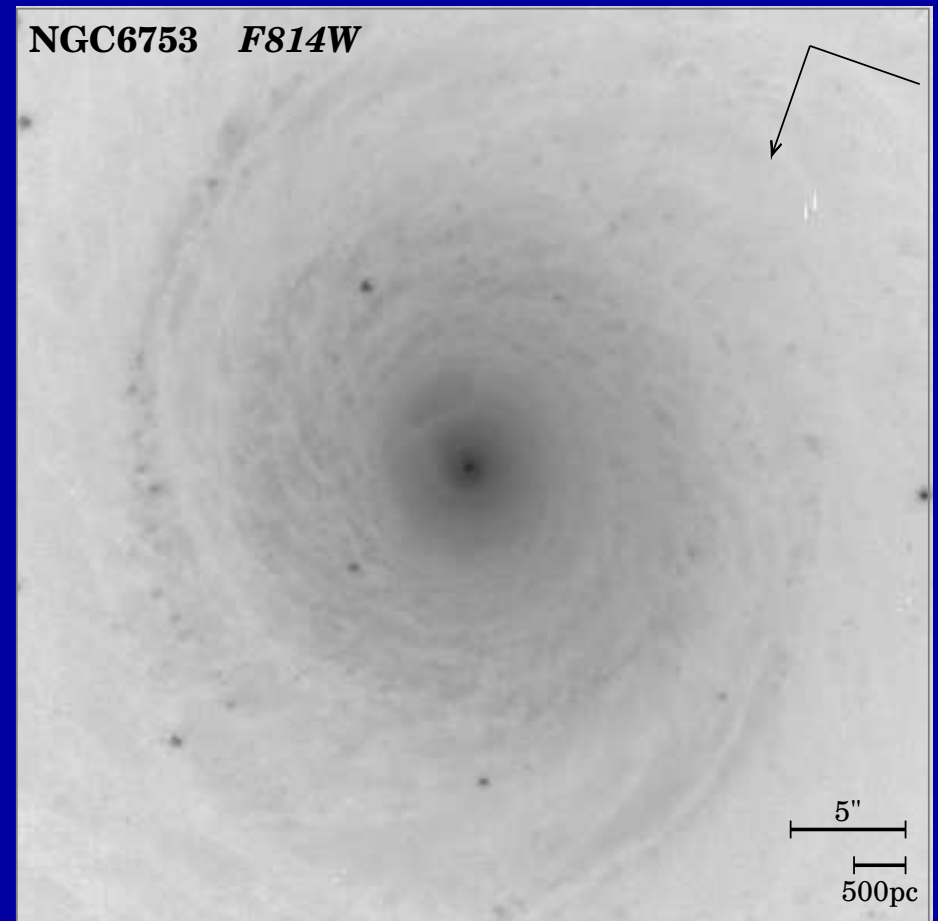
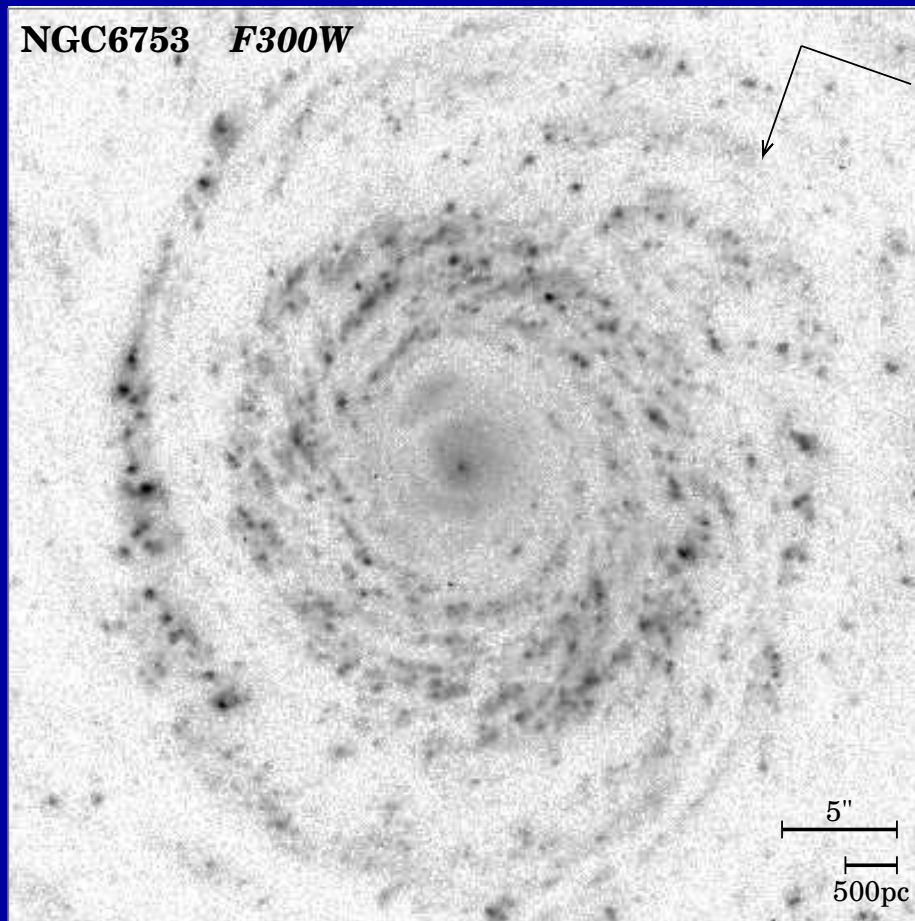
F300W

F814W



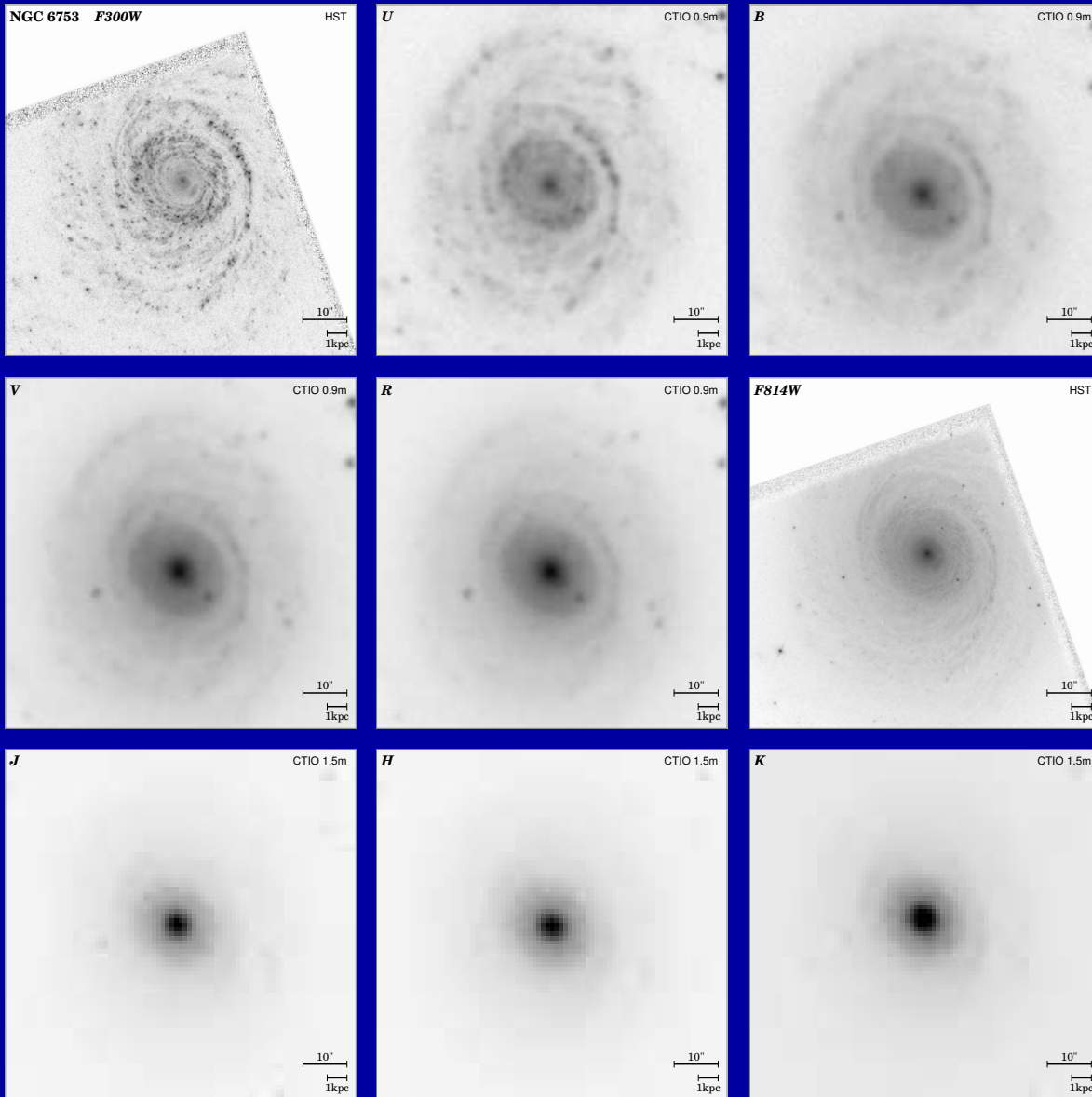
- Early-type spirals are dim in the mid-UV, with faint spiral arms in the UV, and dominant bulges in the red \implies significant K_{morph} .

HST/WFPC2 images of: NGC 6753



- Some grand-design spirals appear of later-type in the mid-UV (due to more pronounced SF in spiral arms),
- Dust lanes are well traceable comparing mid-UV to I_{814} . Visible dust is in lanes (following spiral arms).
- Most spirals show nuclear dust lanes emerging from small bulge.

HST & ground-based images of NGC 6753:

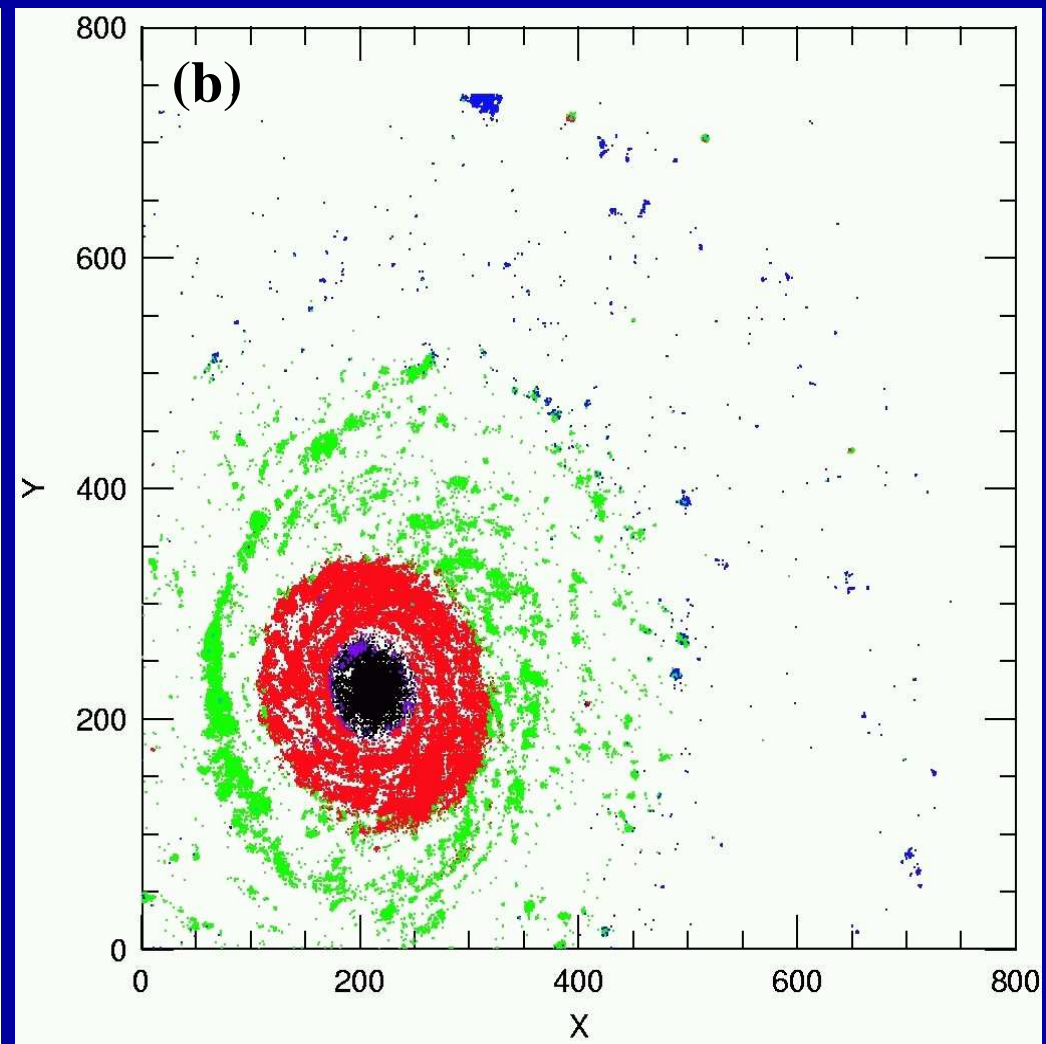
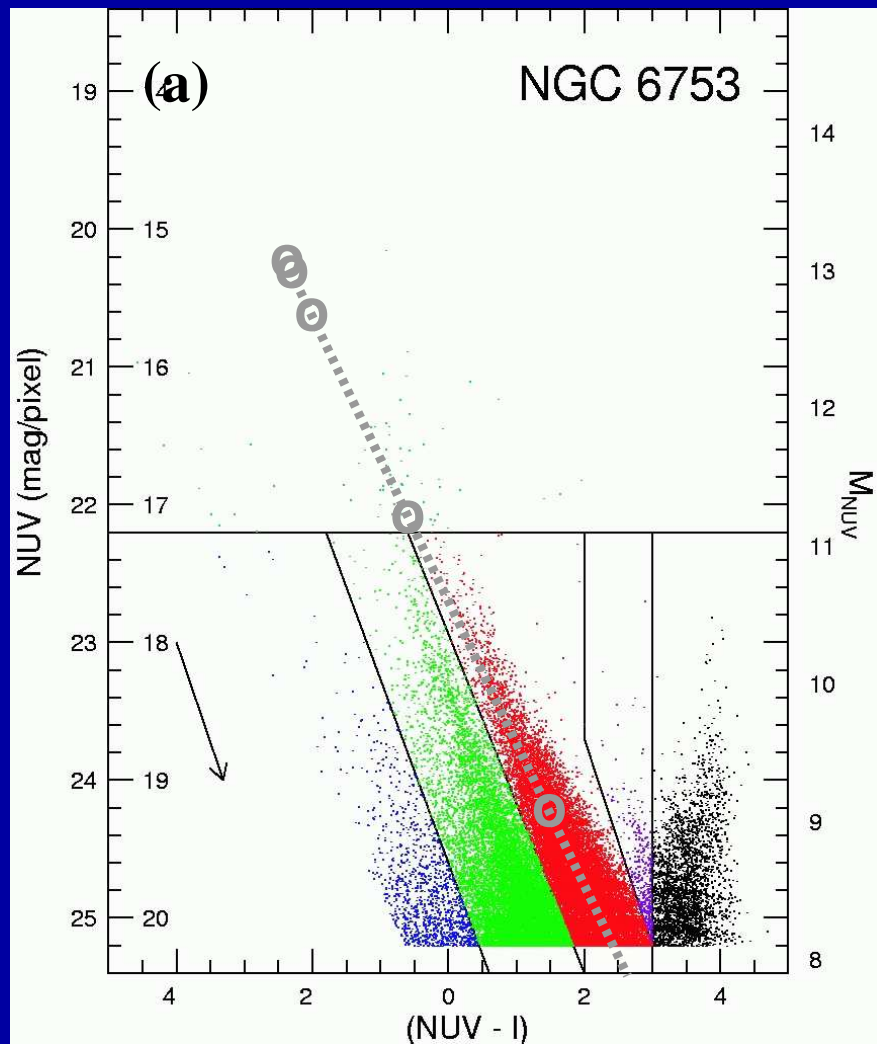


HST F300 g-b U360 g-b B436

g-b V540 g-b R634 HST F814

J1.25 μ m H1.65 μ m K2.2 μ m

- Overall, the mid-UV–red wavelengths broadly indicate the same type, but the near-IR shows an earlier bulge-dominated type.



Eskridge (2003, ApJ, 586, 923): Pixel-to-pixel color-mag diagrams.

These pCMD's show stellar population "plumes" of different ages that are not arbitrarily distributed in the galaxy, but become younger outwards in distinct dynamical entities — from the inner bulge to the outer spiral disk.

⇒ Powerful diagnostic to study ages/evolution of bars (if present).

HST/WFPC2 image of: NGC 6782



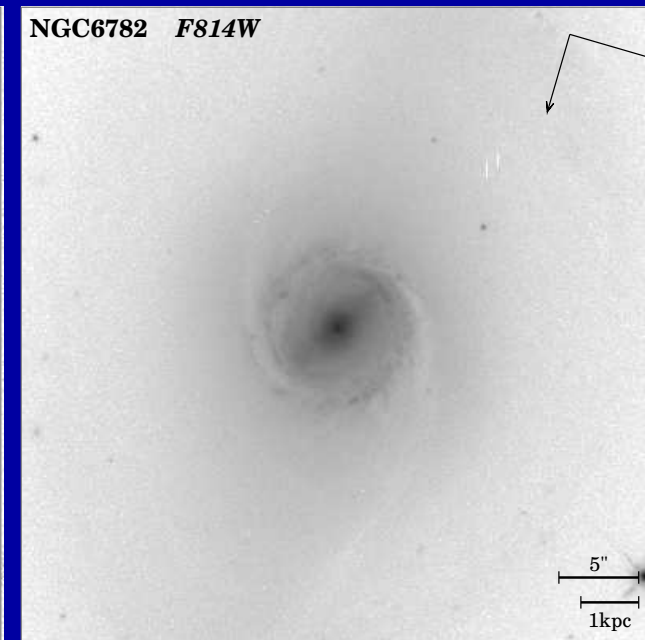
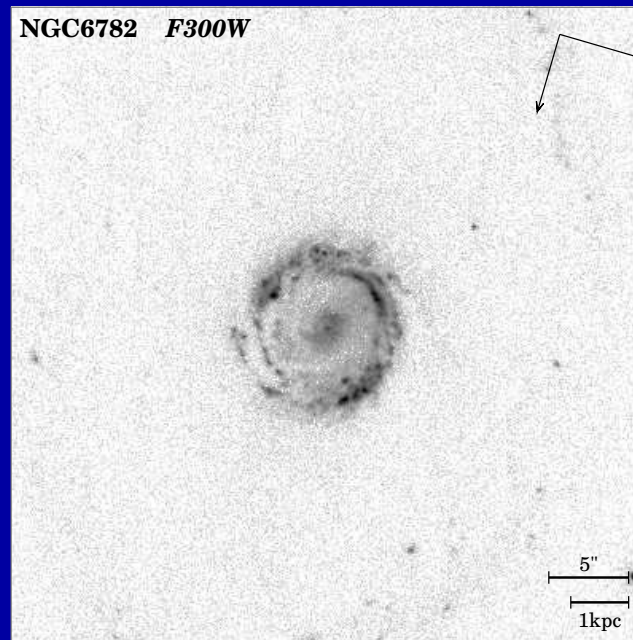
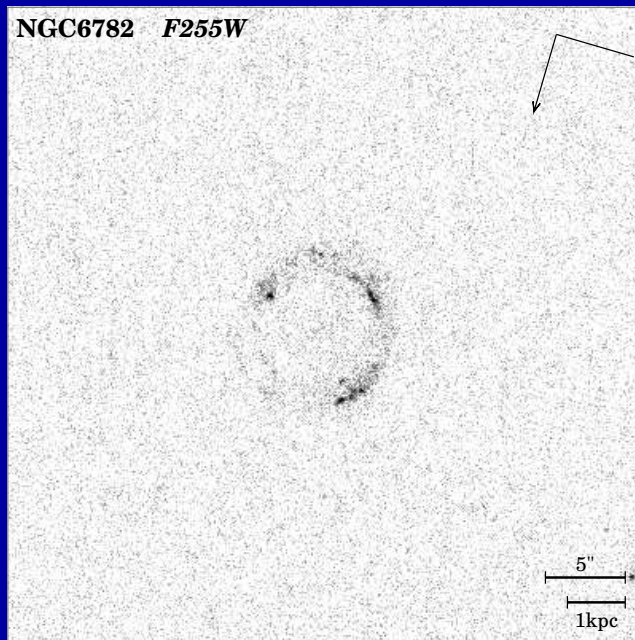
SF-rings (at orbital resonances?) can be spectacular in the mid-UV.

HST/WFPC2 images of: NGC 6782

F255W

F300W

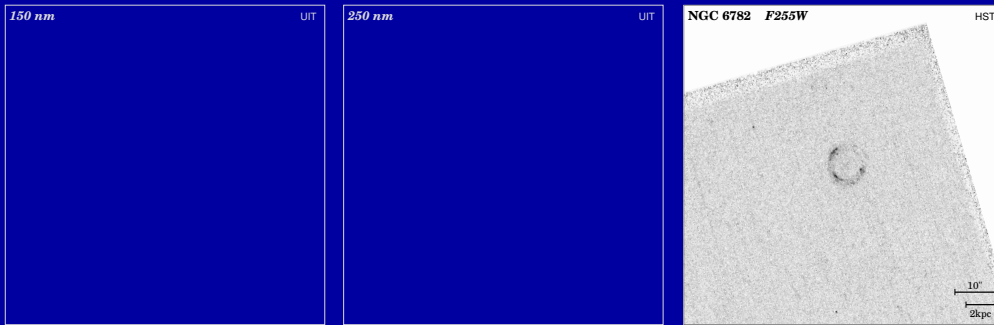
F814W



SF-rings (at orbital resonances?) can be spectacular in the mid-UV.

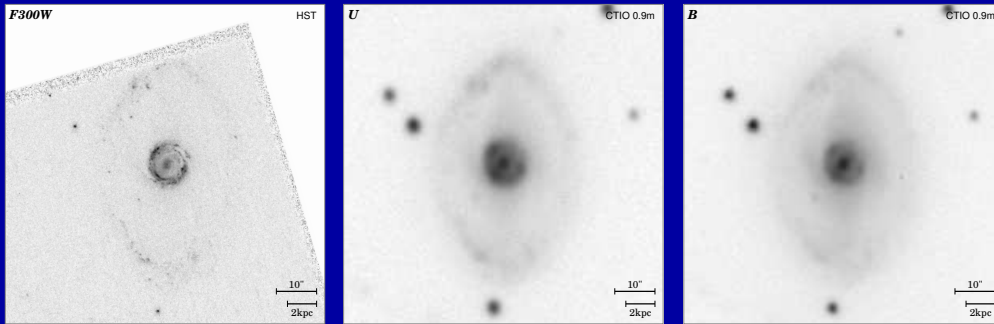
HST pixel-to-pixel CMD's may help address issues like:

- Are bars secular phenomena in the disk? (Kormendy; Hunt; this Conf.).
- What drives SF in the ring, and how does it affect the bar-formation? (various speakers; this Conference).



HST & g-b images of: NGC 6782

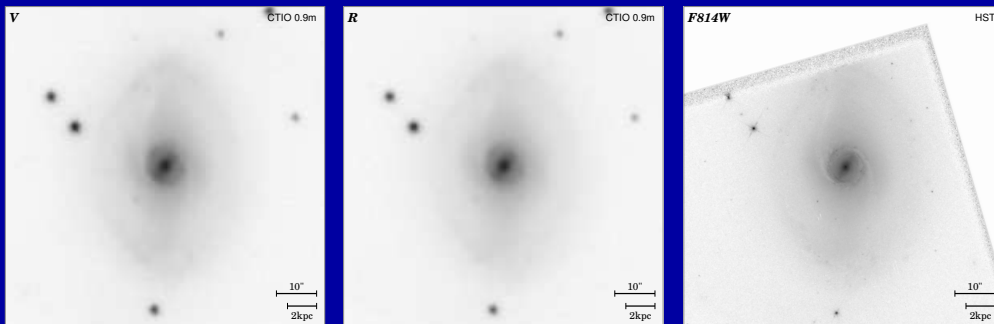
HST F255



HST F300

g-b U360

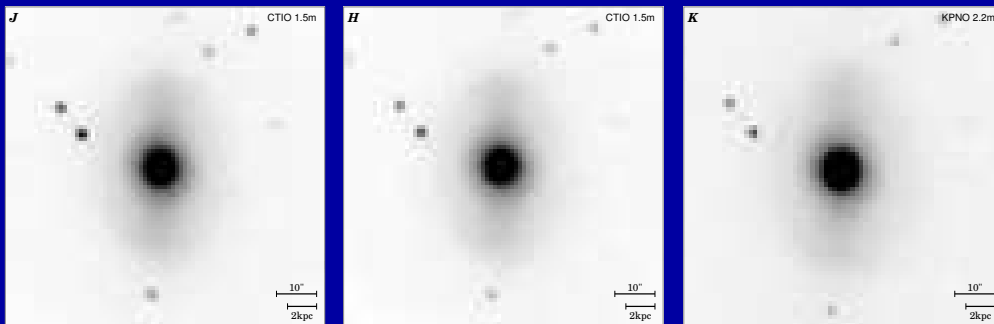
g-b B436



g-b V540

g-b R634

HST F814



g-b J1.25 μ m H1.65 μ m K2.2 μ m

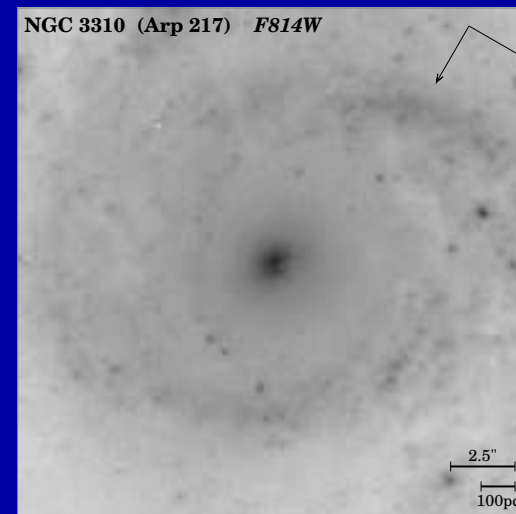
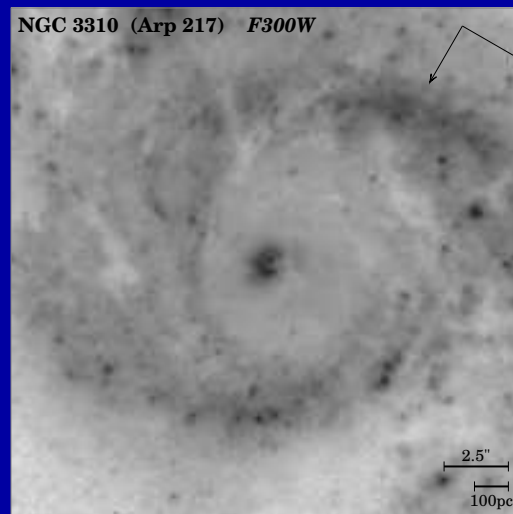
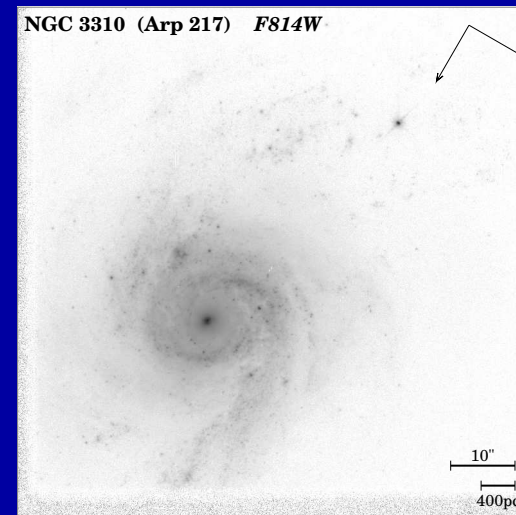
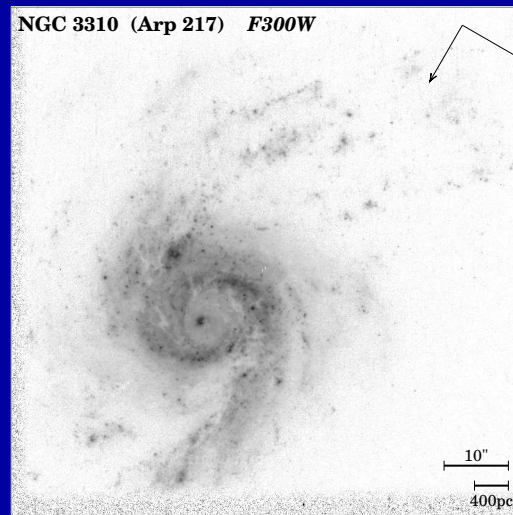
Dominated by resonance ring of hot stars in mid-UV, faint disk+inner bar in optical-red, and bulge+outer bar in red/near-IR. Significant K_{morph} .

HST/WFPC2 images of:

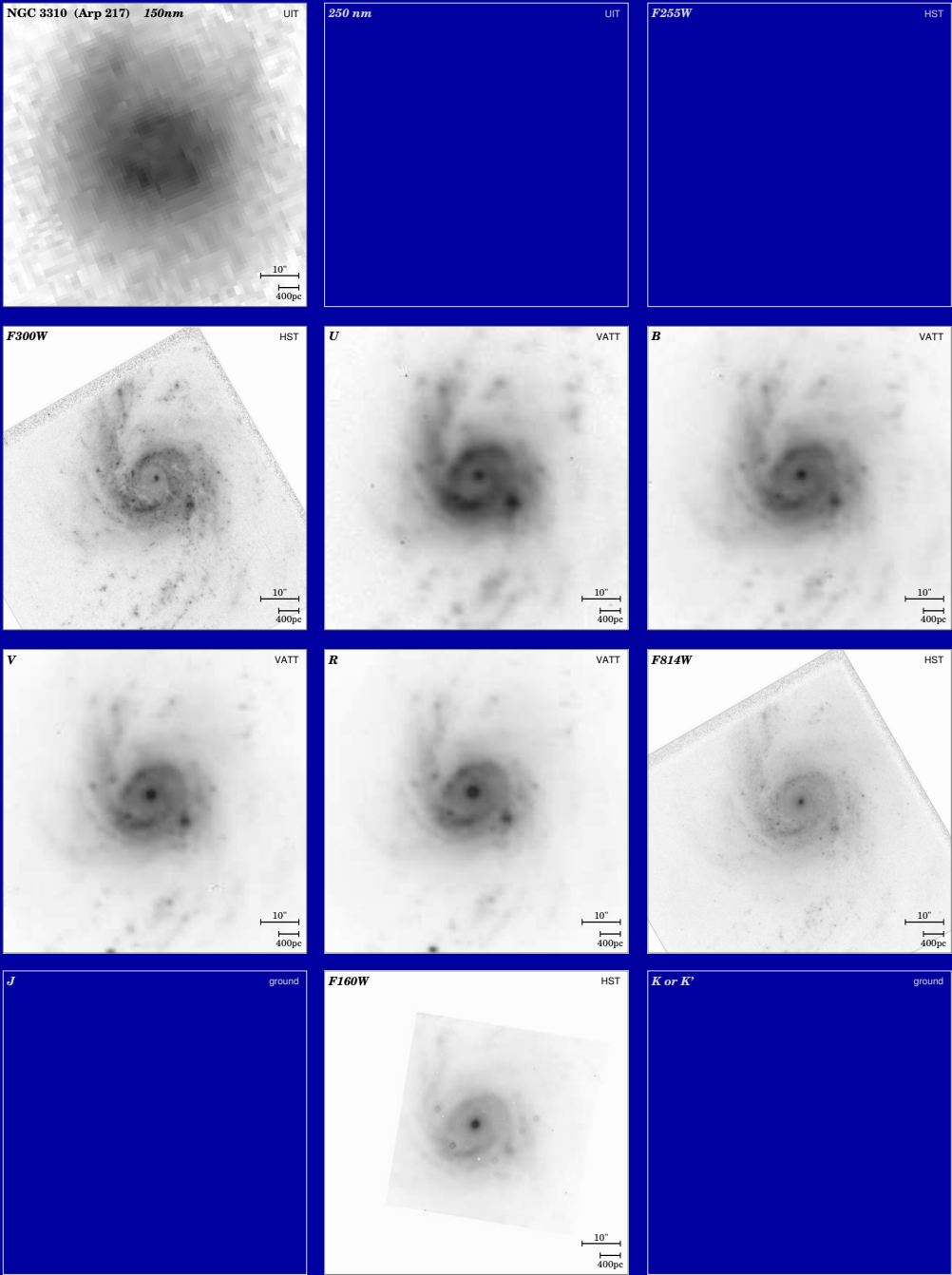
NGC 3310

F300W

F814W



- Other spirals are dominated by a global starburst and similar at all λ 's.
- Most spirals show nuclear dust lanes emerging from small bulge.



UIT, HST & g-b images: NGC 3310

UIT 150nm

HST F300

g-b U360

g-b B436

g-b V540

g-b R634

HST F814

Nic3 F160

- Most actively starforming galaxies are dominated by a global starburst and look similar at all wavelengths (UIT-FUV–near-IR).

HST/WFPC2 images of:

UGC 10043

F300W

F814W

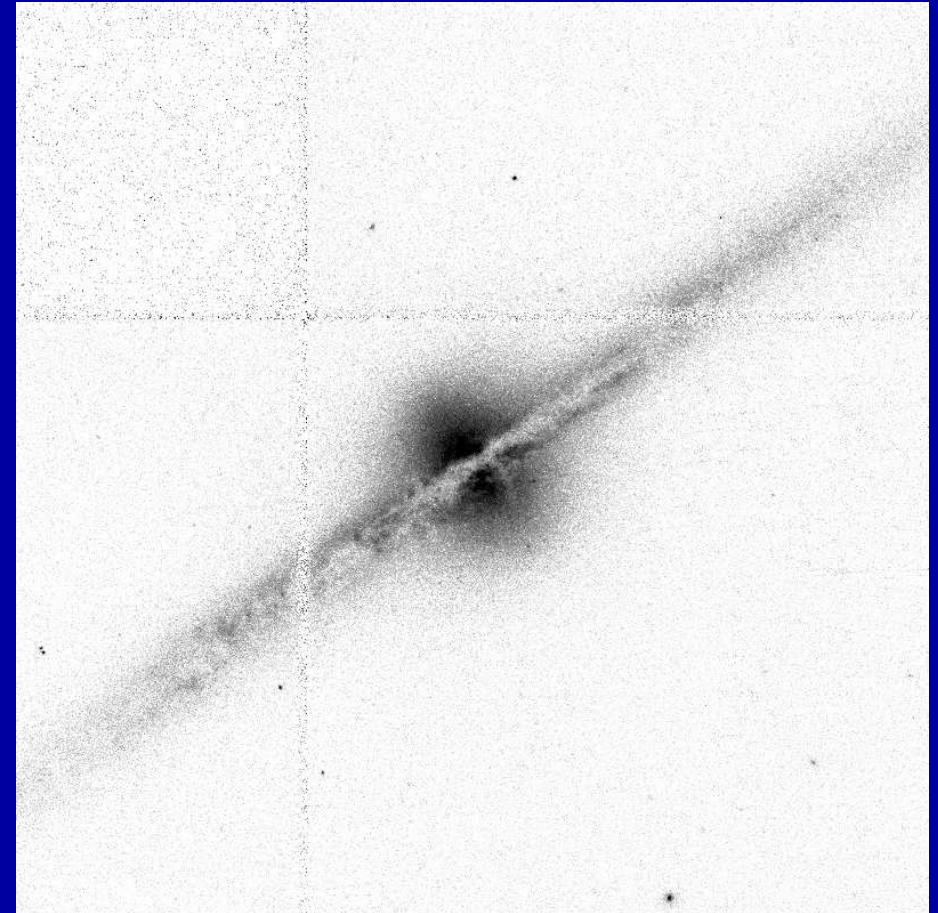
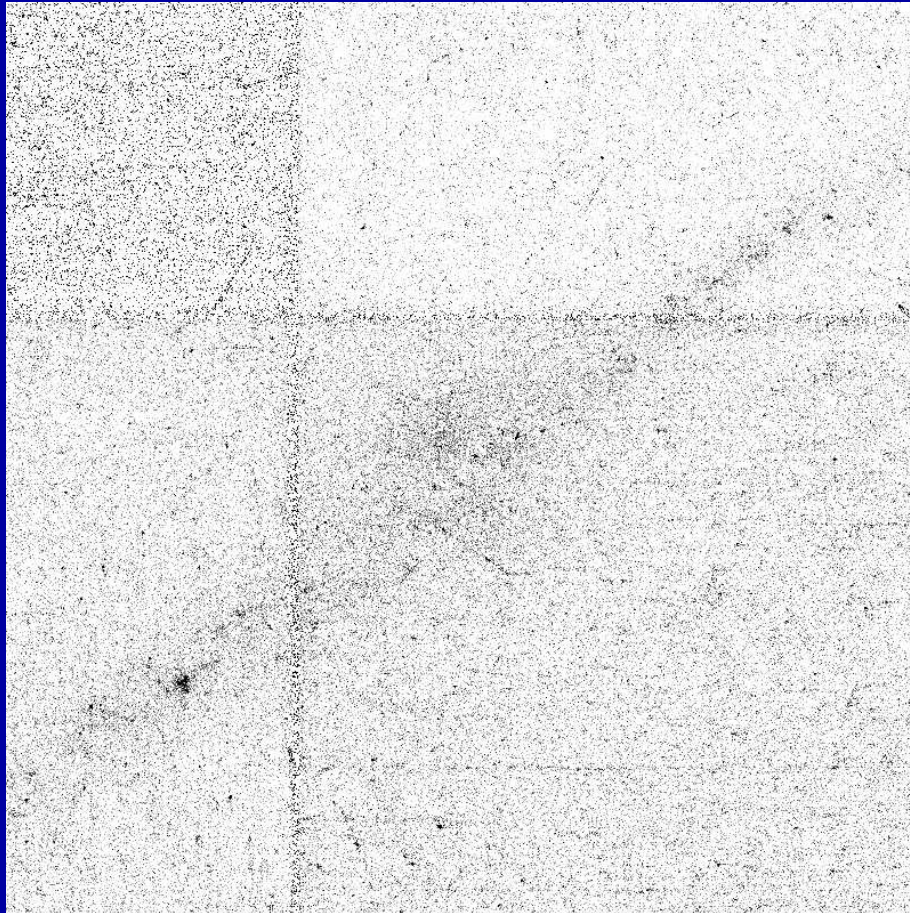


Image edge-on galaxies of all types to find-out where the dust is:

- Many edge-on's are nearly opaque in the mid-UV, some have UV-sources in front of the dust. Most show U_{290} / I_{814} increasing from inside out (younger stellar population with decreasing dust content?).

HST/WFPC2 images of:

ESO 446-G44

F300W

F814W

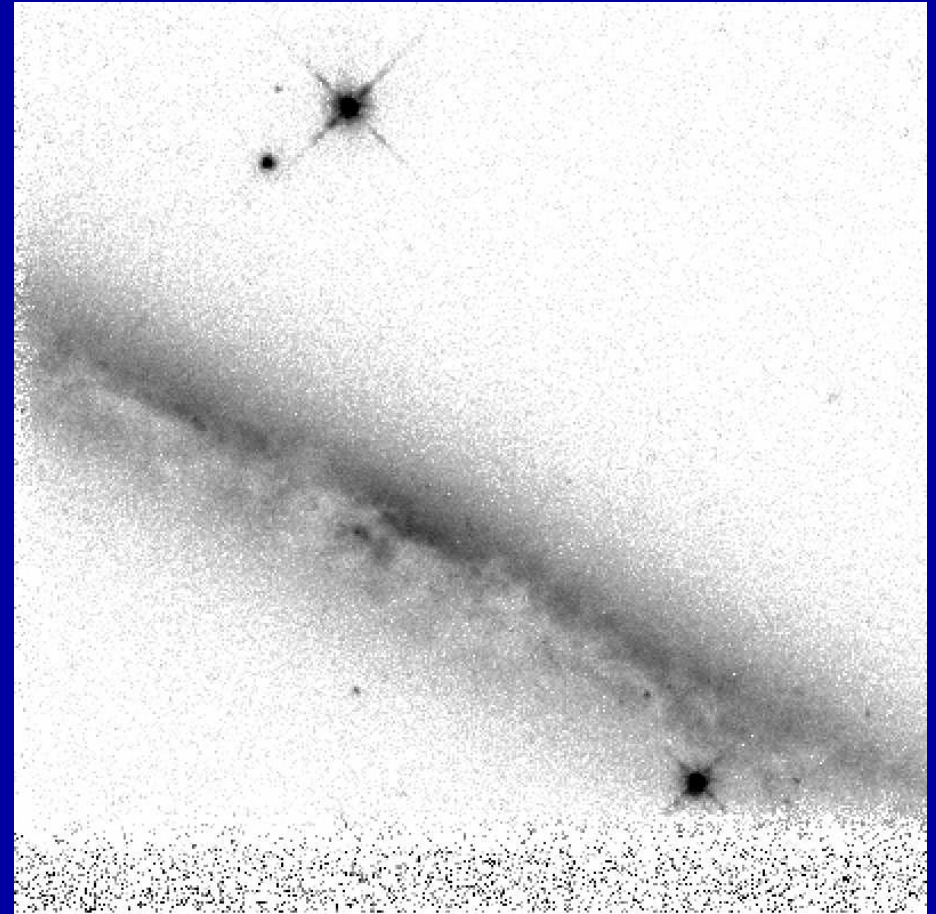
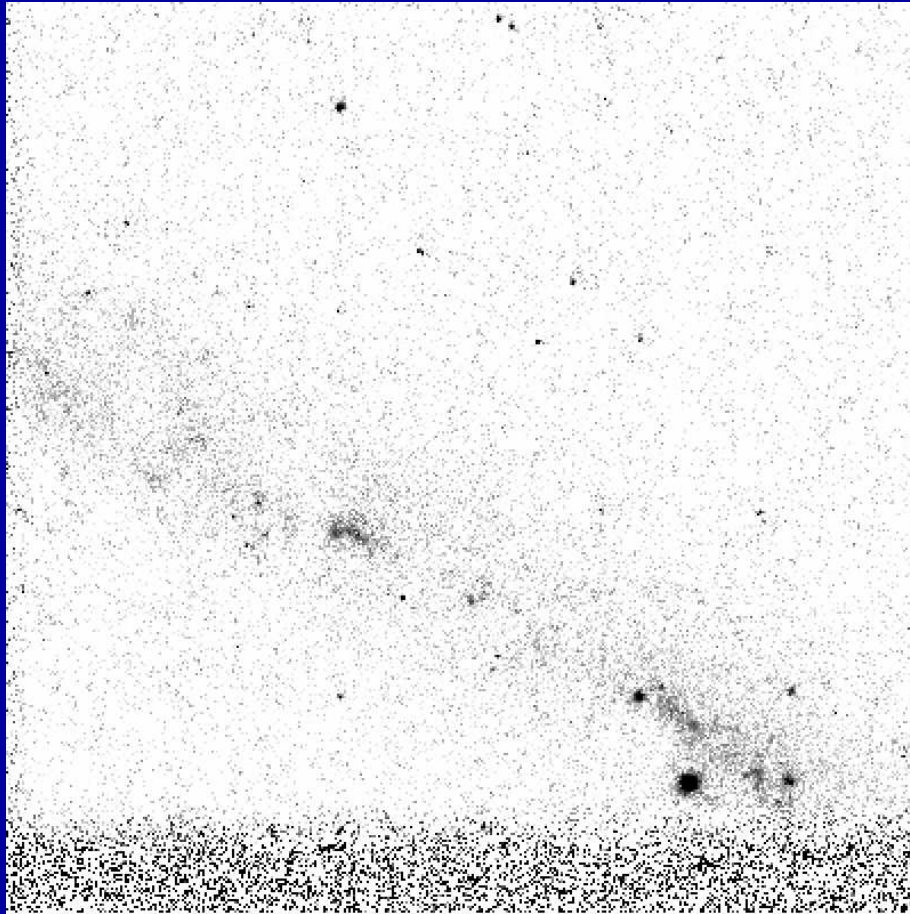


Image edge-on galaxies of all types to find-out where the dust is:

- Many edge-on's are nearly opaque in the mid-UV, some have UV-sources in front of the dust. Most show $F300W/I_{814}$ increasing from inside out (younger stellar population with decreasing dust content?).

4. Results for Late-type Galaxies

(3) MOST LATE-TYPES/IRREGULARS/PECULIARS & MERGERS show similar morphology from the mid-UV to the red, due to their dominant young and hot stellar population.

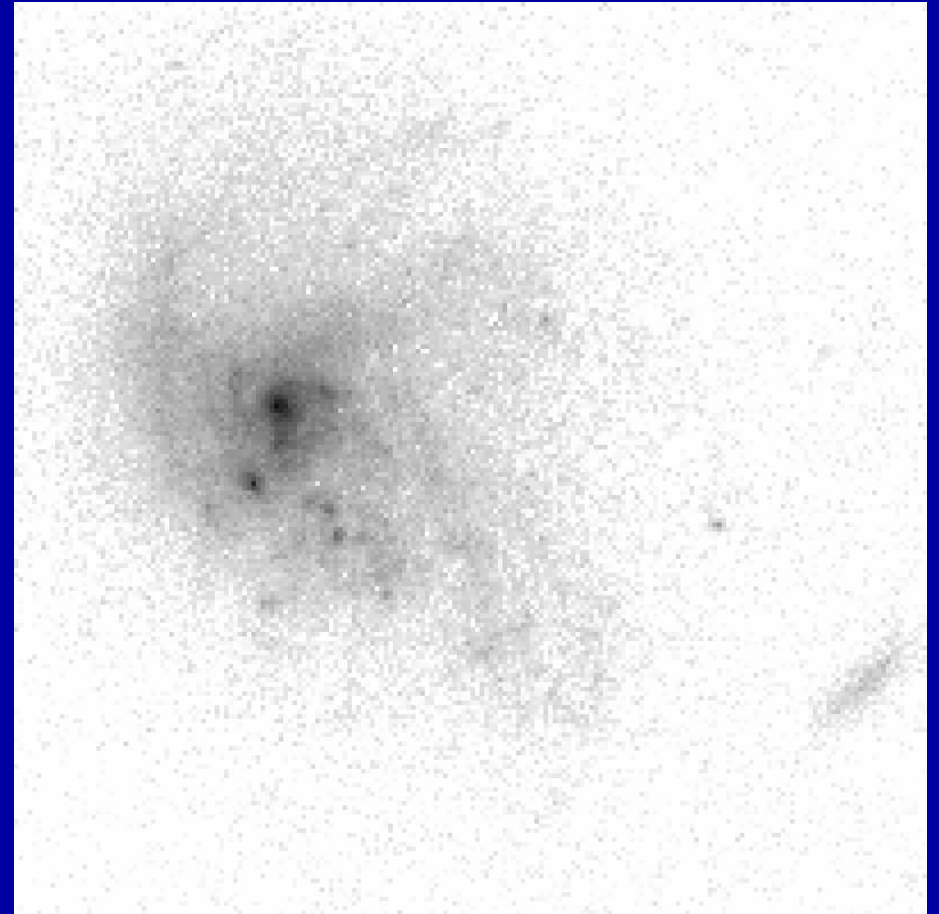
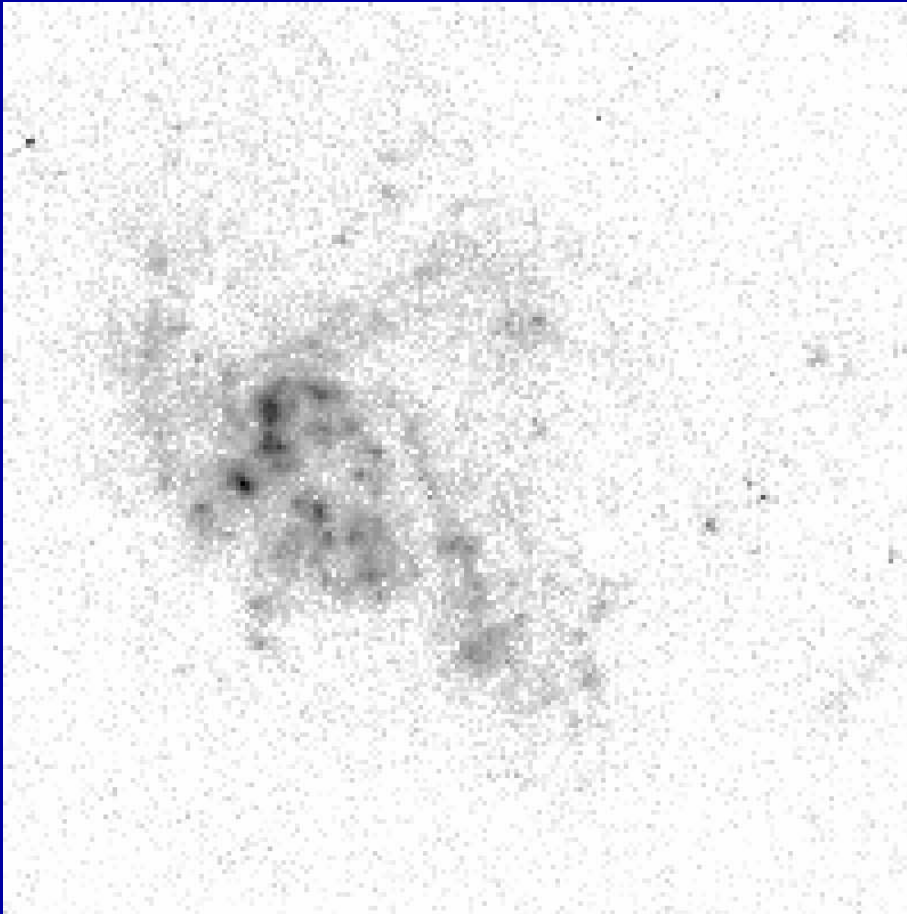
- A few yield significantly different classifications in mid-UV and I_{814} . Important differences due to recognizable dust-lanes blocking out mid-UV light — dust pockets, holes or bubbles (?).
- \exists star-formation “ridges”, hot stars or star-clusters, mostly visible in the mid-UV, but less so in I_{814} .
- In general, bars in late-type galaxies do not disappear in the mid-UV, contrary to most bars in early–mid type spirals.

HST/WFPC2 images of:

CGC G97-114

F300W

F814W



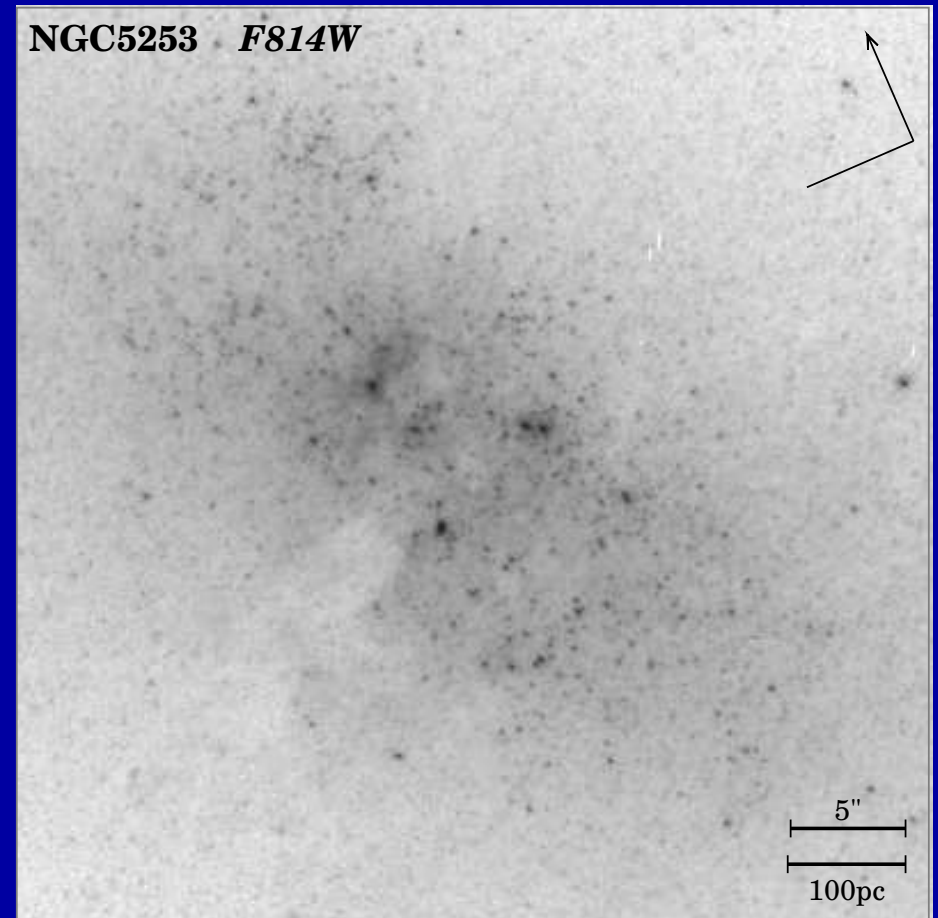
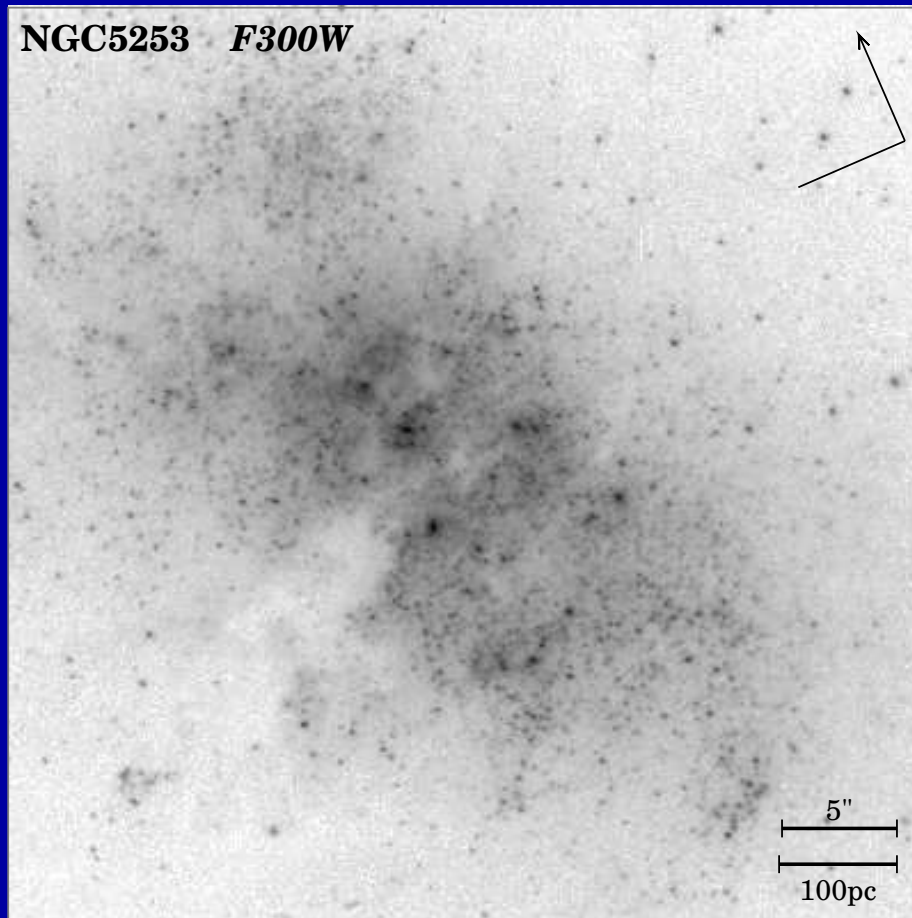
- Possibly the beginning of spiral structure plus stochastic SF.
- Dominated by starburst, so similar appearance at all wavelengths.

HST/WFPC2 images of:

F300W

NGC 5253

F814W



- Small star-forming galaxy with significant super star-clusters.
- Late-type actively star-forming galaxies are possibly local counterparts of the faint blue galaxies at high redshifts, which may be the building blocks of the giant galaxies seen today.

UIT, HST & g-b images: NGC 5253

UIT 150nm

HST F255

HST F300

g-b U360

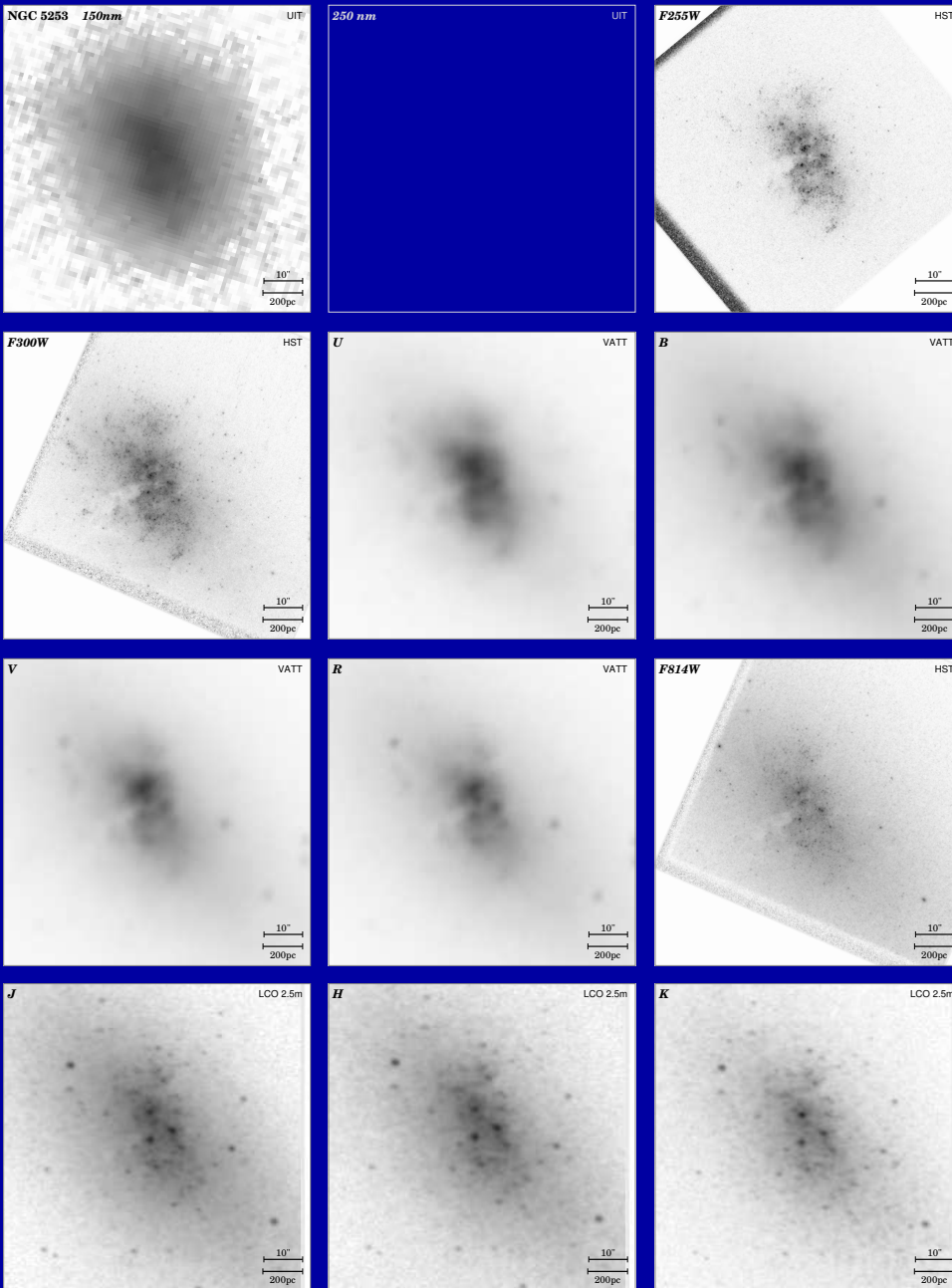
g-b B436

g-b V540

g-b R634

HST F814

g-b J1.25 μ m H1.65 μ m K2.2 μ m



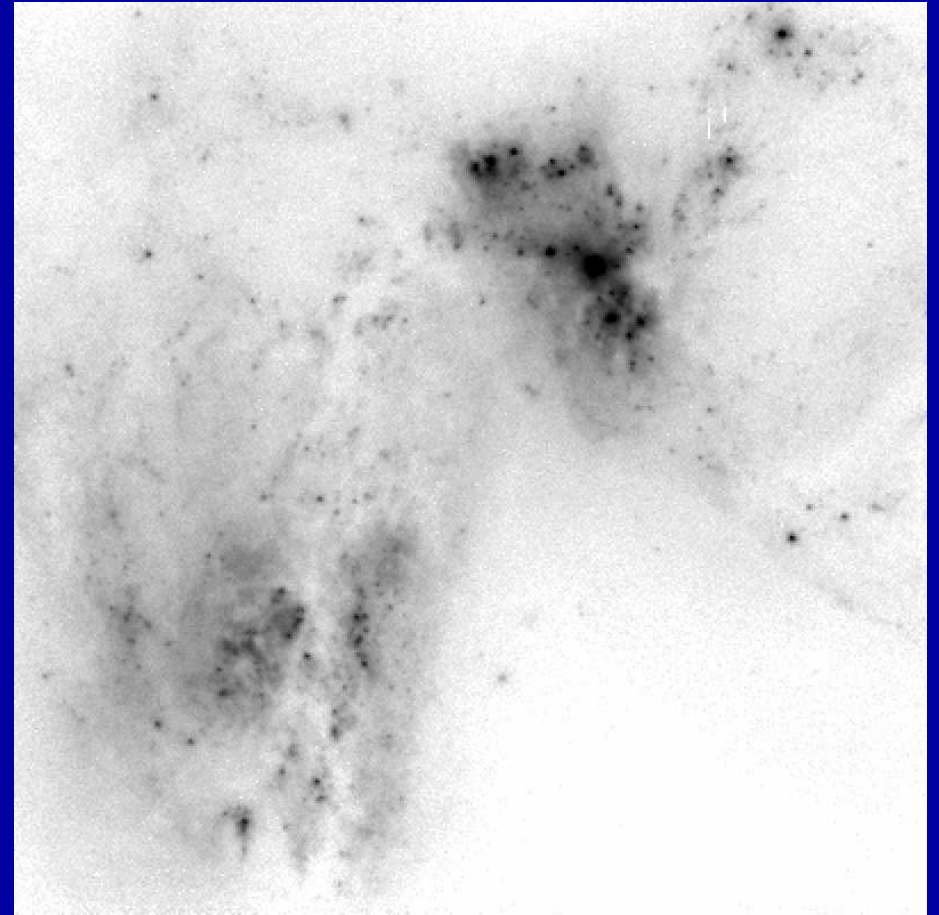
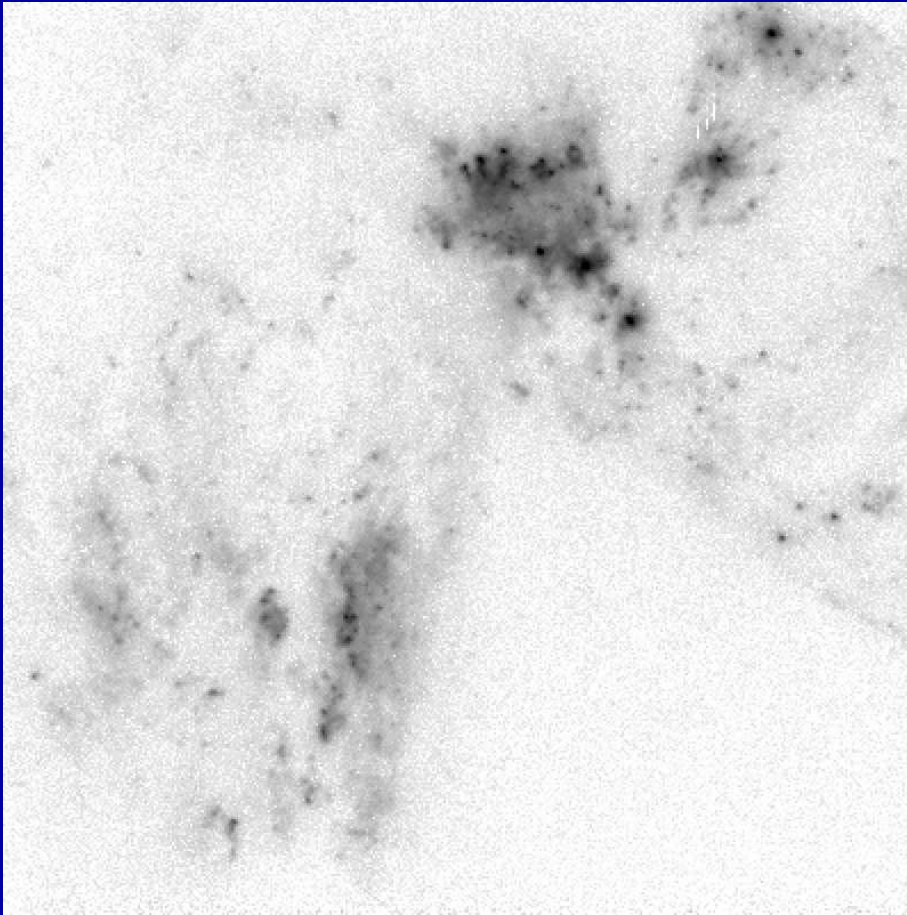
- Most late-type galaxies are dominated by recent star-formation and look similar at all wavelengths (UIT-FUV—near-IR).

HST/WFPC2 images of:

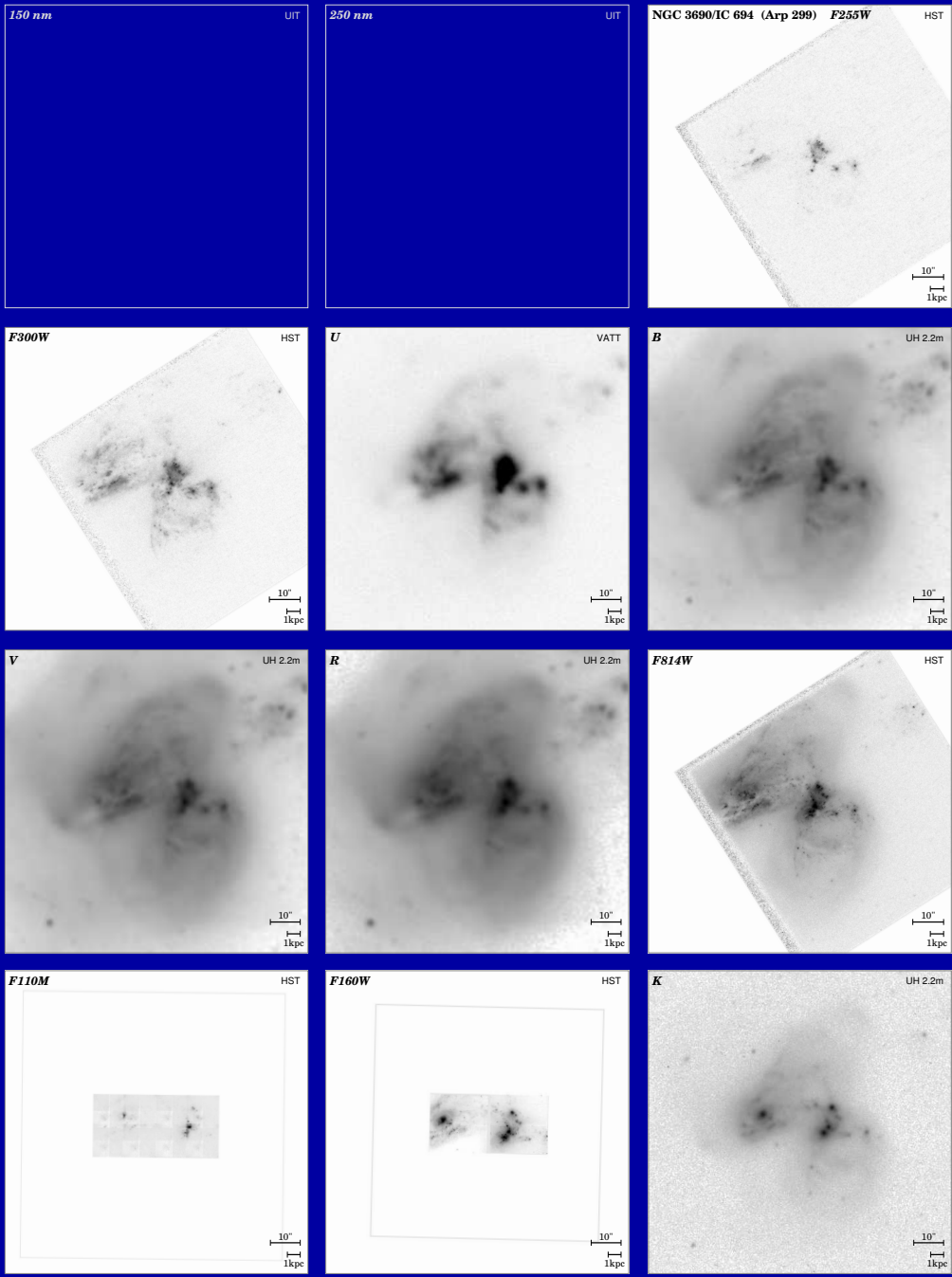
UGC 06471-2

F300W

F814W



- Major merger with active SF that look similar at all wavelengths.
Are the rare local train-wrecks counterparts of high-z star-forming objects?



HST & g-b images of: U06471-2

HST F255

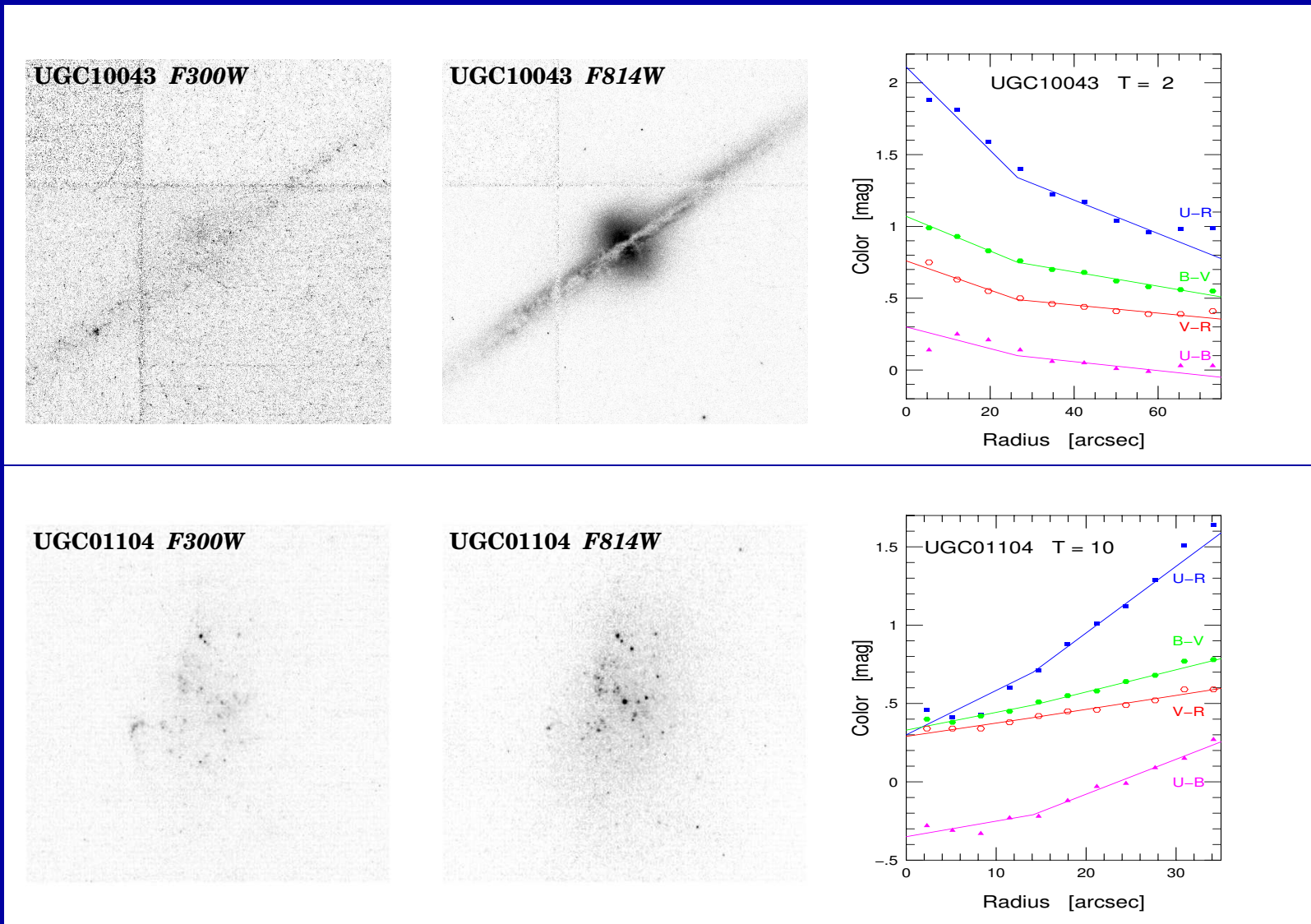
HST F300 g-b U360 g-b B436

g-b V540 g-b R634 HST F814

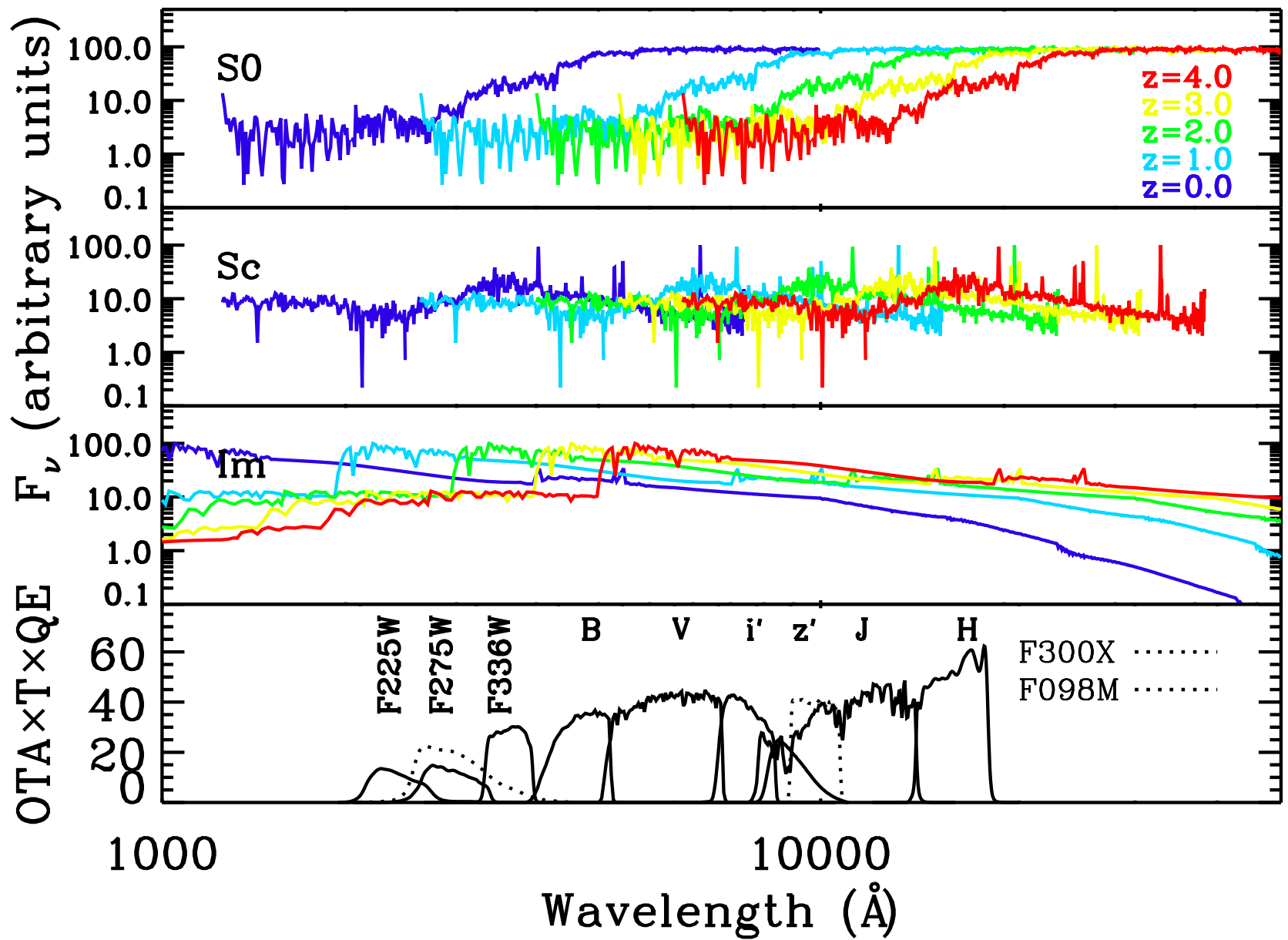
Nic F110M Nic F160W K2.2 μ m

- Most mergers and actively starforming galaxies are dominated by a global starburst and look similar at all wavelengths (HST mid-UV–near-IR).

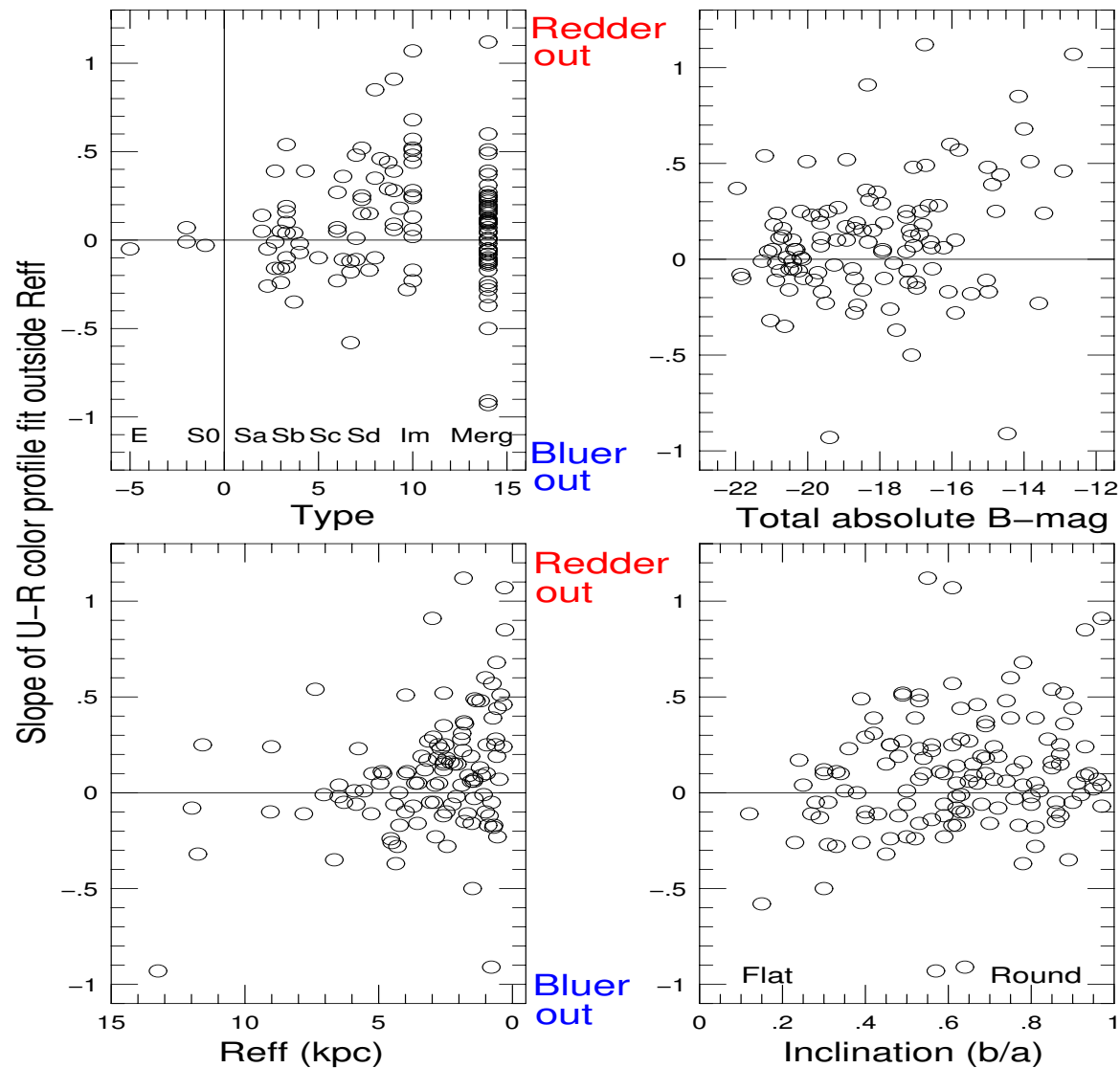
(5) Near-IR images and Ground-based Light-profiles



- Early-mid-type spirals get (slightly) bluer with increasing radius.
- Majority of late-type galaxies get redder outwards.
⇒ Significant halo or (thick) disk of older stars (?)

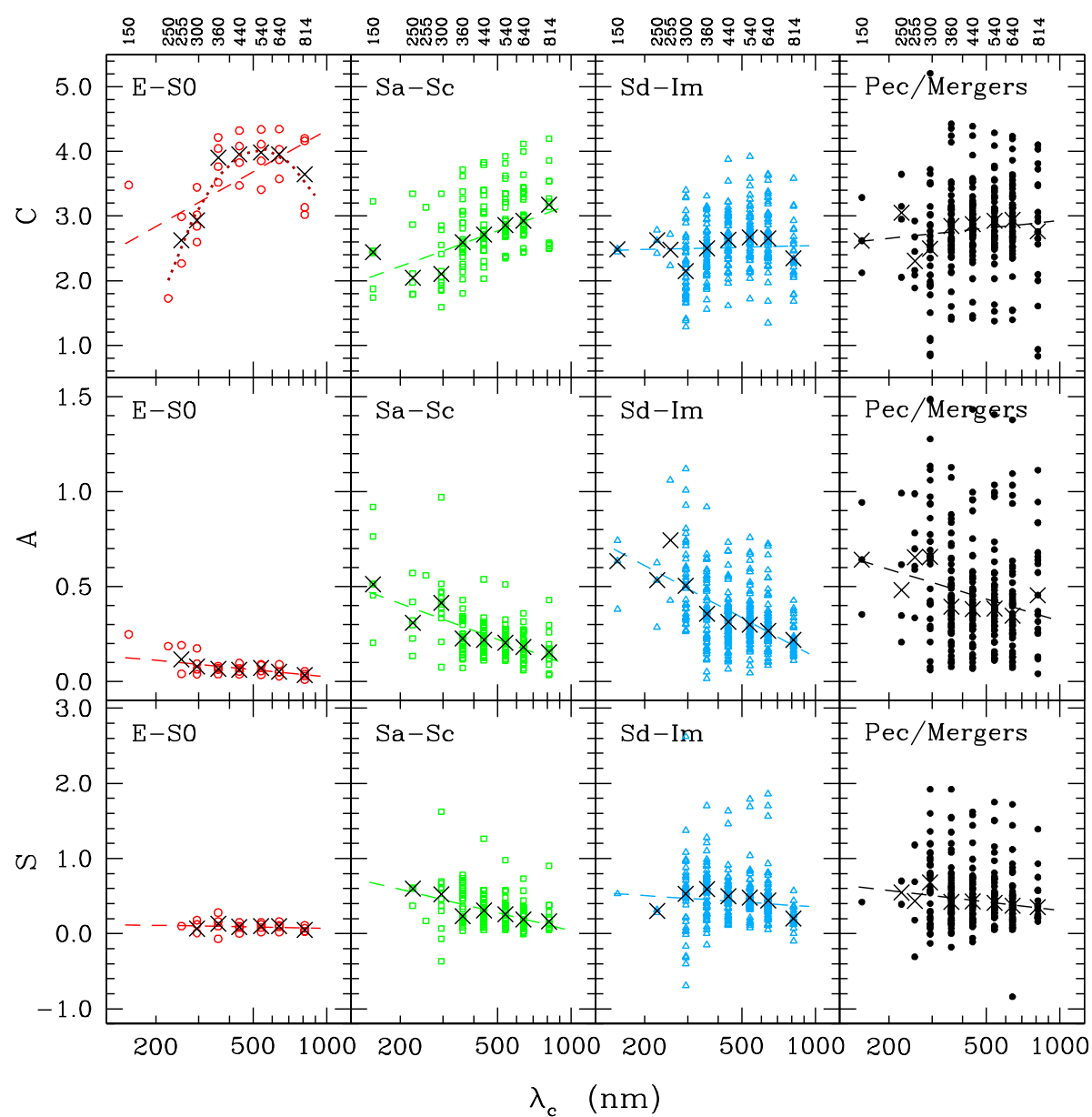


Cardinal WFC3 filters compared to BC03 galaxy SED templates at $z=0-4$.

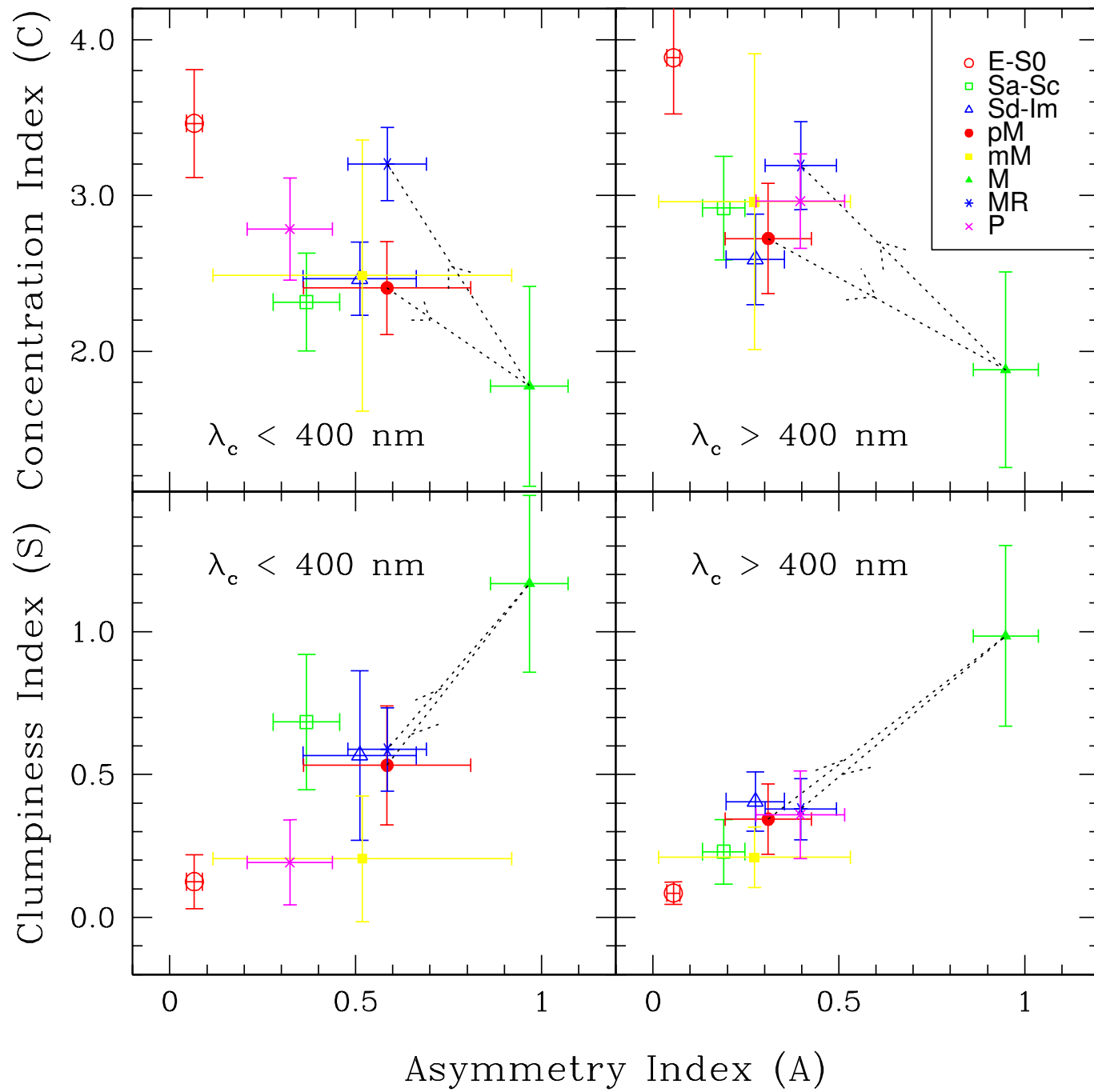


Most later-types get redder outwards, especially those with lower luminosity, smaller r_e , lower average $SB(r < r_e)$, and rounder b/a (Taylor et al. 2005).

⇒ Significant halo or (thick) disk (?) of older stars in late-types.



- V. Taylor et al. (2007): Morphological K-correction now mapped into the UV, and is mostly small, except for **C** in early- and **C, A** in mid-types.
- 12 years of WFPC2 and 3 years of GALEX still leave us still with poor S/N, poor resolution, or poor statistics on nearby galaxies below 3000\AA .

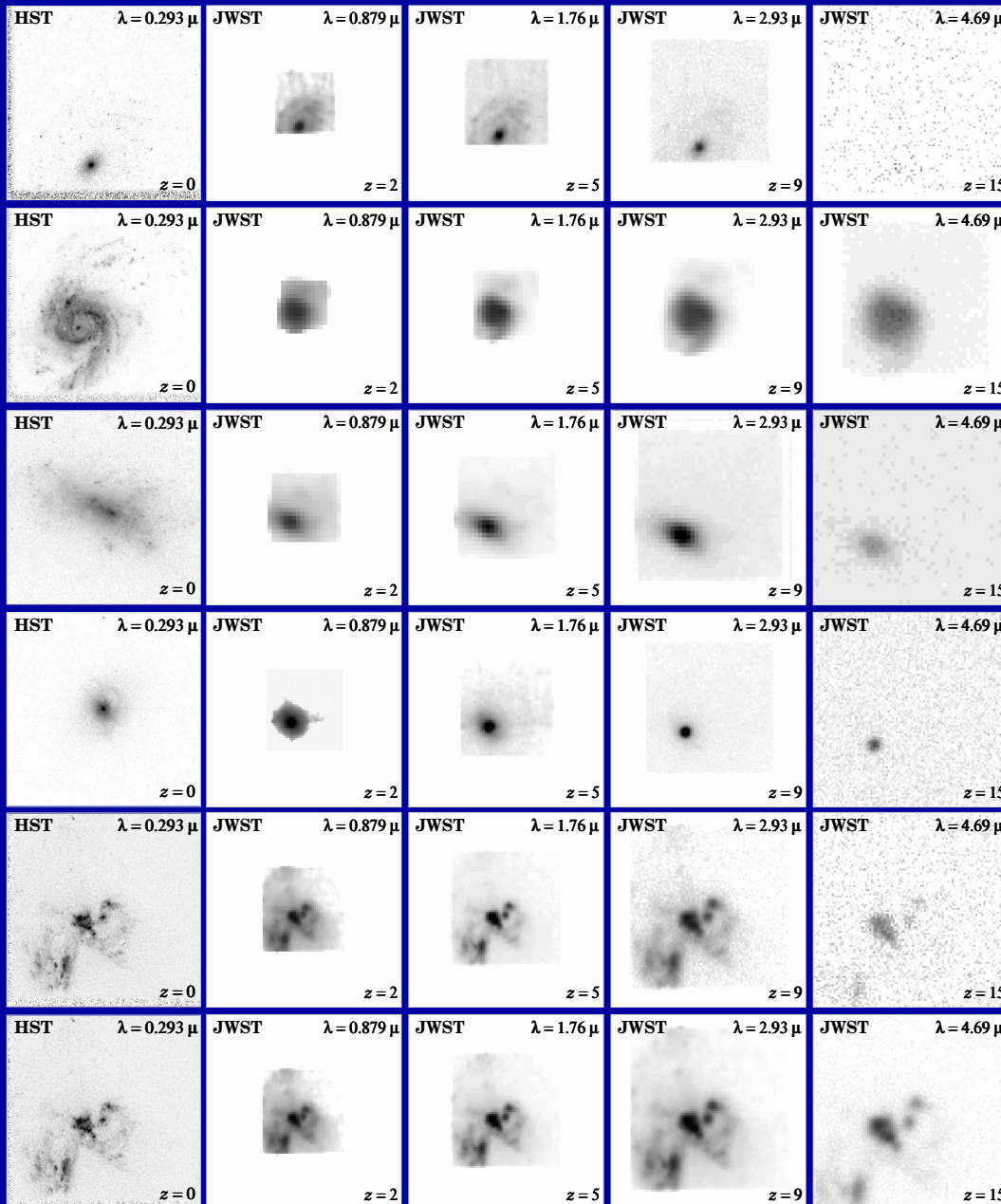


Taylor et al. (2007): $CAS(\lambda)$ traces (some of) galaxy merging sequence.

- WFC3 SNAPs will do this with far superior sampling and statistics !

(6) Predict Galaxy Appearance for JWST at $z \simeq 1-15$

HST $z=0$ JWST $z=2$ $z=5$ $z=9$ $z=15$

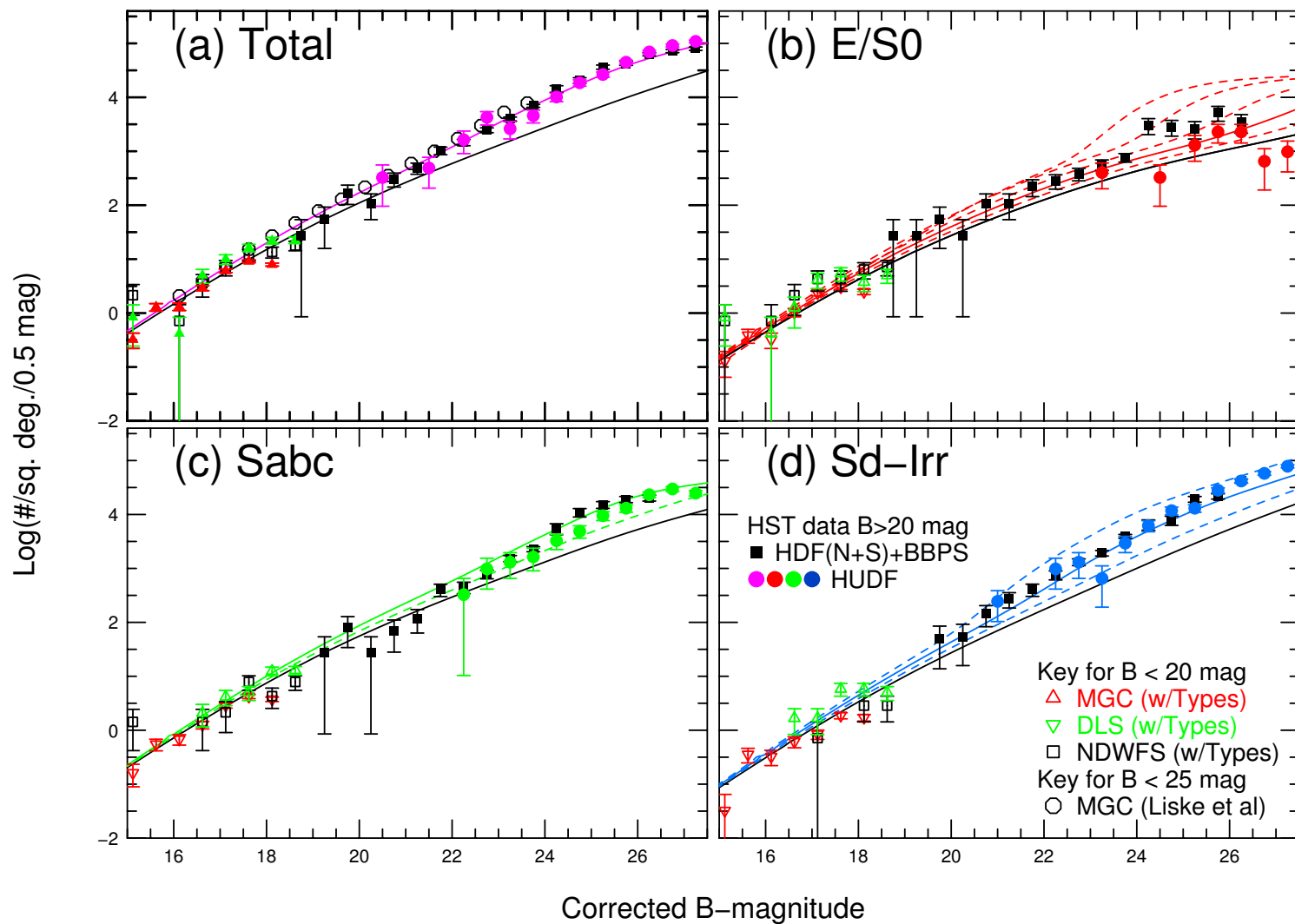


With proper restframe-UV training, JWST can quantitatively measure the evolution of galaxy morphology and structure over a wide range of cosmic time:

- (1) Most disks will SB-dim away at high z , but they formed at $z \lesssim z_{form} \simeq 1-2$.
- (2) High SB structures are visible to very high z .
- (3) Point sources (AGN) are visible to very high z .
- (4) High SB-parts of mergers/train-wrecks are visible to very high z .

(7) Summary and Conclusions

- (1) In the rest-frame mid-UV, early- to mid-type galaxies are more likely to be misclassified as later-types than late-type galaxies are misclassified as earlier-types.
- (2) The change of galaxy morphology with rest-frame wavelength can explain part ($\lesssim 20\text{--}30\%$) but not all of the excess faint blue late-type/irregular/peculiar galaxies seen in the deepest HST fields.
- (3) The excess of late-type/irregular/peculiar galaxies at $AB \gtrsim 22$ mag is thus real, and an essential clue to the process of galaxy formation — the building blocks or merging stages of giant galaxies seen today?
- (4) and ...



Cohen et al. (2003): ● Artificial Neural Networks calibrated in the mid-UV.
 ● Available ground-based and HST images covering AB=15–29 mag.
 ⇒ Faint late-types have largest excess compared to local LF, but early- & mid-types have some excess too. This is now a secure result, since their rest-frame mid-UV mis-classifications go mostly in the opposite direction.

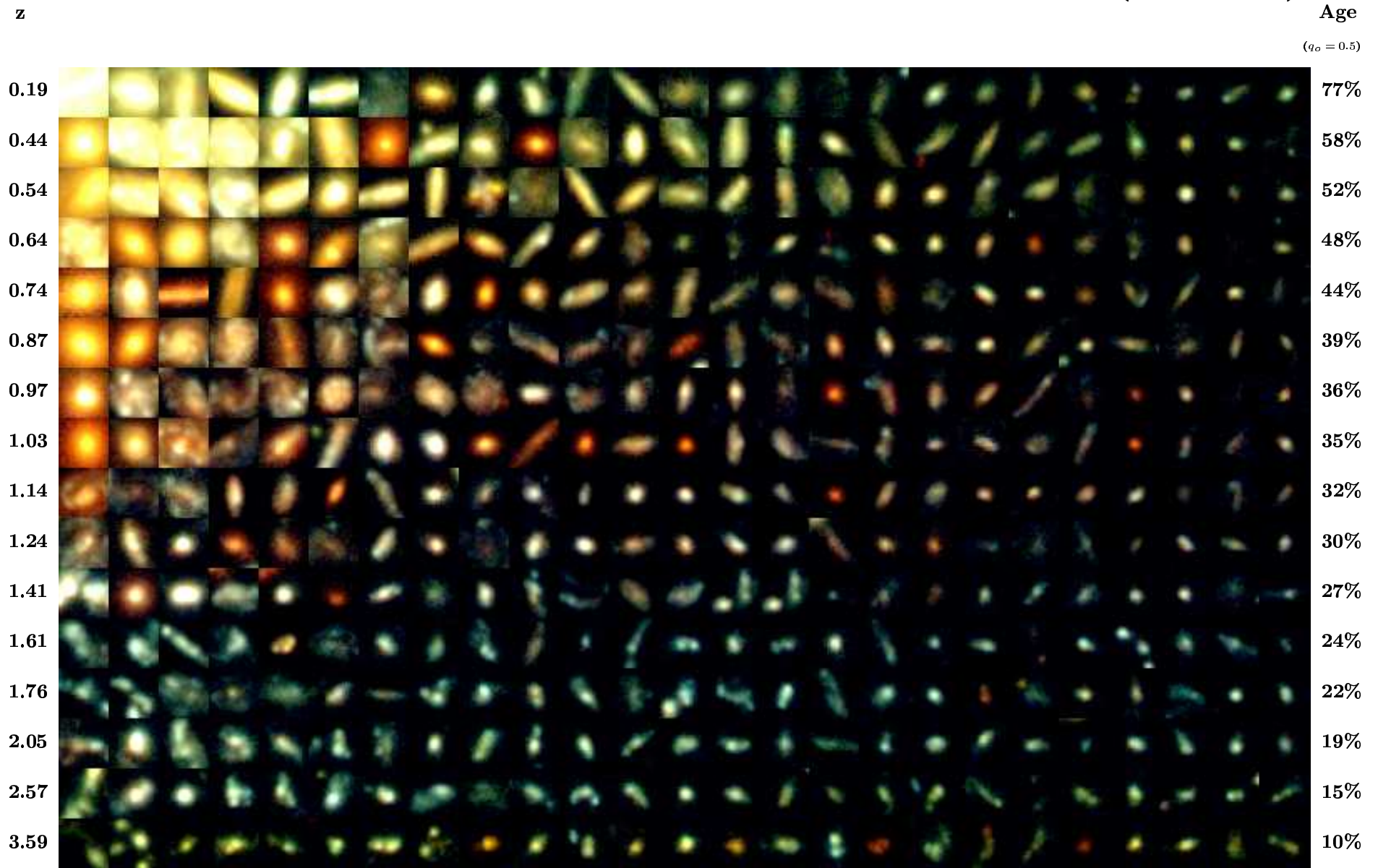
(7) Summary and Conclusions

- (1) In the rest-frame mid-UV, early- to mid-type galaxies are more likely to be misclassified as later-types than late-type galaxies are misclassified as earlier-types.
- (2) The change of galaxy morphology with rest-frame wavelength can explain part ($\lesssim 20\text{--}30\%$) but not all of the excess faint blue late-type/irregular/peculiar galaxies seen in the deepest HST fields.
- (3) The excess of late-type/irregular/peculiar galaxies at $AB \gtrsim 22$ mag is thus real, and an essential clue to the process of galaxy formation — the building blocks or merging stages of giant galaxies seen today?
- (4) Early-mid types also show an excess for $AB \gtrsim 23$ mag, possibly caused by the Cosmological Constant winding down the strongly epoch-dependent rate of (minor) mergers when it forever took over the expansion at:

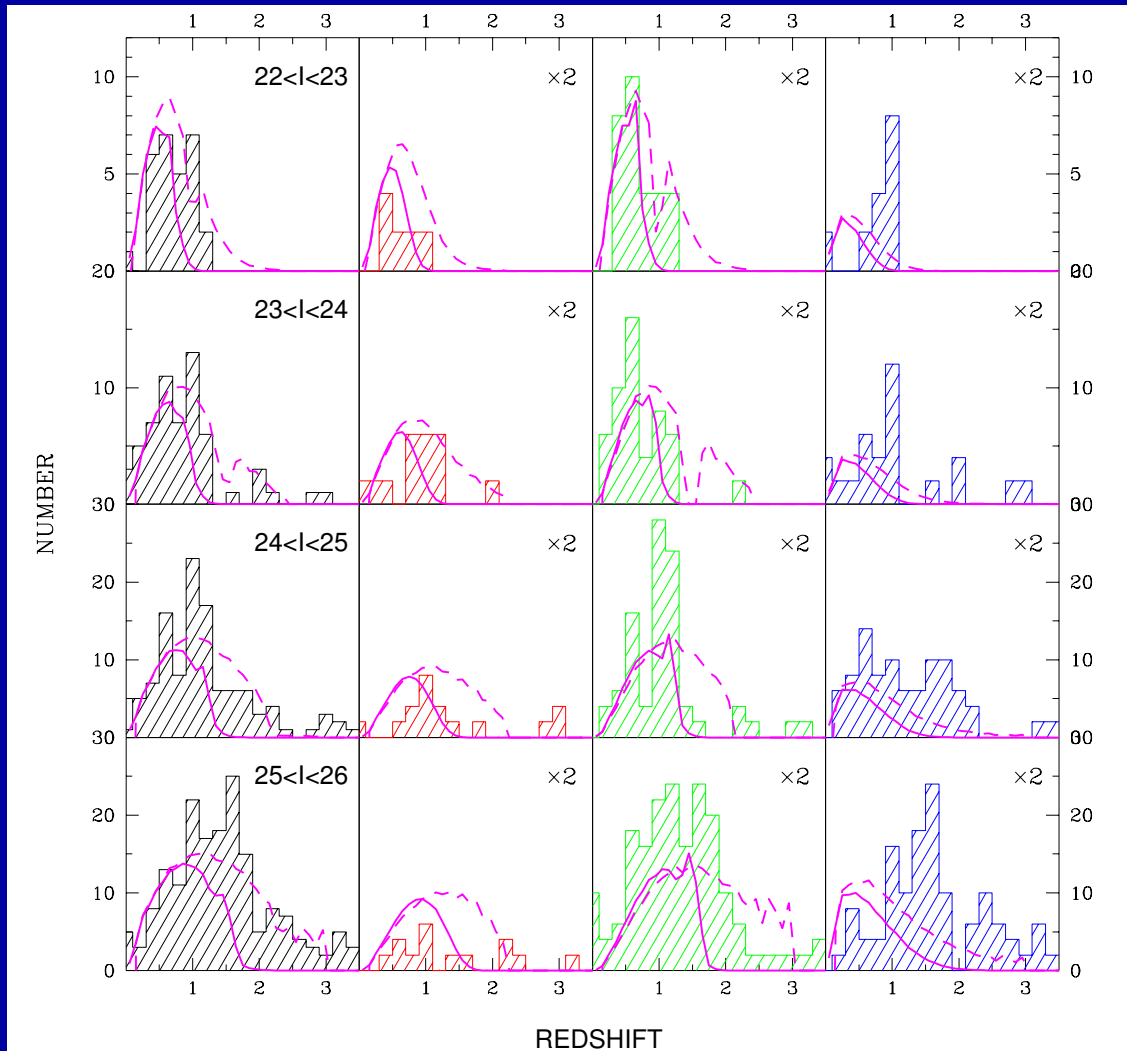
$$z_{m-\Lambda} \lesssim (\Omega_m/\Omega_\Lambda)^{1/3} - 1 = 0.39 \quad (\text{WMAP value}).$$

SPARE CHARTS

THE HUBBLE DEEP FIELD CORE SAMPLE ($I < 26.0$)



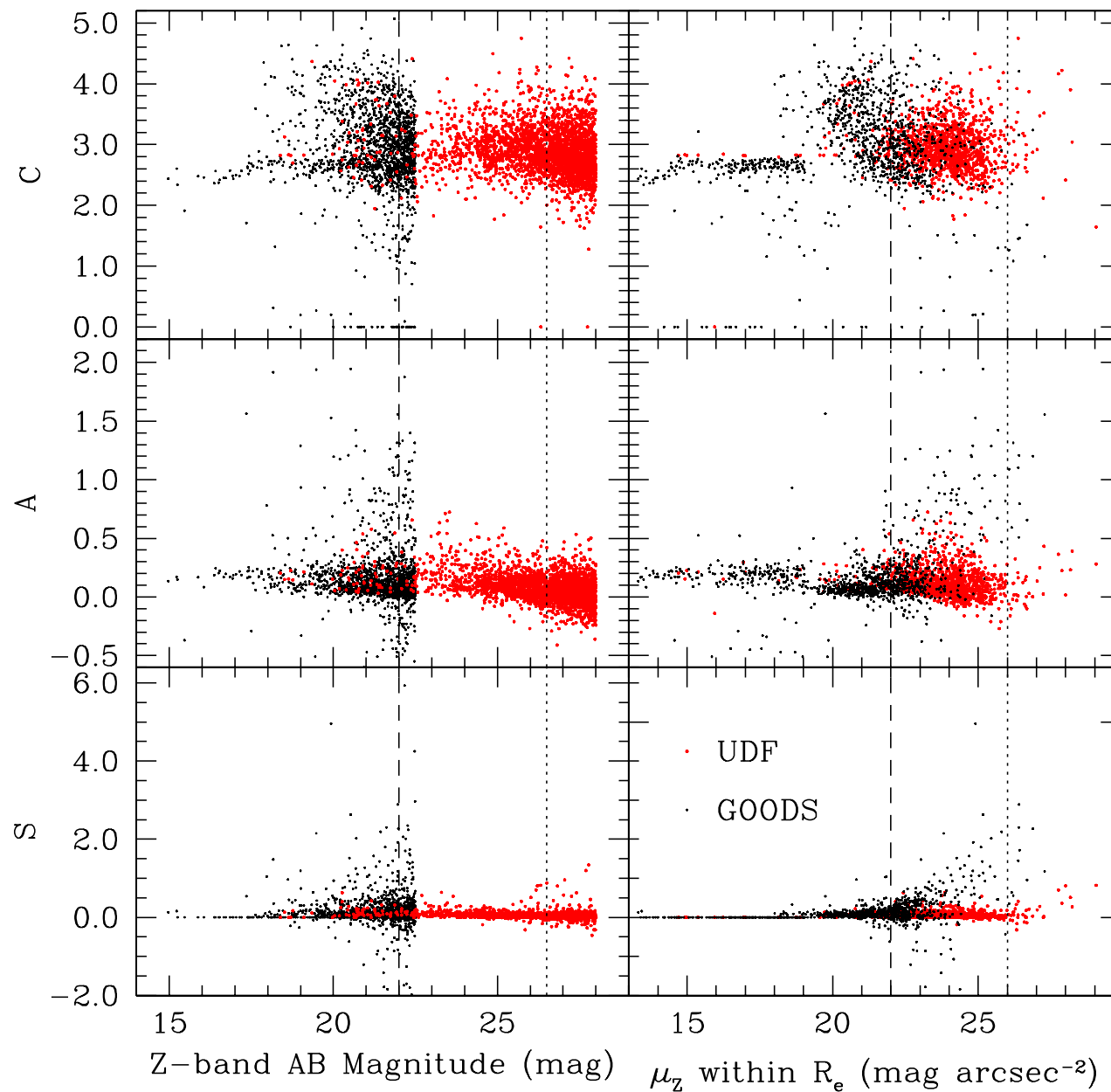
Total EII/S0 Sabc Irr/Mergers



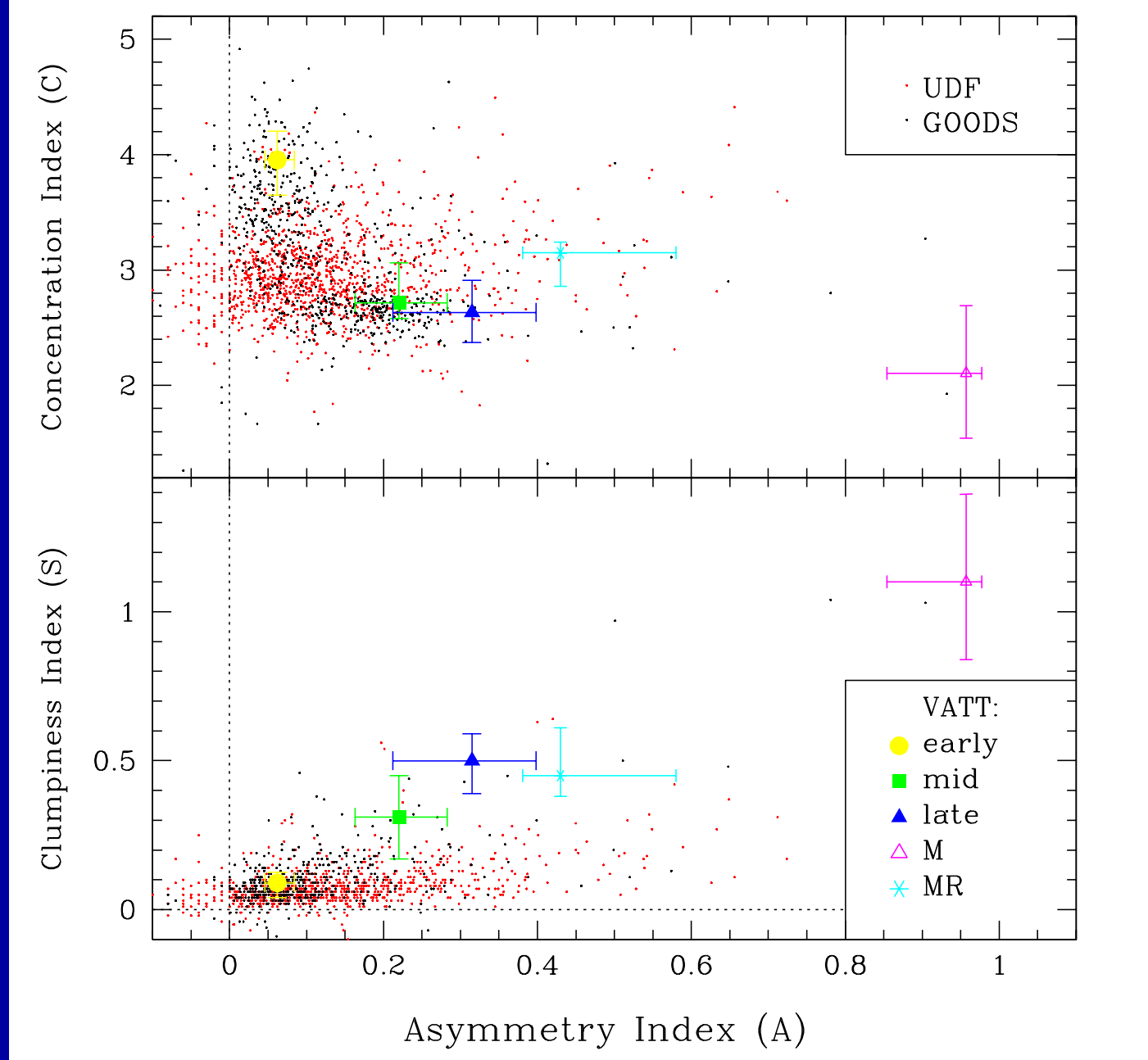
- $N(z, \text{Type})$ can measure how galaxies of all Hubble types formed over a wide range of cosmic time, by measuring their redshift distribution as a function of rest-frame type.

- For this, the types must be reliably measured for large samples from deep, uniform and high quality multi-wavelength images.

Driver et al. 1998, ApJL, 496, L93



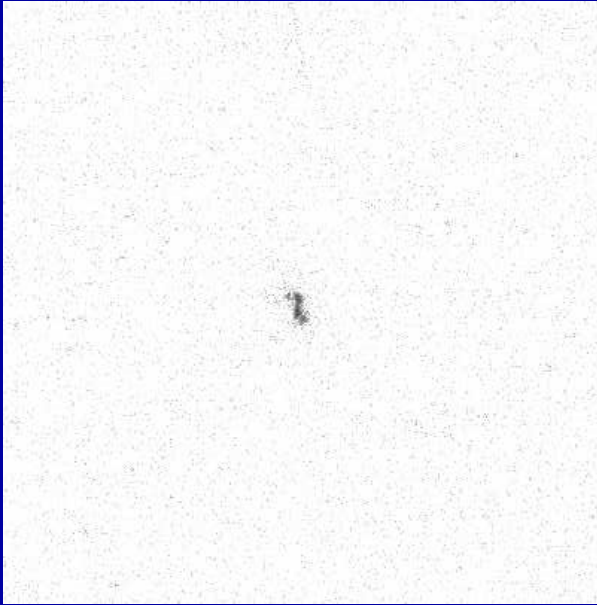
Taylor et al. (2007): CAS in GOODS and HUDF match well, given completeness limits. Galaxies don't get a whole lot more asymmetric or clumpy at faint mags. Improper S/N cutoffs in CAS affected previous studies.



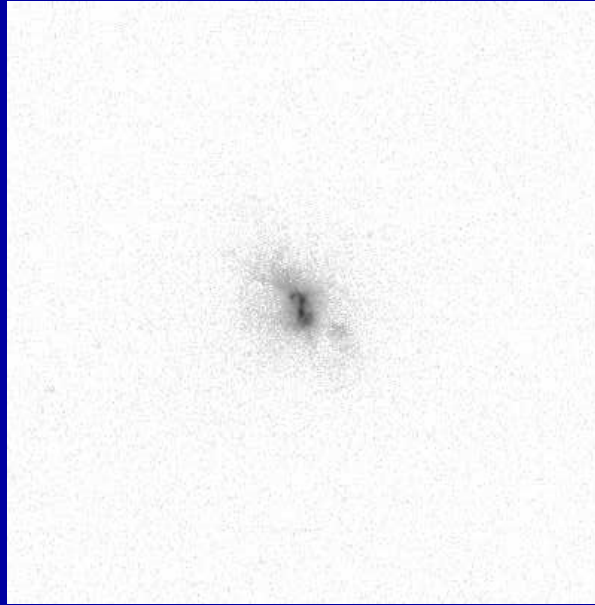
- Taylor et al. (2007): $CAS(\lambda, S/N, \text{resolution/sampling})$ may be used to quantitatively classify & compare high and low redshift merger sequence.
- WFC3 SNAPs will do this with far superior sampling and statistics !

HST/WFPC2 images of: UGC 03426

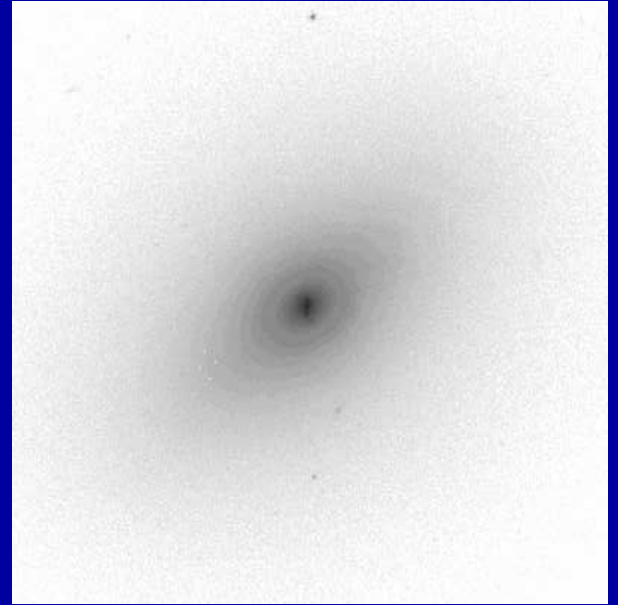
F255W



F300W



F814W



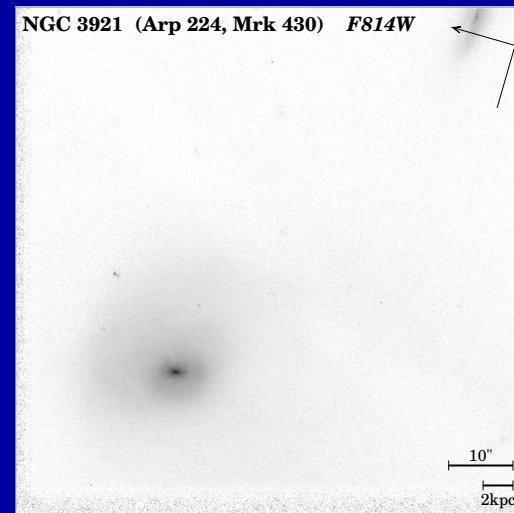
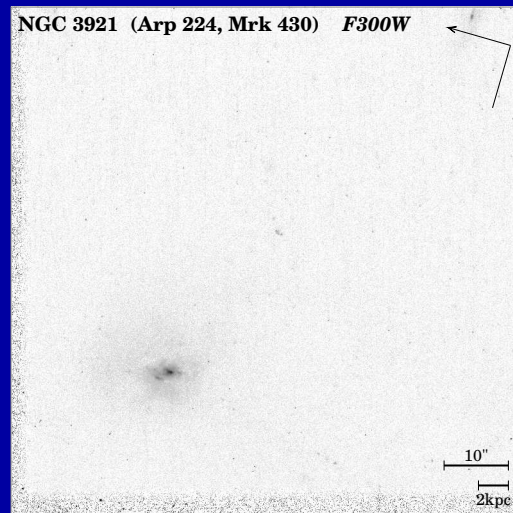
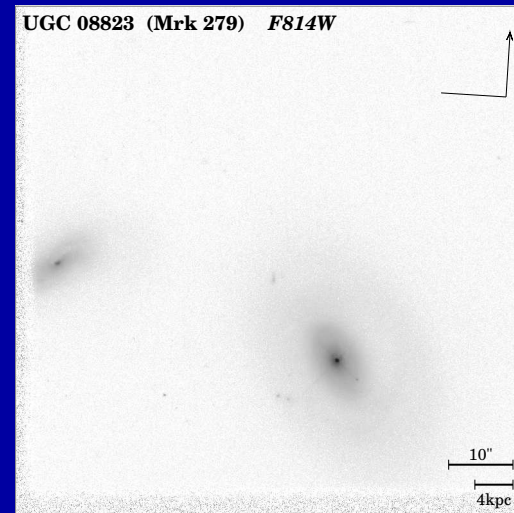
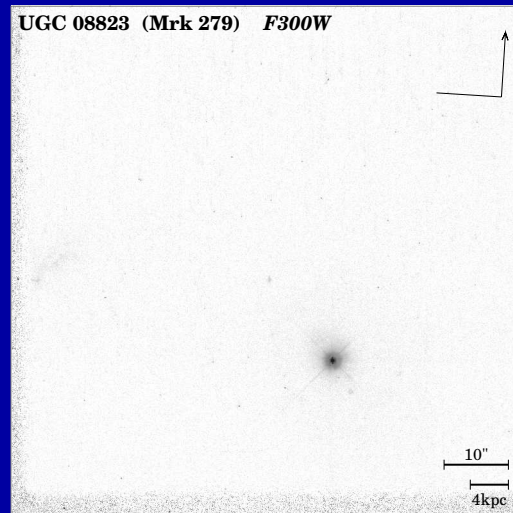
- Early-type galaxies can be full of surprises in the mid-UV ...

HST/WFPC2 images of:

UGC 08823 and NGC 3921

F300W

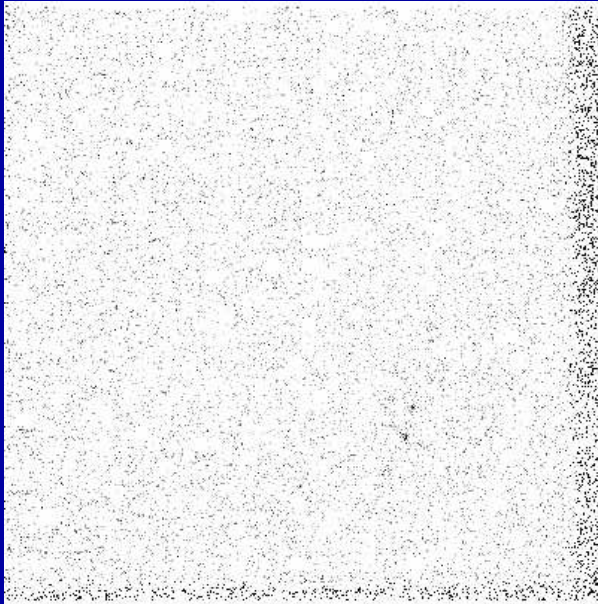
F814W



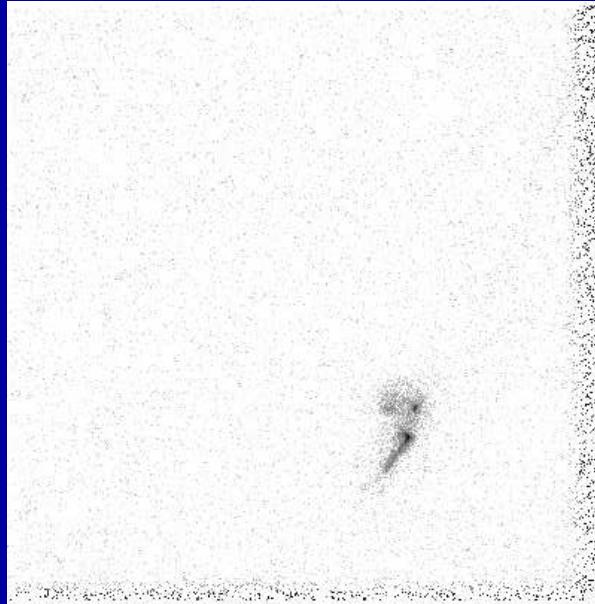
- Early-type galaxies that are AGN dominated in the mid-UV (UGC 00823).
- Others are merger remnants (NGC 3921).

HST/WFPC2 images of: UGC 08696

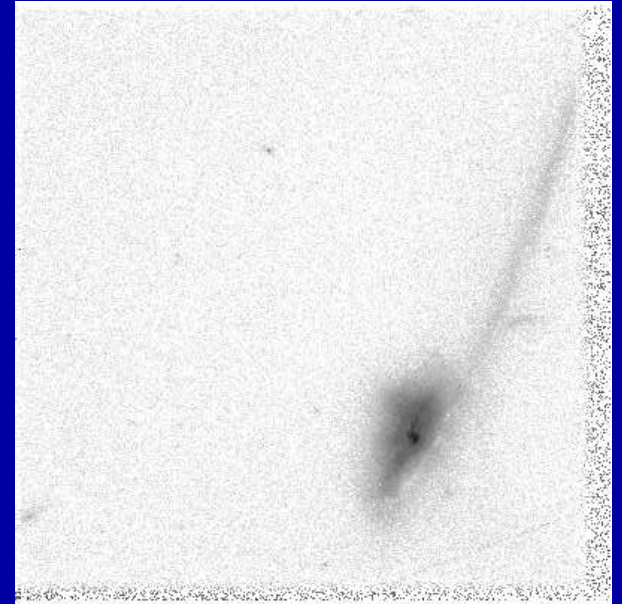
F255W



F300W



F814W



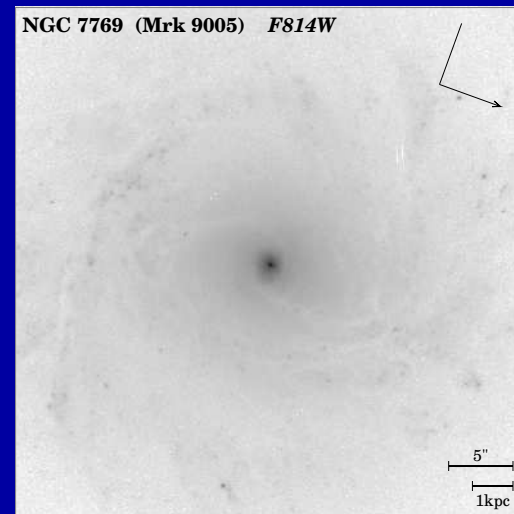
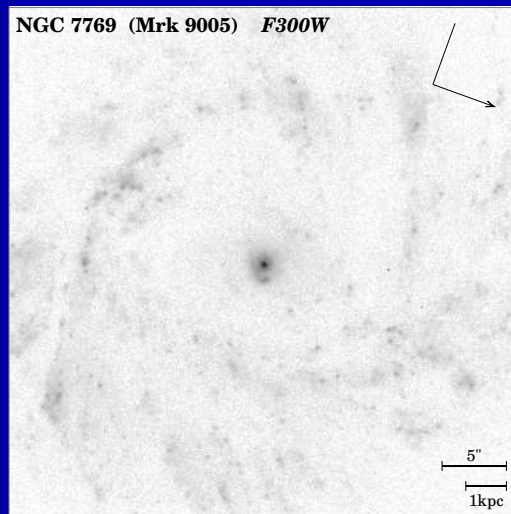
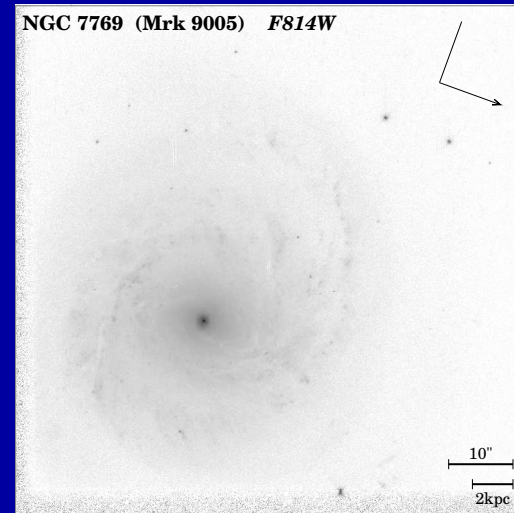
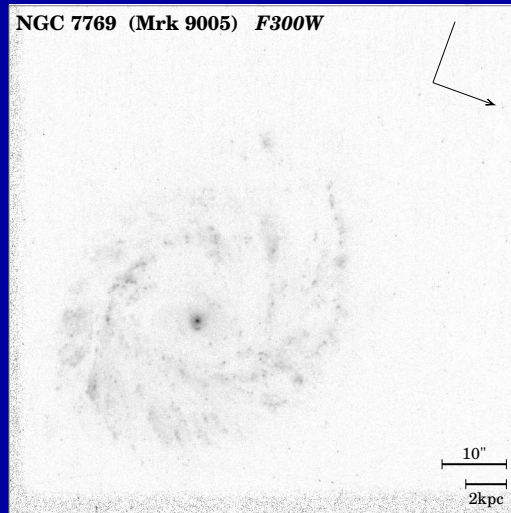
- Dust can hide most of the SF-regions \Rightarrow sample many objects and many inclination angles.

HST/WFPC2 images of:

NGC 7769

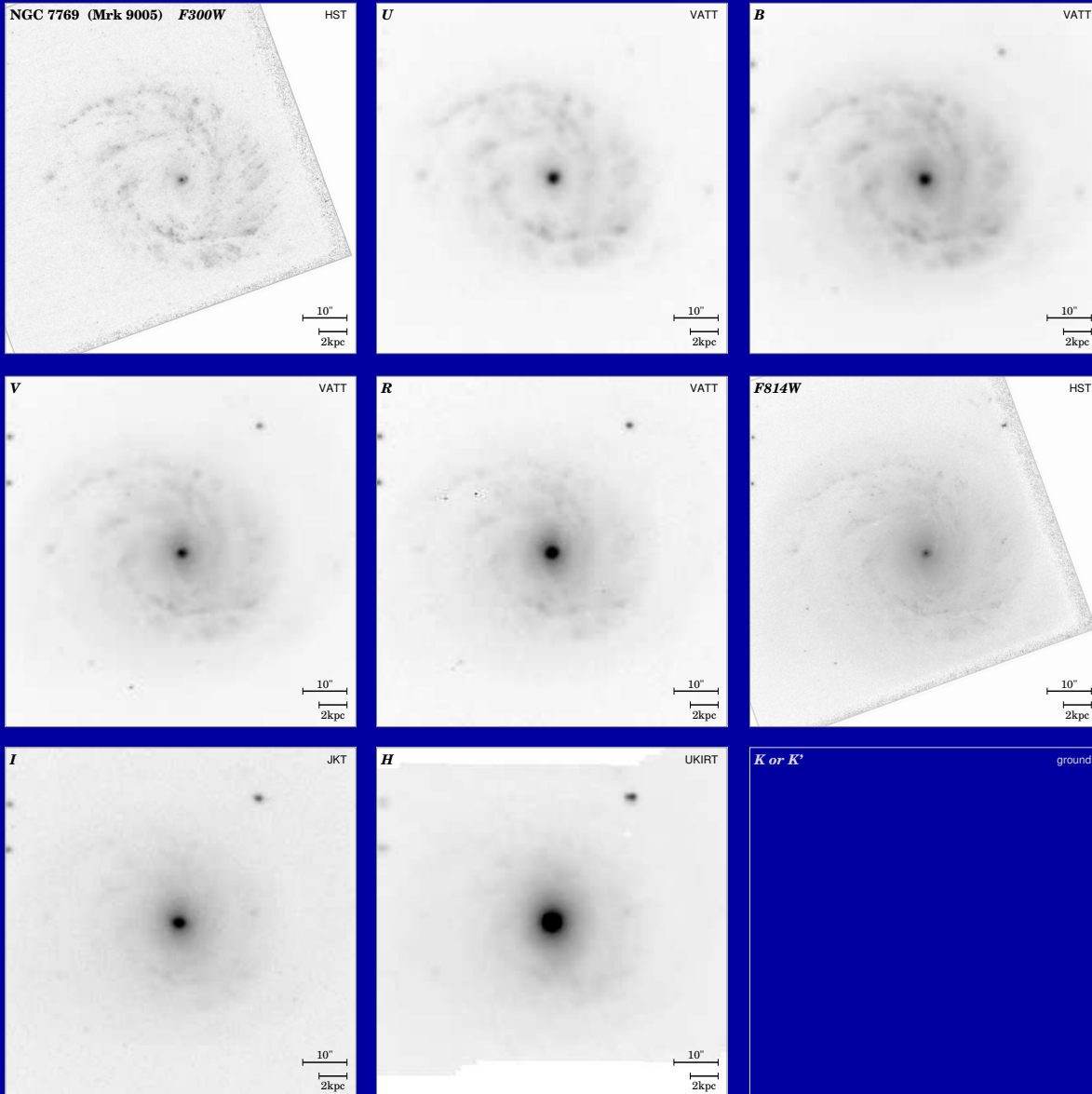
F300W

F814W



- Some grand-design spirals appear of later-type in the mid-UV due to more pronounced SF in spiral arms.
- Most spirals show nuclear dust lanes emerging from small bulge.

UIT, HST & ground-based images of NGC 7769:

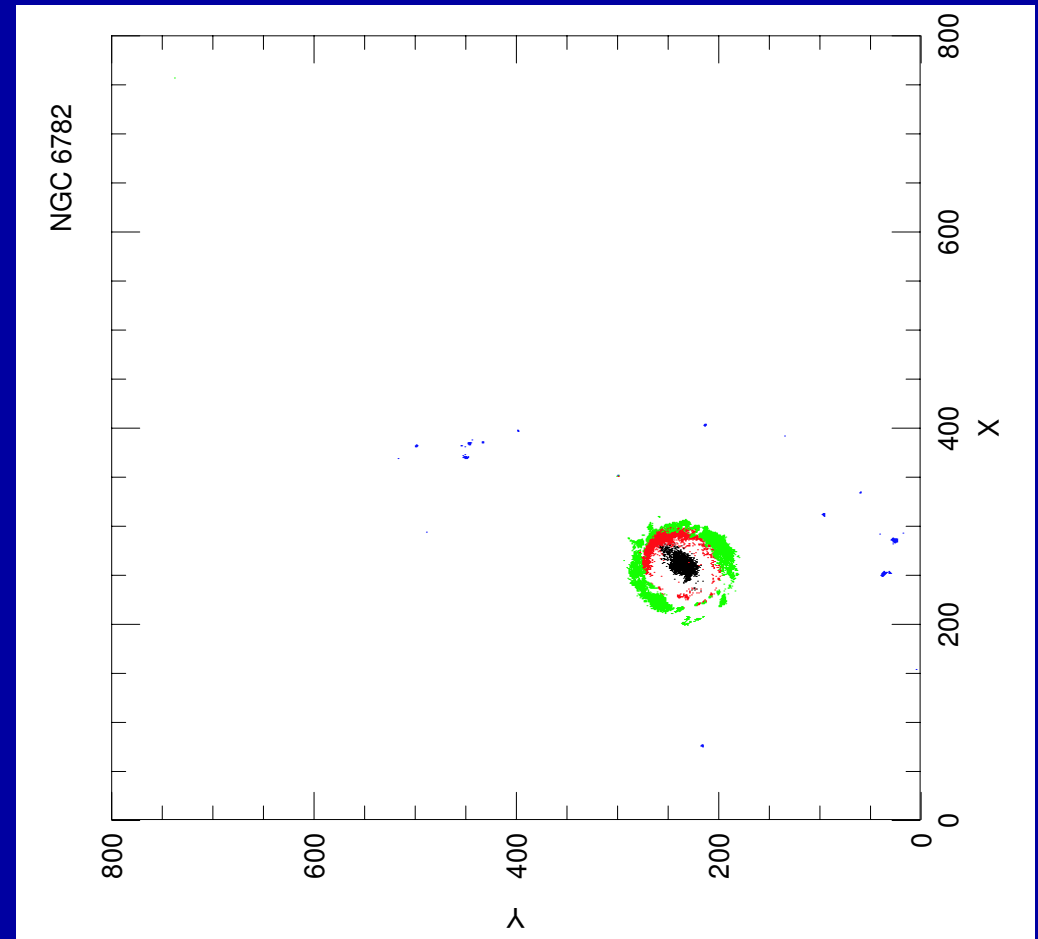
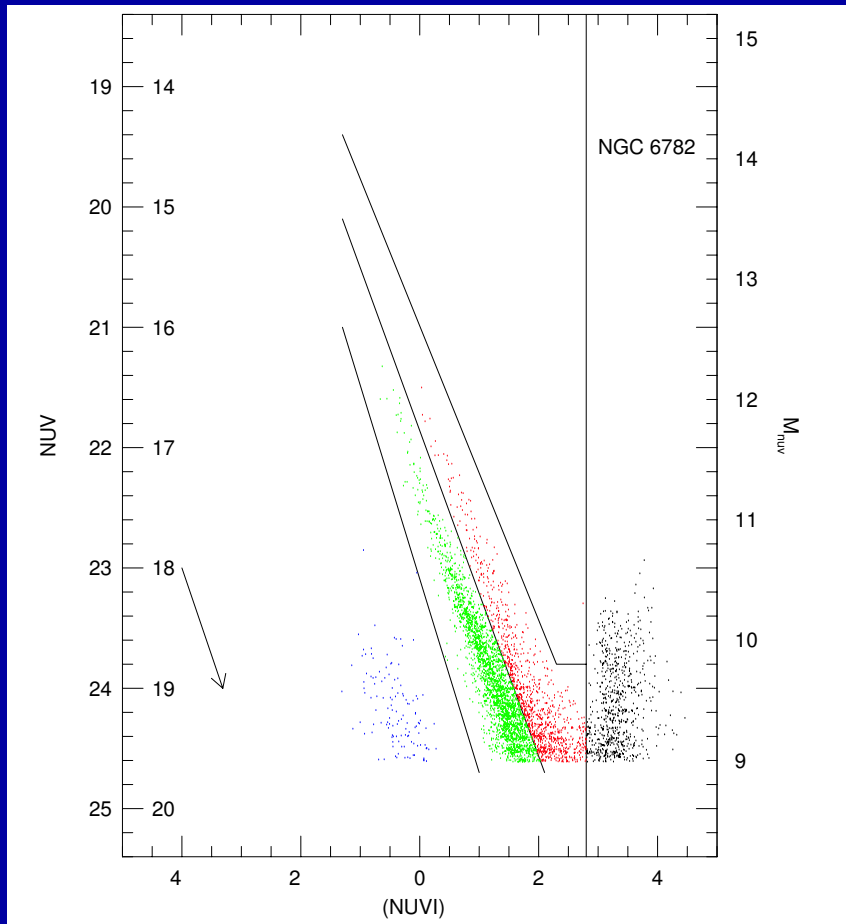


HST F300 g-b U360 g-b B436

g-b V540 g-b R634 HST F814

g-b I-band H1.6 μ m

- Dominated by spiral structure in mid-UV and bulge+bar in red/near-IR.



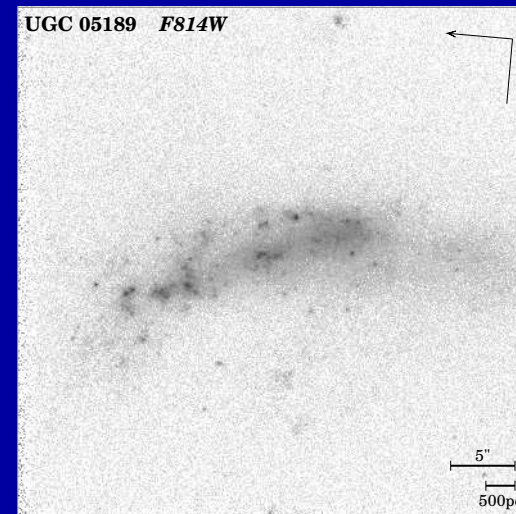
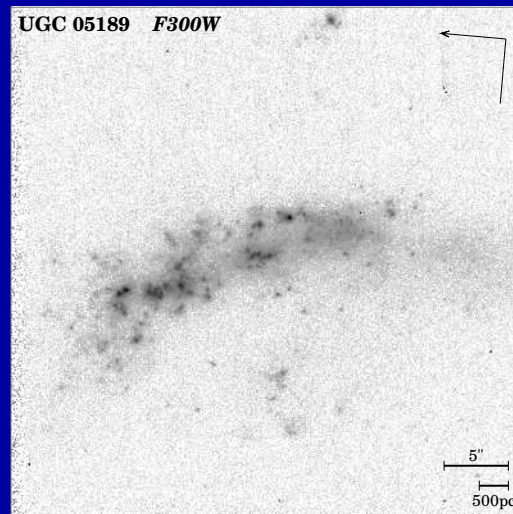
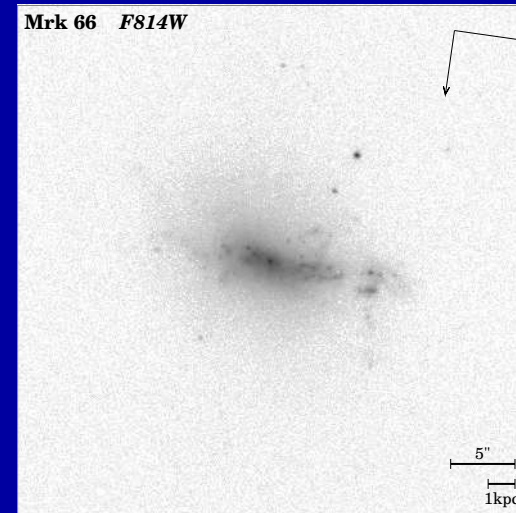
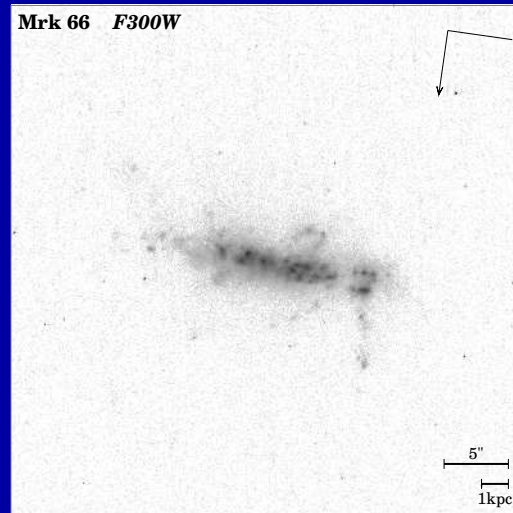
Eskridge et al. (2003, ApJ, 586, 923): Pixel-to-pixel color-mag diagrams.
 \implies Powerful diagnostic to study ages/evolution of bars, rings, spiral arms, and other distinct dynamical entities.

HST/WFPC2 images of:

Mrk 66 and UGC 05189

F300W

F814W



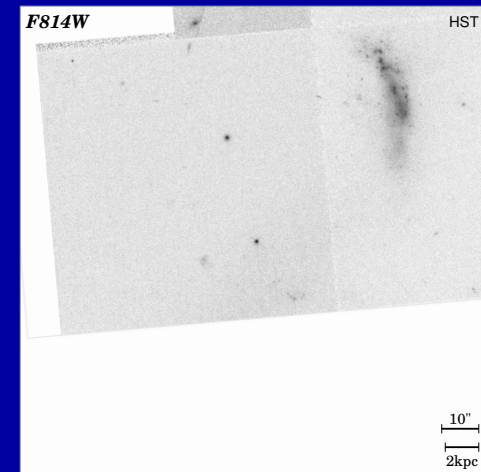
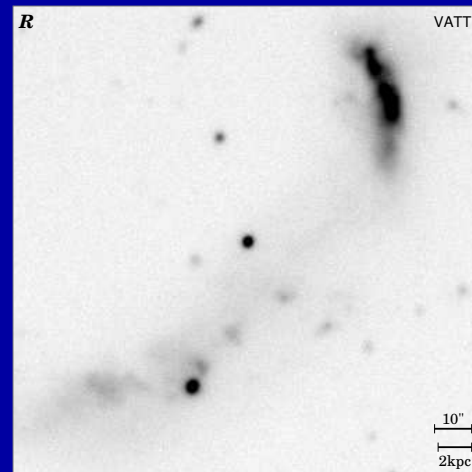
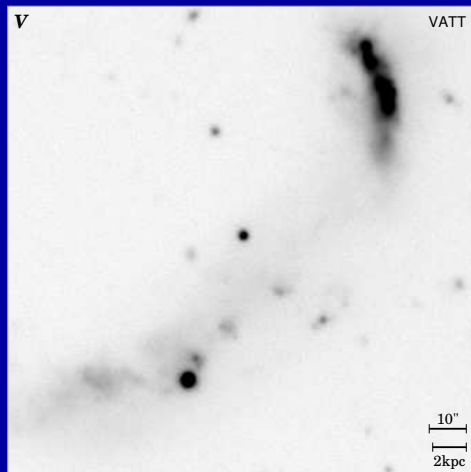
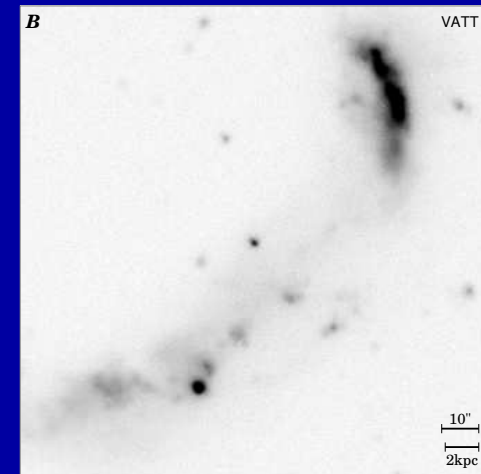
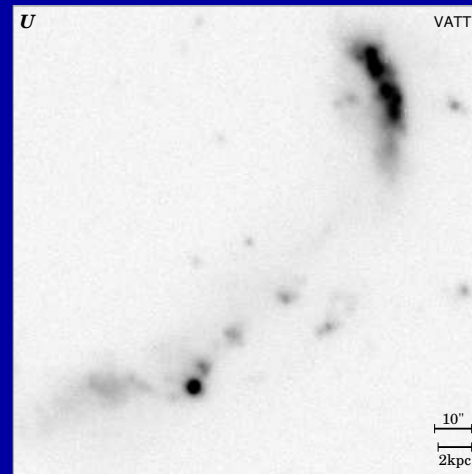
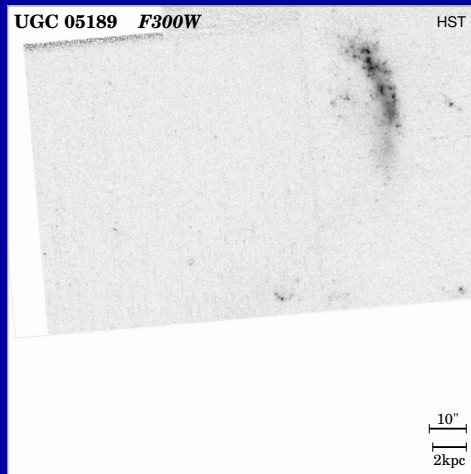
- Most late-type galaxies are dominated by a global starburst and similar at all wavelengths.

HST and ground-based images of UGC 05189:

F300W

U360

B436

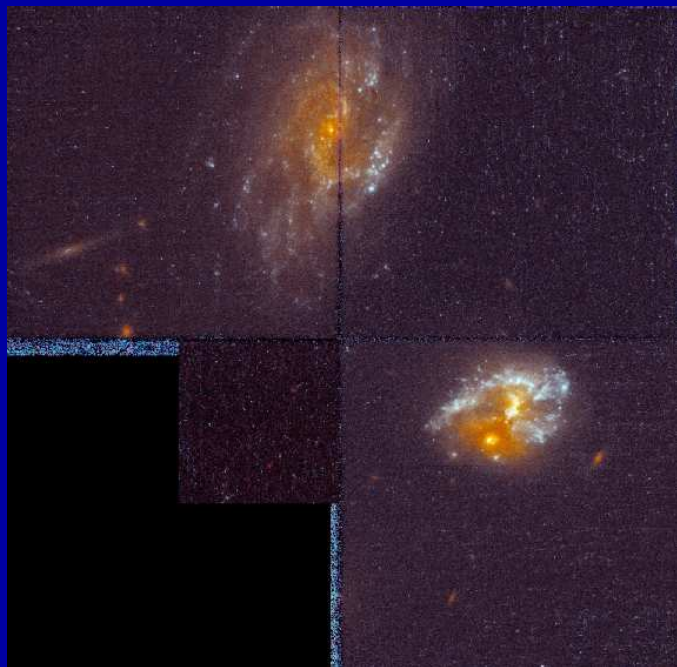
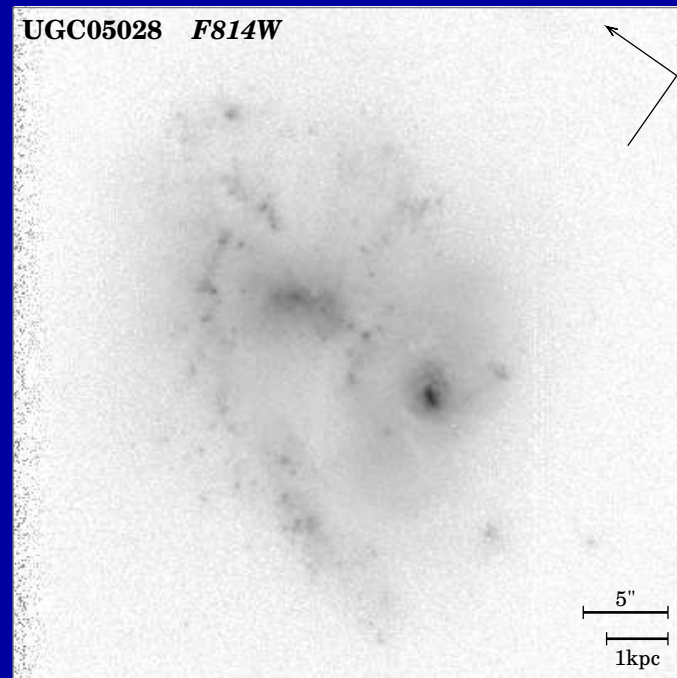
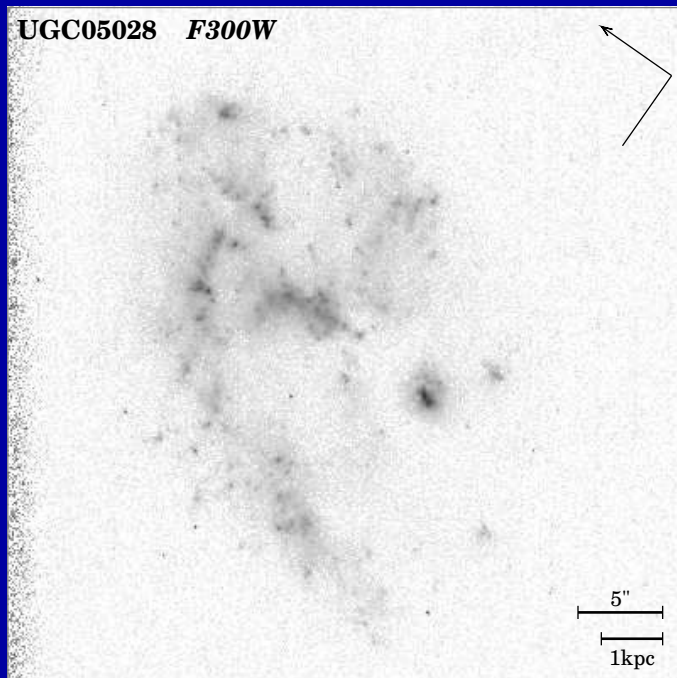


V540

R634

F814

- Most mergers and actively starforming galaxies are dominated by a global starburst and similar at all wavelengths (HST mid-UV–near-IR).



Lop-sided star-forming spiral galaxy in pair, with interaction likely triggering starbursts. Spatially resolved (Integral Field) spectra can provide powerful constraints on the influence of the dynamical environment on SF (see S. Odewahn's talk):

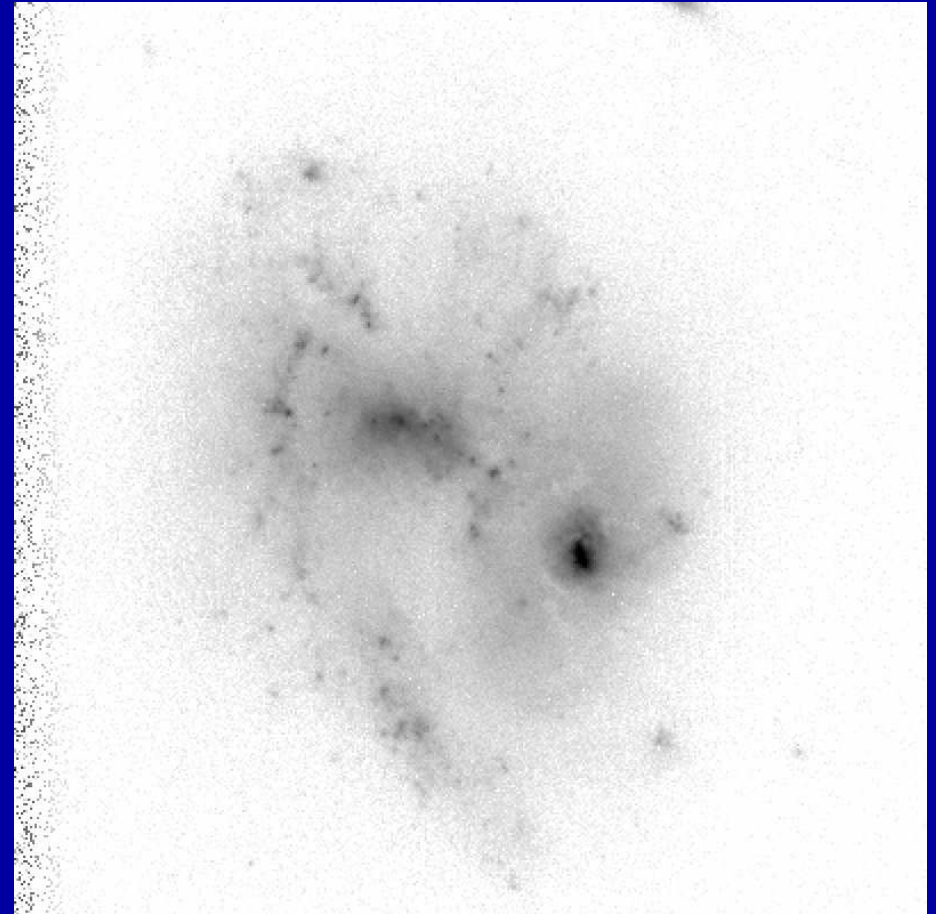
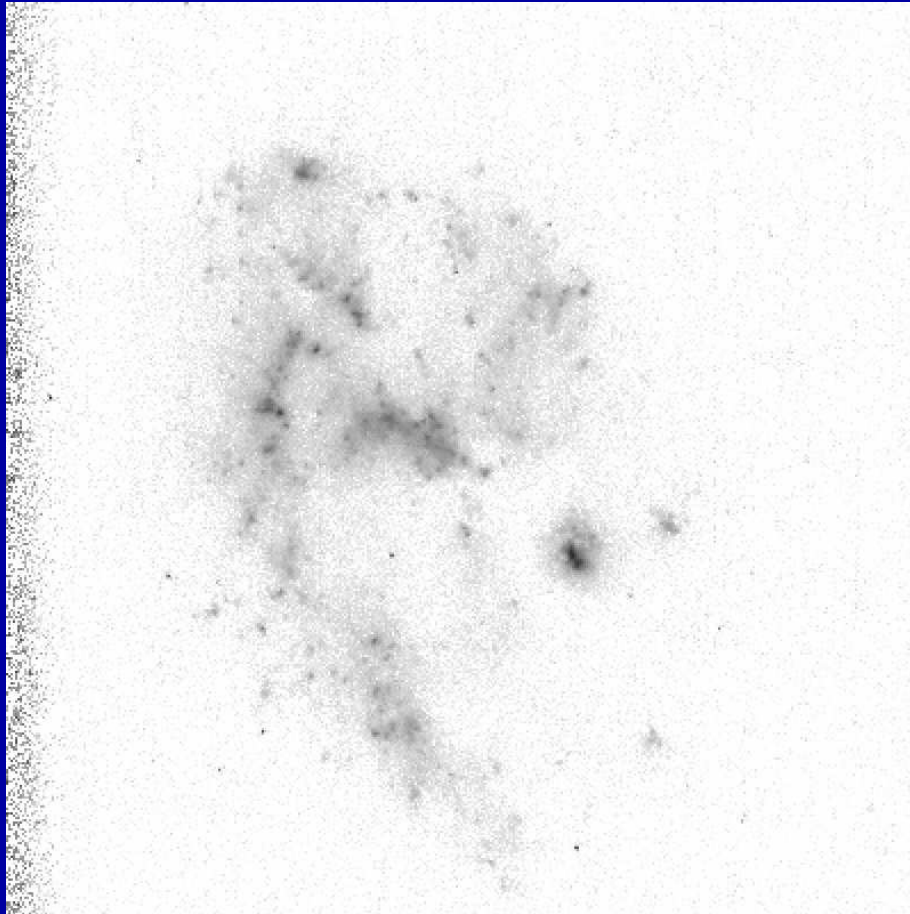
Mid-UV/Blue \iff Recent SF \iff large-scale bulk velocities ($v \lesssim v_{rot}$)?

HST/WFPC2 images of:

UGC 05028

F300W

F814W

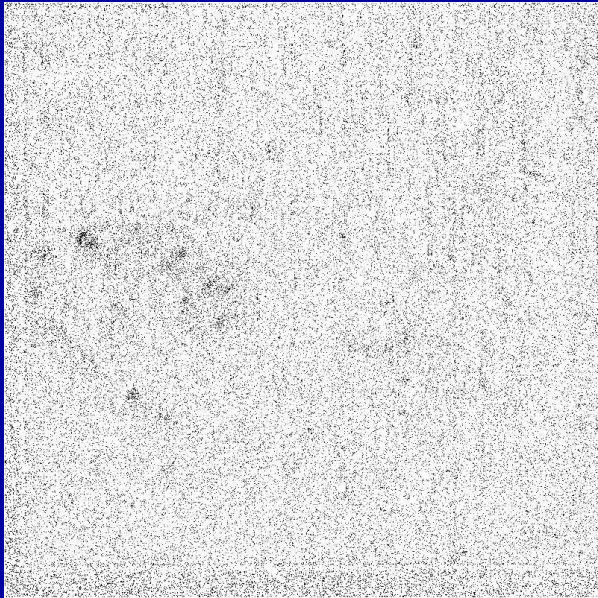


Lop-sided star-forming spiral galaxy in pair, with interaction likely triggering star-bursts. Spatially resolved (Integral Field) spectra can provide powerful constraints on the influence of the dynamical environment on SF:

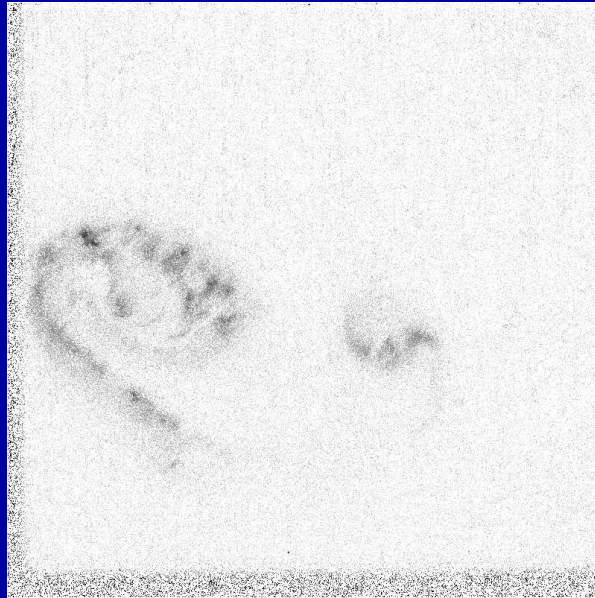
Mid-UV/Blue \longleftrightarrow Recent SF \longleftrightarrow large-scale bulk velocities ($v \lesssim v_{rot}$)?

HST/WFPC2 images of: UGC 08677-8

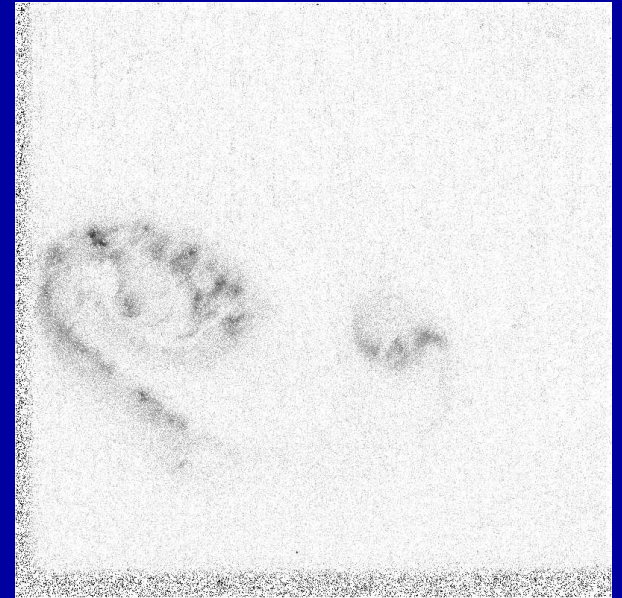
F255W



F300W



F814W



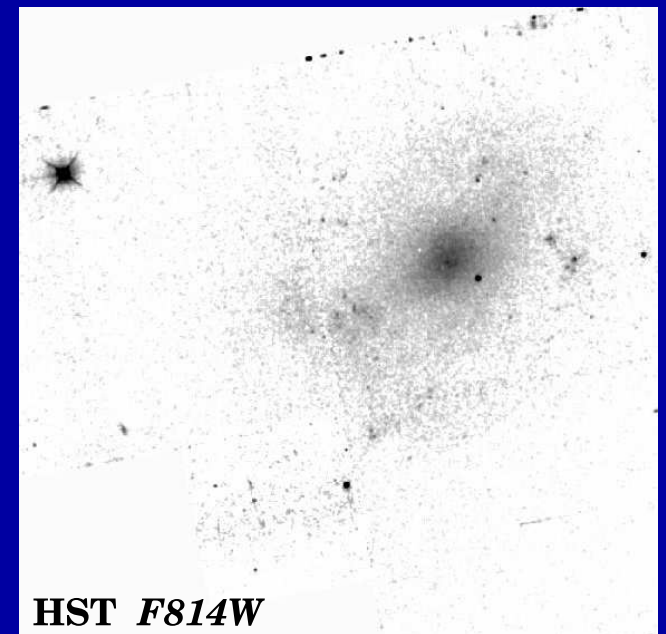
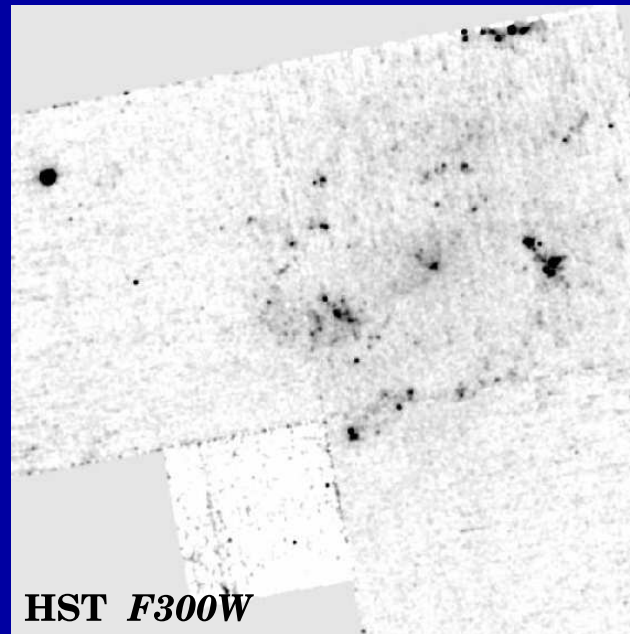
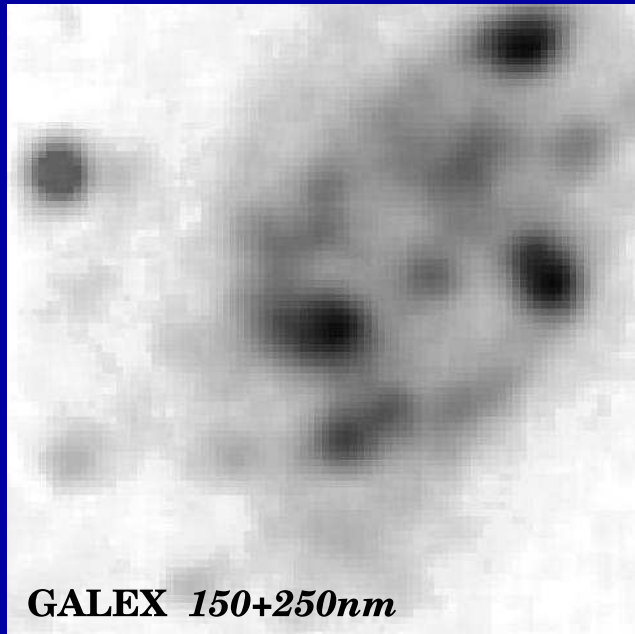
- Major merger with active SF that look similar at in mid-UV and red, but with significant dust superimposed.

GALEX and HST/WFPC2 images of UGC 10445:

GALEX 150+230nm

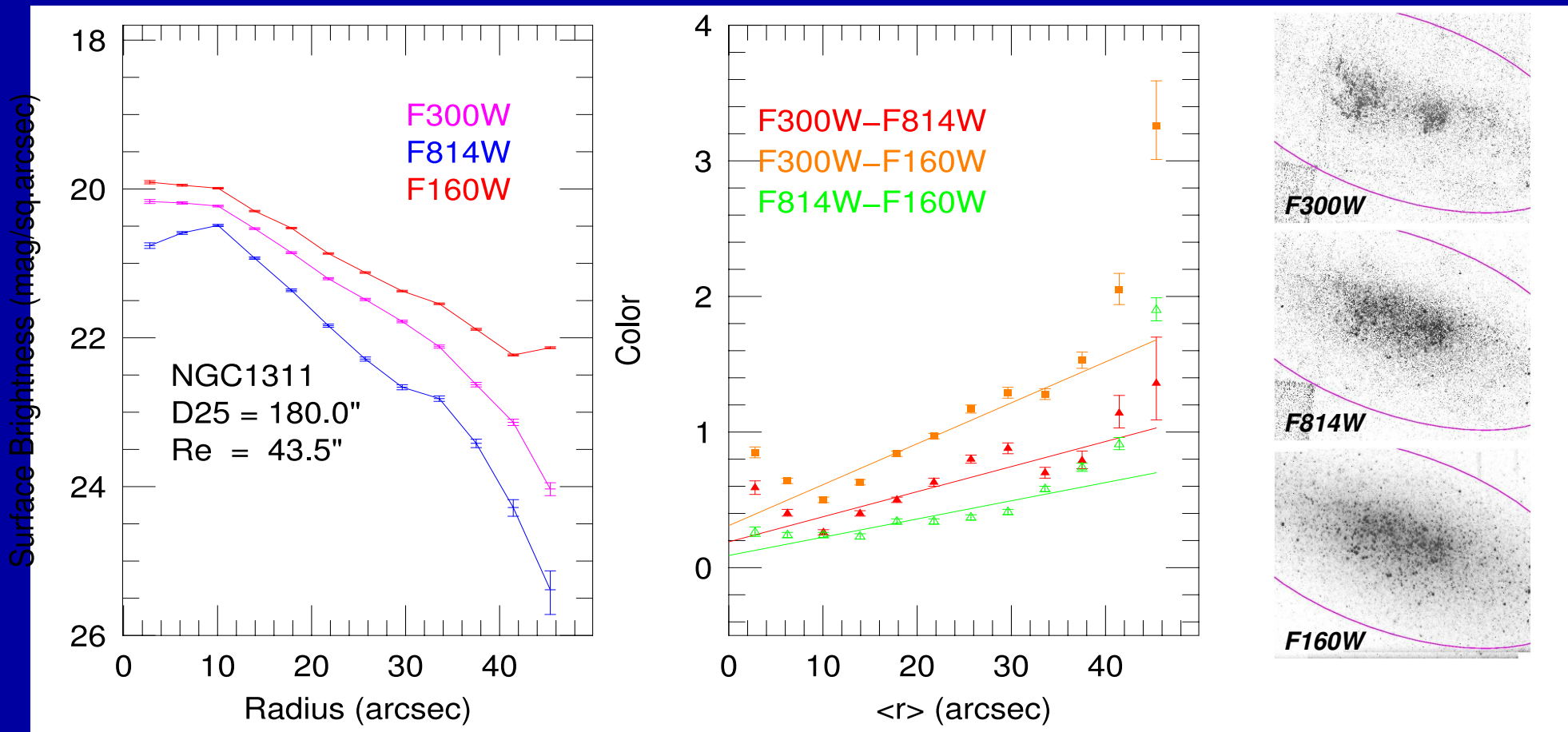
F300W

F814W



GALEX 150+230 nm images will measure the total FUV flux at low SB-levels escaping from the young hot stellar population, while comparison of the high-resolution HST F300W and F814W images locates the individual hot stars, SF clusters and dust, and locates the possible paths of the escaping FUV light.

(5) mid-UV–Near-IR images and Light-profiles



- Majority of late-types get redder outwards, including in the NIC3 H-band.
⇒ Significant halo or (thick) disk of older stars (?)

(7) Consequences of more reliable galaxy classifications

- (1) For $AB < 23-24$ mag ($z_{med} < 0.3-0.4$), early-types follow the $L(z) = L(0) (1+z)^{1.4}$ model. The CFRS redshift survey found this a good representation of the luminosity evolution of early-types to $z < 1$.
- (2) For $AB < 22$ ($z_{med} < 0.2$), late-types follow the $L(z) = L(0) (1+z)^{1.4}$ model.
- (3) For $AB > 23-24$ mag ($z_{med} > 0.4$), early-, mid- AND late-types follow the $L(z) = L(0) (1+z)^{2.0-2.5}$ model, suggesting an additional excess in numbers of all types for $z > 0.4$.
- (4) This can be explained if the Cosmological Constant itself was winding down the strongly epoch-dependent rate of (minor) mergers for $z < 0.4$, when it forever took over the expansion at:

$$z_{m-\Lambda} = (\Omega_m / \Omega_\Lambda)^{1/3} - 1 = 0.39 \quad (\text{WMAP value}).$$

(6) Predict Galaxy Appearance for JWST at $z \simeq 1-15$

Use HST mid-UV images to simulate galaxy appearance to the 6.0m James Webb Space Telescope (≥ 2011) at $z \simeq 1-15$:

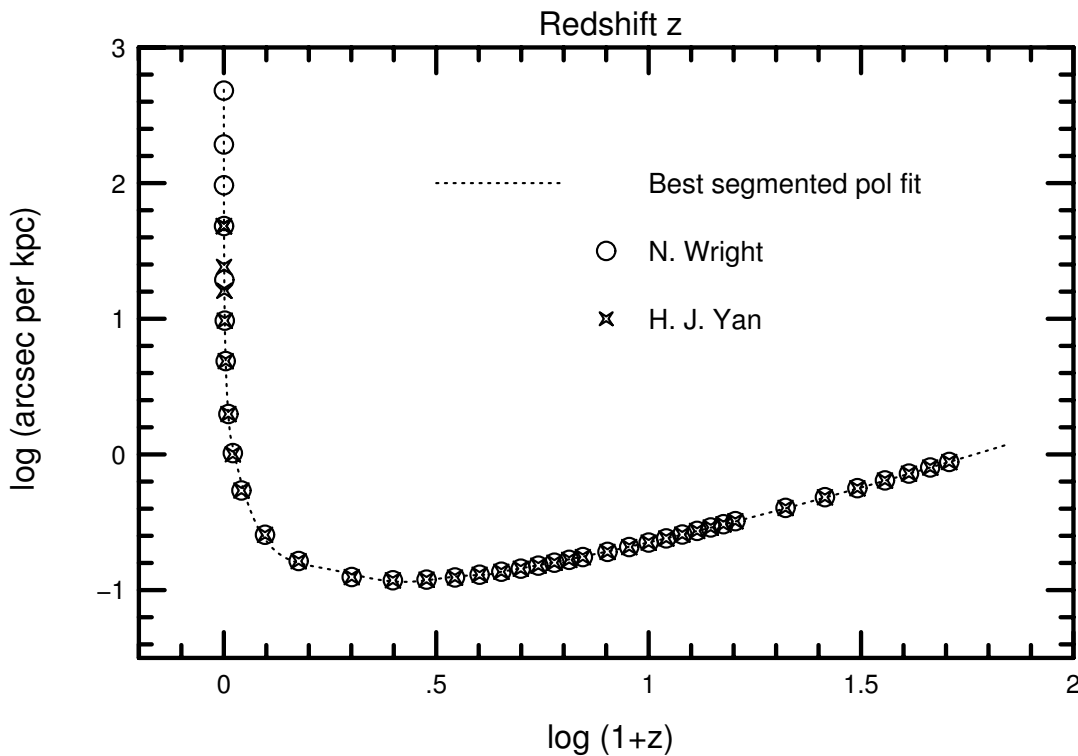
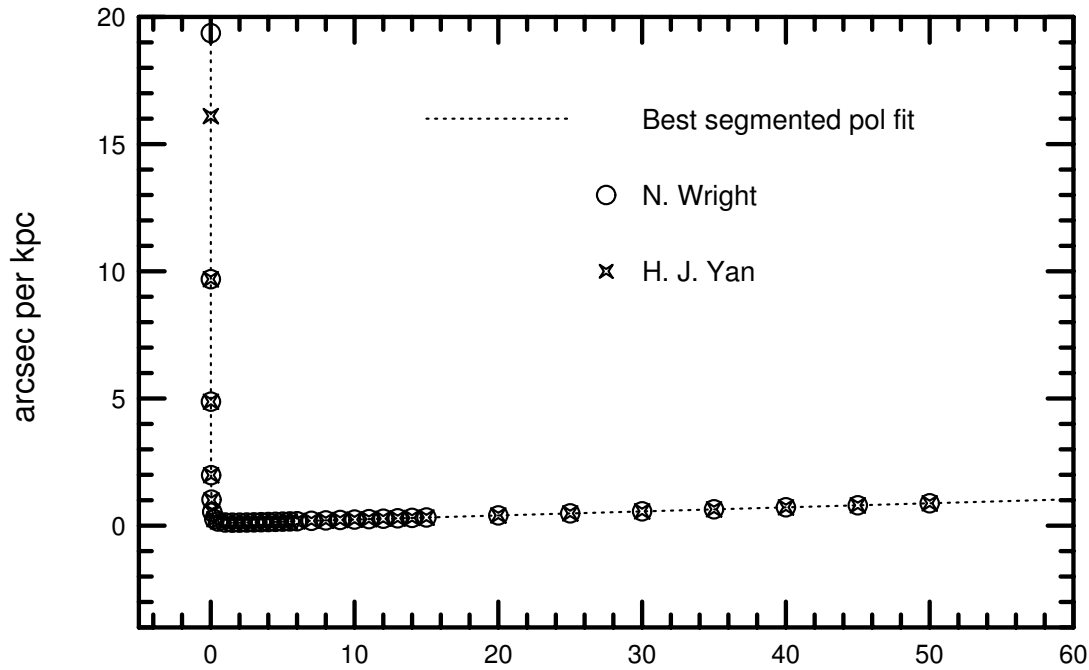
- (1) Galaxies detectable to $z \simeq 10-15$ and structures recognizable to $z \simeq 7-10$, if the average rest-frame mid-UV SB($\leq r_e$) is brighter than 18.0–20.0 mag arcsec $^{-2}$ (at $z=0$, i.e., top few % of the RC3).
- (2) Faint extensions are not well visible beyond $z \simeq 5-7$ due to cosmological SB-dimming, but $z \gtrsim 5$ objects will be point sources anyway.
- (3) Regions of very high SB or star-formation rate, and AGN, are generally visible to $z \simeq 10-15$. Population III star clusters to $z \gtrsim 20$ (see poster).
- (4) The minimum in the Θ - z relation (at $z \simeq 1.7$) and the JWST diffraction limit at $\lambda \gtrsim 2\mu\text{m}$ conspire to improve the effective JWST resolution from $z \simeq 2$ to $z \simeq 7$ for objects of very high SB.

Details on JWST image simulations:

- Based on HST/WFPC2 F300W images from the HST mid-UV survey of nearby galaxies (Windhorst et al. 2002, ApJS, 143, 113)
- WMAP COSMOLOGY: $H_0=71$ km/s/Mpc, $\Omega_m=0.27$, $\Omega_\Lambda=0.73$.
- INSTRUMENT: 6.0 m effective aperture, diffraction limited at $\lambda \gtrsim 2.0 \mu\text{m}$, JWST/NIRCam, $0''.034/\text{pix}$, read-noise= $5.0 e^-$, dark-current= $0.02 e^-/\text{s}$, NEP-Sky($1.6 \mu\text{m}$)= $21.7 \text{ mag}/('')^2$ in L2, Zodi spectrum, $t_{exp}=4 \times 900\text{s}$.

Row	Telesc.	Redshift	λ (μm)	FWHM ($''$)
1	HST	$z \sim 0$	$0.293 \mu\text{m}$	$0''.04$
	JWST	$z=1.0$	$0.586 \mu\text{m}$	$0''.084$
	JWST	$z=2.0$	$0.879 \mu\text{m}$	$0''.084$
2	JWST	$z=3.0$	$1.17 \mu\text{m}$	$0''.084$
	JWST	$z=5.0$	$1.76 \mu\text{m}$	$0''.084$
	JWST	$z=7.0$	$2.34 \mu\text{m}$	$0''.098$
3	JWST	$z=09.0$	$2.93 \mu\text{m}$	$0''.122$
	JWST	$z=12.0$	$3.81 \mu\text{m}$	$0''.160$
	JWST	$z=15.0$	$4.69 \mu\text{m}$	$0''.197$

Theta-z relation for $H_0=71$, $\Omega_m=0.27$, $\Omega_\Lambda=0.73$



Angular size vs. redshift relation in a Lambda dominated cosmology of $H_0=71 \text{ km s}^{-1} \text{ Mpc}^{-1}$, $\Omega_m=0.27$, $\Omega_\Lambda=0.73$.

In the top panel the relation is nearly linear in $1/z$ for $z \lesssim 0.05$ (the small angle approximation) and linear in z for $z \gtrsim 3$ (the Lambda dominated universe).

All curvature occurs in the range $0.05 \lesssim z \lesssim 3$, which is coded up in the IRAF script that does the JWST simulations.

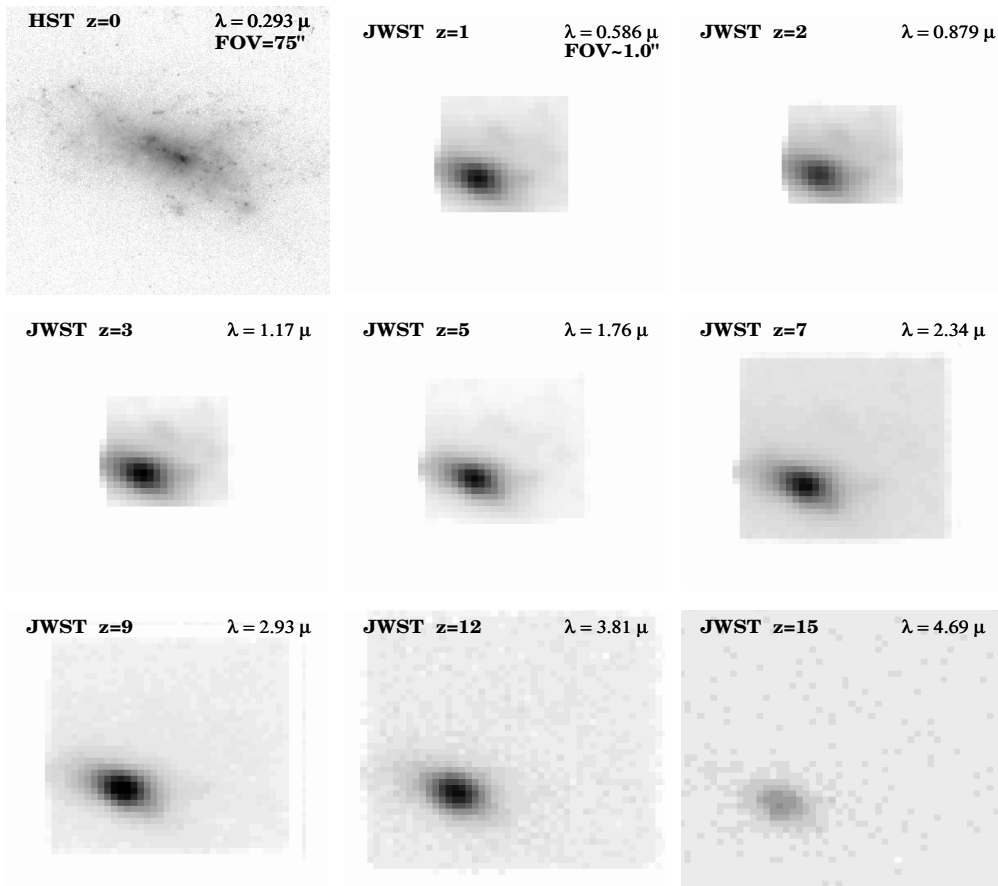


Fig. 4.01. JWST simulations based on HST/WFPC2 F300W images of the dwarf irregular NGC1140 ($z=0.0050$). This compact high SB object would be visible to $z \simeq 15$, but hard to classify at all $z \geq 1$.

ASSUMPTIONS: COSMOLOGY: $H_0=71$ km/s/Mpc, $\Omega_m=0.27$, and $\Omega_\Lambda=0.73$.

INSTRUMENT: 6.0 m effective aperture, JWST/NIRCam, $0.034''$ /pix, $RN=5.0 e^-$, $Dark=0.020 e^-/sec$, NEP H-band $Sky=21.7$ mag/arcsec² in L2, Zodiacal spectrum, $t_{exp}=1.0$ hrs, read-out every 900 sec.

Row 1: $z=0.0$ (HST $\lambda=0.293\mu m$, $FWHM=0.04''$), $z=1.0$ (JWST $\lambda=0.586\mu m$, $FWHM=0.084''$), and $z=2.0$ (JWST $\lambda=0.879\mu m$, $FWHM=0.084''$).

Row 2: $z=3.0$ (JWST $\lambda=1.17\mu m$, $FWHM=0.084''$), $z=5.0$ (JWST $\lambda=1.76\mu m$, $FWHM=0.084''$), and $z=7.0$ (JWST $\lambda=2.34\mu m$, $FWHM=0.098''$).

Row 3: $z=9.0$ (JWST $\lambda=2.93\mu m$, $FWHM=0.122''$), $z=12.0$ (JWST $\lambda=3.81\mu m$, $FWHM=0.160''$), and $z=15.0$ (JWST $\lambda=4.69\mu m$, $FWHM=0.197''$).

The compact high-SB dwarf irregular galaxy NGC1140 ($z=0.0050$).

With JWST, this object would be visible to $z \simeq 15$, but it will be hard to classify at all redshifts $z \geq 1$.

Note that the object indeed reaches a minimum angular size at $z \simeq 1.7$.

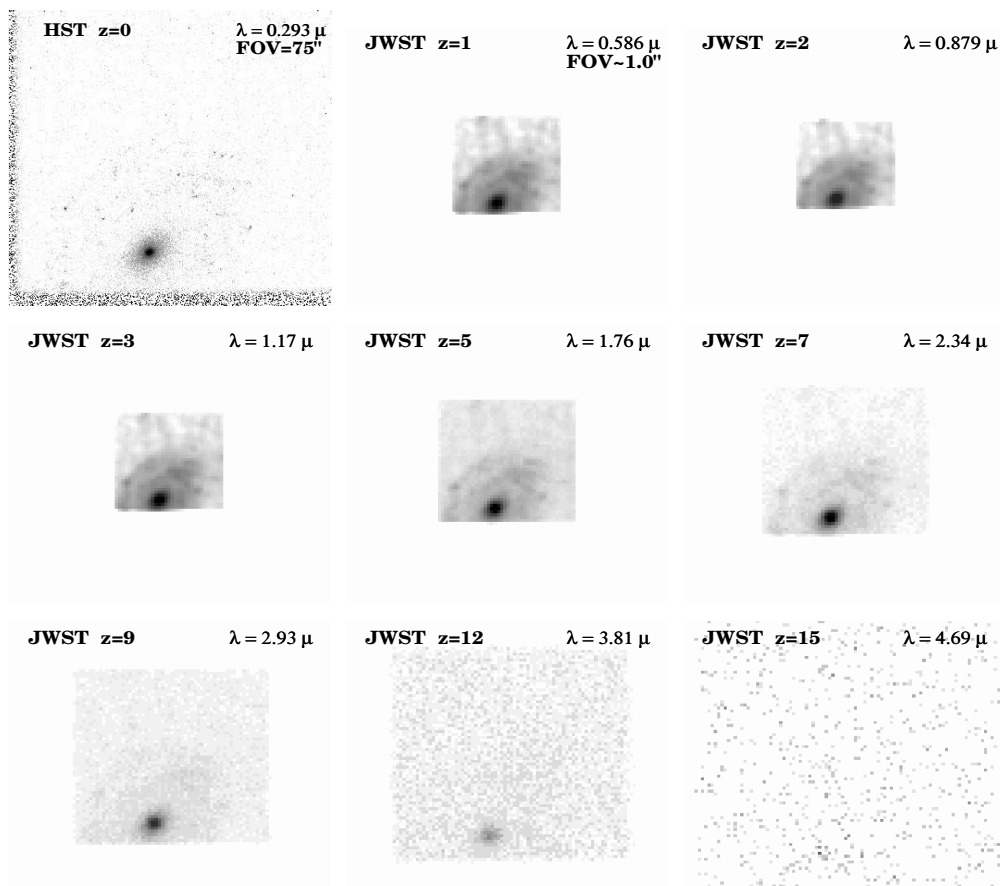


Fig. 4.02. JWST simulations based on HST/WFPC2 F300W images of the mid-type spiral NGC2551 (0.0078). Such an object would be visible to $z \lesssim 10$, but only recognizable to $z \lesssim 7$.

ASSUMPTIONS: COSMOLOGY: $H_0=71$ km/s/Mpc, $\Omega_m=0.27$, and $\Omega_\Lambda=0.73$.

INSTRUMENT: 6.0 m effective aperture, JWST/NIRCam, $0.034''$ /pix, $RN=5.0 e^-$, $Dark=0.020 e^-/sec$, NEP H-band $Sky=21.7$ mag/arcsec² in L2, Zodiacal spectrum, $t_{exp}=1.0$ hrs, read-out every 900 sec.

Row 1: $z=0.0$ (HST $\lambda=0.293\mu m$, $FWHM=0.04''$), $z=1.0$ (JWST $\lambda=0.586\mu m$, $FWHM=0.084''$), and $z=2.0$ (JWST $\lambda=0.879\mu m$, $FWHM=0.084''$).

Row 2: $z=3.0$ (JWST $\lambda=1.17\mu m$, $FWHM=0.084''$), $z=5.0$ (JWST $\lambda=1.76\mu m$, $FWHM=0.084''$), and $z=7.0$ (JWST $\lambda=2.34\mu m$, $FWHM=0.098''$).

Row 3: $z=9.0$ (JWST $\lambda=2.93\mu m$, $FWHM=0.122''$), $z=12.0$ (JWST $\lambda=3.81\mu m$, $FWHM=0.160''$), and $z=15.0$ (JWST $\lambda=4.69\mu m$, $FWHM=0.197''$).

The mid-type spiral NGC2551 ($z=0.0078$) would be visible out to $z \lesssim 10$, but only recognizable out to $z \lesssim 7$.

Its disk is in principle visible to $z \gtrsim 5-7$. Hence, if such objects are not seen by JWST at $z \lesssim 3$, then disks likely form at $z \lesssim 3$.

With HST we have seen glimpses of this, but with JWST these will become robust conclusions.

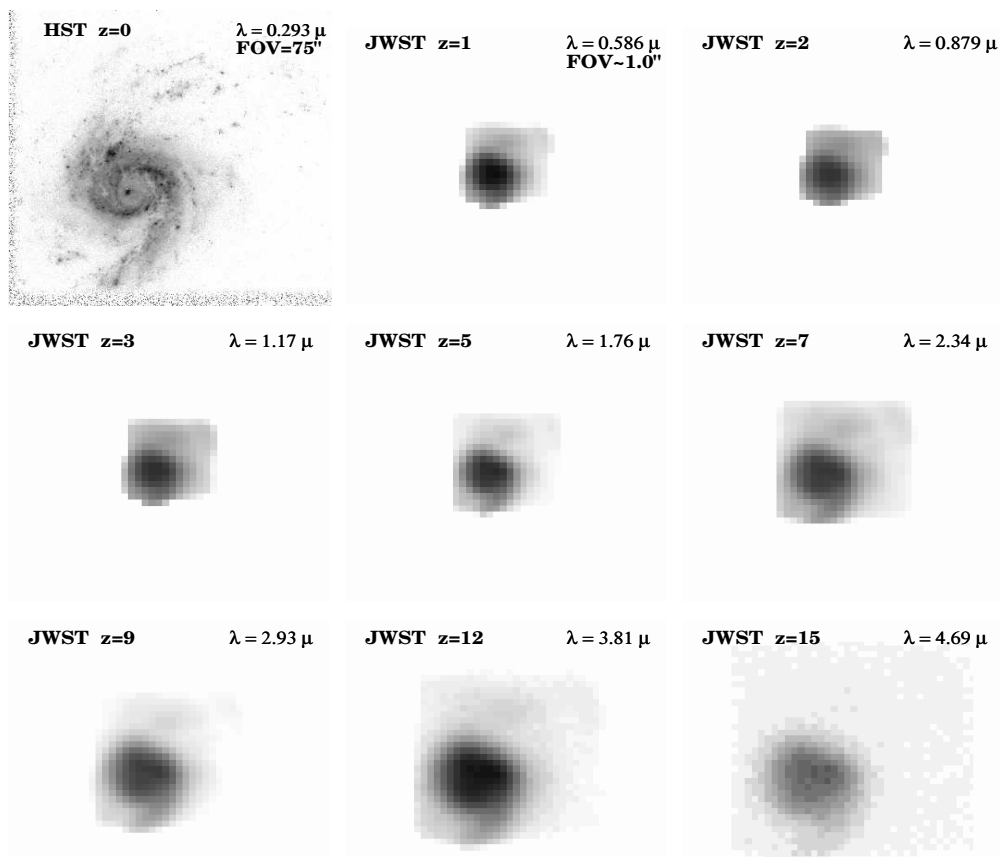


Fig. 4.03. JWST simulations based on HST/WFPC2 F300W images of the high-SB starbursting dwarf spiral galaxy NGC3310 (0.0033). The minimum in the Θ - z relation at $z \simeq 1.7$ and the JWST diffraction limit at $\lambda \geq 2.2 \mu\text{m}$ — combined with the object's very high rest-frame UV SB — conspire to improve the effective JWST resolution on the mid-UV morphology of this object from $z \simeq 2$ to $z \simeq 7$.

ASSUMPTIONS: COSMOLOGY: $H_0=71$ km/s/Mpc, $\Omega_m=0.27$, and $\Omega_\Lambda=0.73$. INSTRUMENT: 6.0 m effective aperture, JWST/NIRCam, $0.034''$ /pix, RN=5.0 e^- , Dark=0.020 e^- /sec, NEP H-band Sky=21.7 mag/arcsec² in L2, Zodiacal spectrum, $t_{exp}=1.0$ hrs, read-out every 900 sec.

Row 1: $z=0.0$ (HST $\lambda=0.293 \mu\text{m}$, FWHM=0.04"), $z=1.0$ (JWST $\lambda=0.586 \mu\text{m}$, FWHM=0.084"), and $z=2.0$ (JWST $\lambda=0.879 \mu\text{m}$, FWHM=0.084"). **Row 2:** $z=3.0$ (JWST $\lambda=1.17 \mu\text{m}$, FWHM=0.084"), $z=5.0$ (JWST $\lambda=1.76 \mu\text{m}$, FWHM=0.084"), and $z=7.0$ (JWST $\lambda=2.34 \mu\text{m}$, FWHM=0.098"). **Row 3:** $z=9.0$ (JWST $\lambda=2.93 \mu\text{m}$, FWHM=0.122"), $z=12.0$ (JWST $\lambda=3.81 \mu\text{m}$, FWHM=0.160"), and $z=15.0$ (JWST $\lambda=4.69 \mu\text{m}$, FWHM=0.197")

The very high-SB, compact starbursting dwarf spiral galaxy NGC3310 ($z=0.0033$).

The minimum in the Θ - z relation at $z \simeq 1.7$ and the JWST diffraction limit at $\lambda \geq 2.2 \mu\text{m}$ — combined with the object's very high rest-frame UV-SB — conspire to improve the effective JWST resolution on the mid-UV morphology of this object from $z \simeq 2$ to $z \simeq 7$.

A rather exceptional case of where nasty cosmology doesn't appear to cost you prohibitive sensitivity, but gains you resolution!

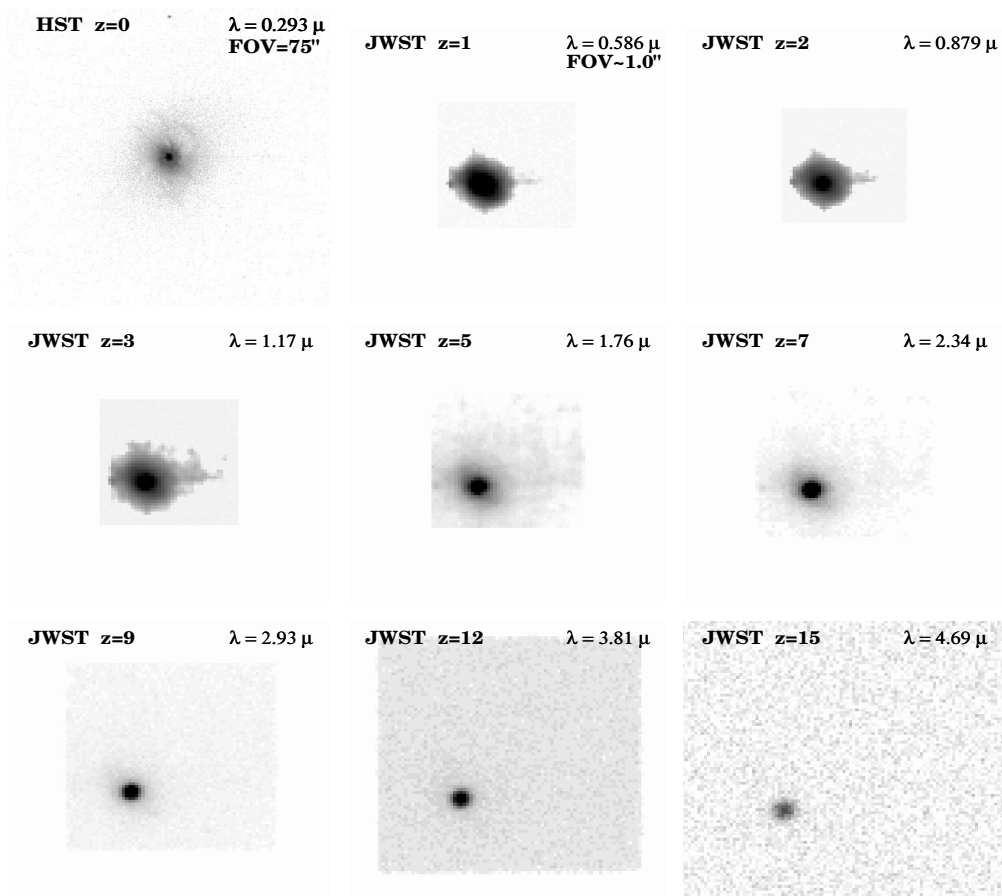


Fig. 4.04. JWST simulations based on HST/WFPC2 F300W images of the Seyfert galaxy NGC3516 (0.0088). Note that the faint nebulosity surrounding the AGN in the mid-UV at $z=0$ essentially disappears at $z \geq 7$, so that at high redshifts such objects would look like a pure AGN.

ASSUMPTIONS: COSMOLOGY: $H_0=71$ km/s/Mpc, $\Omega_m=0.27$, and $\Omega_\Lambda=0.73$.

INSTRUMENT: 6.0 m effective aperture, JWST/NIRCam, $0.034''$ /pix, $RN=5.0 e^-$, $Dark=0.020 e^-/sec$, NEP H-band $Sky=21.7 mag/arcsec^2$ in L2, Zodiacal spectrum, $t_{exp}=1.0$ hrs, read-out every 900 sec.

Row 1: $z=0.0$ (HST $\lambda=0.293\mu m$, $FWHM=0.04''$), $z=1.0$ (JWST $\lambda=0.586\mu m$, $FWHM=0.084''$), and $z=2.0$ (JWST $\lambda=0.879\mu m$, $FWHM=0.084''$). **Row 2:** $z=3.0$ (JWST $\lambda=1.17\mu m$, $FWHM=0.084''$), $z=5.0$ (JWST $\lambda=1.76\mu m$, $FWHM=0.084''$), and $z=7.0$ (JWST $\lambda=2.34\mu m$, $FWHM=0.098''$). **Row 3:** $z=9.0$ (JWST $\lambda=2.93\mu m$, $FWHM=0.122''$), $z=12.0$ (JWST $\lambda=3.81\mu m$, $FWHM=0.160''$), and $z=15.0$ (JWST $\lambda=4.69\mu m$, $FWHM=0.197''$).

The Seyfert galaxy NGC3516 ($z=0.0088$) has a faint nebulosity surrounding its AGN in the mid-UV, while at longer wavelengths the surrounding elliptical galaxy is present (not shown here).

The nebulosity surrounding the AGN is essentially SB-dimmed away at $z \geq 7$, so that at high redshifts these objects would look like purely stellar objects (“quasars”).

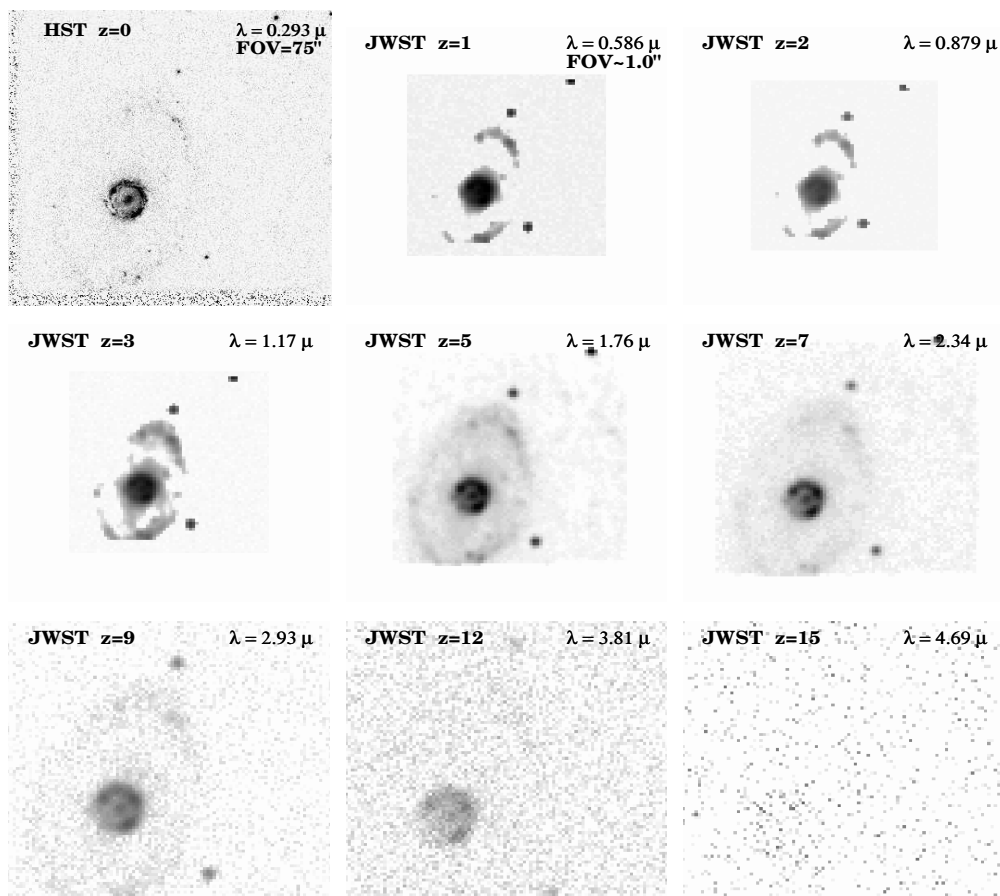


Fig. 4.05. JWST simulations based on HST/WFPC2 F300W images of the barred ring galaxy NGC6782 (0.0125). Note again that for $z \gtrsim 2-7$, the effective resolution on the bright star-forming ring improves with increasing redshift, until the $(1+z)^4$ -dimming completely kills it for $z \gtrsim 10$.

ASSUMPTIONS: COSMOLOGY: $H_0=71$ km/s/Mpc, $\Omega_m=0.27$, and $\Omega_\Lambda=0.73$.

INSTRUMENT: 6.0 m effective aperture, JWST/NIRCam, $0.034''$ /pix, $RN=5.0 e^-$, $Dark=0.020 e^-/sec$, NEP H-band Sky= $21.7 \text{ mag}/arcsec^2$ in L2, Zodiacal spectrum, $t_{exp}=1.0$ hrs, read-out every 900 sec.

Row 1: $z=0.0$ (HST $\lambda=0.293\mu m$, FWHM= $0.04''$), $z=1.0$ (JWST $\lambda=0.586\mu m$, FWHM= $0.084''$), and $z=2.0$ (JWST $\lambda=0.879\mu m$, FWHM= $0.084''$). **Row 2:** $z=3.0$ (JWST $\lambda=1.17\mu m$, FWHM= $0.084''$), $z=5.0$ (JWST $\lambda=1.76\mu m$, FWHM= $0.084''$), and $z=7.0$ (JWST $\lambda=2.34\mu m$, FWHM= $0.098''$). **Row 3:** $z=9.0$ (JWST $\lambda=2.93\mu m$, FWHM= $0.122''$), $z=12.0$ (JWST $\lambda=3.81\mu m$, FWHM= $0.160''$), and $z=15.0$ (JWST $\lambda=4.69\mu m$, FWHM= $0.197''$)

The barred ring galaxy NGC6782 (0.0125) shows that at $z \simeq 2$ to $z \simeq 7$, the effective resolution on its high-SB bright star-forming ring improves with increasing redshift, until the $(1+z)^4$ -dimming completely kills it for $z \gtrsim 10-12$.

Another good case showing why cosmology is not "WYSIWYG".

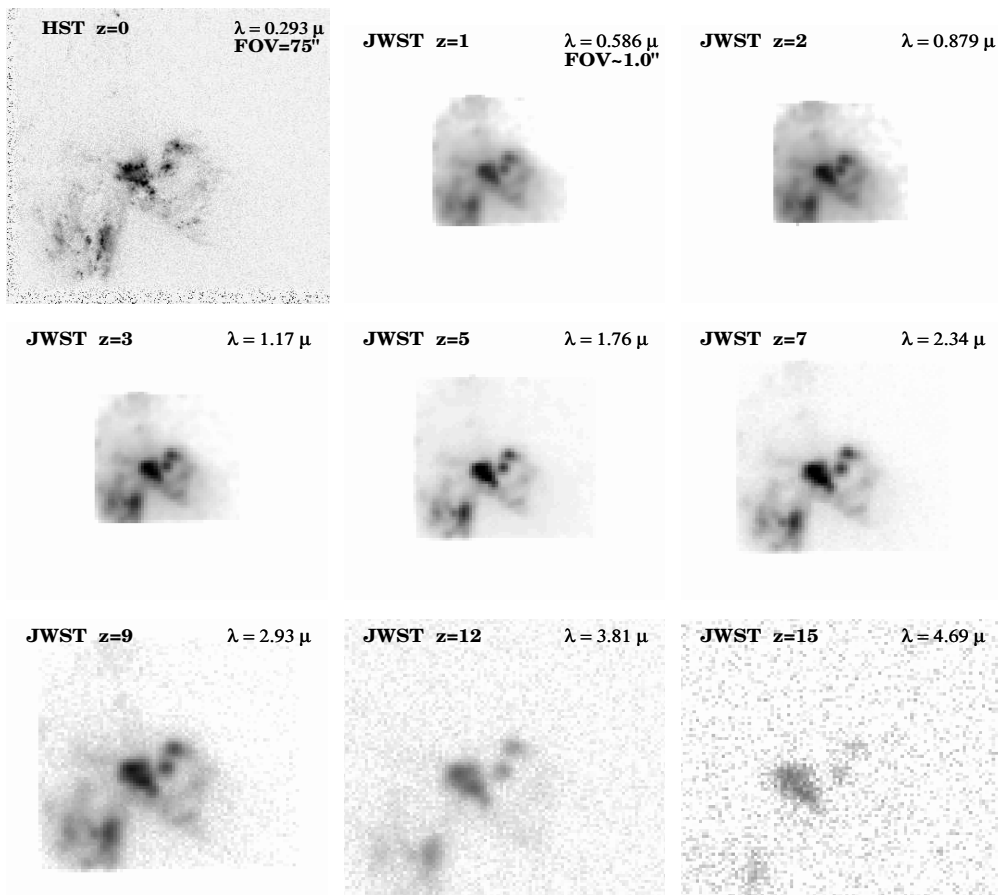


Fig. 4.06.a. JWST simulations based on HST/WFPC2 F300W images of the merger UGC06471-2 ($z=0.0104$). Note that the two unresolved star-bursting knots in the center remain visible until $z \sim 12$, beyond which the SB-dimming also kills their flux. This is the NOMINAL JWST [= (GOALS+REQUIREMENTS)/2].

ASSUMPTIONS: COSMOLOGY: $H_0=71$ km/s/Mpc, $\Omega_m=0.27$, and $\Omega_\Lambda=0.73$.

INSTRUMENT: 6.0 m effective aperture, JWST/NIRCam, $0.034''$ /pix, $RN=5.0 e^-$, $Dark=0.020 e^-/sec$, NEP H-band Sky= 21.7 mag/arcsec² in L2, Zodiacal spectrum, $t_{exp}=1.0$ hrs, read-out every 900 sec ("NOMINAL").

Row 1: $z=0.0$ (HST $\lambda=0.293 \mu m$, FWHM= $0.04''$), $z=1.0$ (JWST $\lambda=0.586 \mu m$, FWHM= $0.084''$), and $z=2.0$ (JWST $\lambda=0.879 \mu m$, FWHM= $0.084''$). **Row 2:** $z=3.0$ (JWST $\lambda=1.17 \mu m$, FWHM= $0.084''$), $z=5.0$ (JWST $\lambda=1.76 \mu m$, FWHM= $0.084''$), and $z=7.0$ (JWST $\lambda=2.34 \mu m$, FWHM= $0.098''$). **Row 3:** $z=9.0$ (JWST $\lambda=2.93 \mu m$, FWHM= $0.122''$), $z=12.0$ (JWST $\lambda=3.81 \mu m$, FWHM= $0.160''$), and $z=15.0$ (JWST $\lambda=4.69 \mu m$, FWHM= $0.197''$)

The galaxy merger UGC06471-2 ($z=0.0104$) is a major and very dusty collision of two massive disk galaxies.

It shows two bright unresolved star-bursting knots to the upper-right of the center, which remain visible until $z \simeq 12$, beyond which the cosmic SB-dimming kills their flux. These are more typical for the small star-forming objects expected at $z \simeq 10-15$.

This is the NOMINAL JWST = (GOALS+REQUIREMENTS)/2.

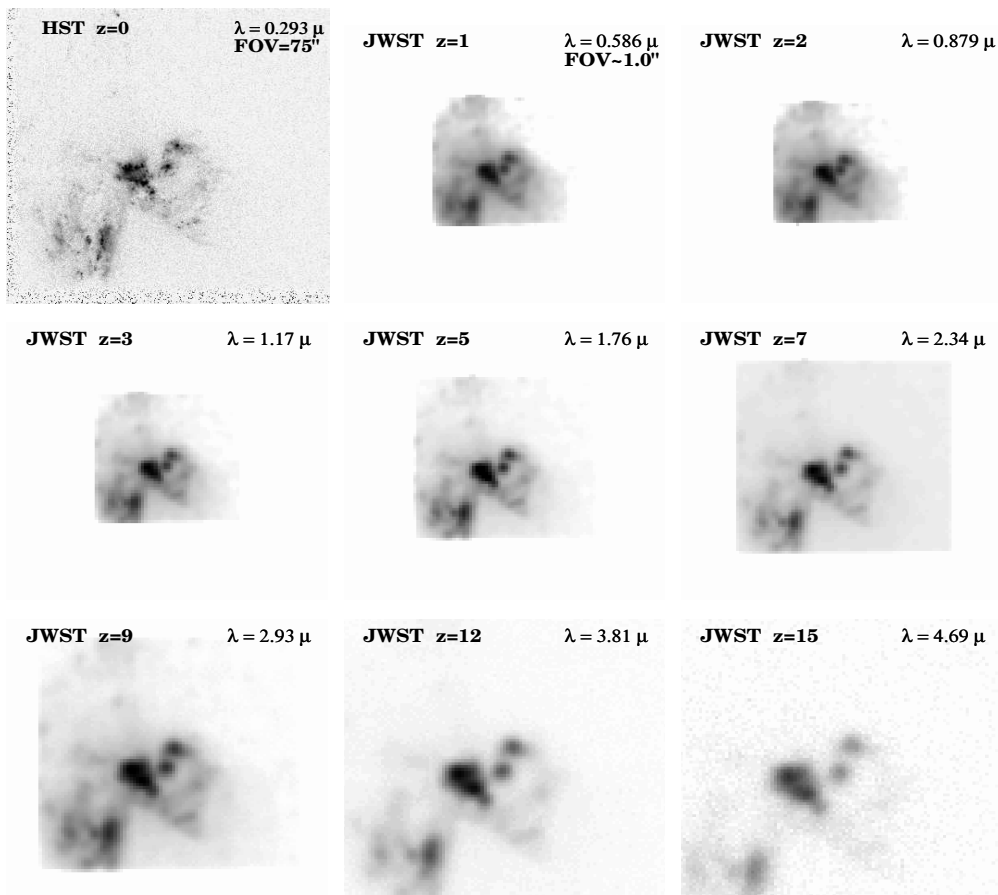


Fig. 4.06.c. JWST simulations based on HST/WFPC2 F300W images of the merger UGC06471-2 ($z=0.0104$). This is the BEST CASE JWST [meeting all GOALS, and $t_{exp}=100$ hrs]. The object is recognizable to $z \simeq 15$.

ASSUMPTIONS: COSMOLOGY: $H_0=71$ km/s/Mpc, $\Omega_m=0.27$, and $\Omega_\Lambda=0.73$.

INSTRUMENT: 6.0 m effective aperture, JWST/NIR camera, $0.034''$ /pix, $RN=3.0 e^-$, $Dark=0.010 e^-/sec$, NEP H-band Sky= 21.7 mag/arcsec² in L2, Zodi spectrum, $t_{exp}=100.0$ hrs, read-out every 900 sec ("GOALS").

Row 1: $z=0.0$ (HST $\lambda=0.293\mu m$, FWHM= $0.04''$), $z=1.0$ (JWST $\lambda=0.586\mu m$, FWHM= $0.084''$), and $z=2.0$ (JWST $\lambda=0.879\mu m$, FWHM= $0.084''$). **Row 2:** $z=3.0$ (JWST $\lambda=1.17\mu m$, FWHM= $0.084''$), $z=5.0$ (JWST $\lambda=1.76\mu m$, FWHM= $0.084''$), and $z=7.0$ (JWST $\lambda=2.34\mu m$, FWHM= $0.098''$). **Row 3:** $z=9.0$ (JWST $\lambda=2.93\mu m$, FWHM= $0.122''$), $z=12.0$ (JWST $\lambda=3.81\mu m$, FWHM= $0.160''$), and $z=15.0$ (JWST $\lambda=4.69\mu m$, FWHM= $0.197''$)

The galaxy merger UGC06471-2 ($z=0.0104$).

This is the BEST CASE JWST. It assumes that all GOALS are met, and that $t_{exp}=100$ hrs. The whole object (including the two star-forming knots) is recognizable to $z \simeq 15$.

This does not imply that observing galaxies at $z=15$ with JWST will be easy. On the contrary, since galaxies formed through hierarchical merging, real objects at $z \simeq 10-15$ will be $10^1-10^4 \times$ less luminous, requiring to push JWST to its limits.

8. Future plans

- Rest-frame Artificial Neural Network construction using Fourier decompositions (Odewahn, Jansen, Taylor).
- Pixel-to-pixel decomposition, asymmetry (Taylor, Eskridge et al.)
- Correlations with other imaging data: H- α , H-I, etc (Jansen).
- Follow-up with Chandra, XMM in X-rays (hot gas, weak hidden AGN) and Spitzer in mid-IR (dust), and GALEX in FUV (Lyman escape fraction).
- WFC3 in 2007-2010 (?): Systematic UV survey of 1000 nearby galaxies and $\sim 10\times$ better sensitivity.
- JWST in 2011-2015: Quantitative measurement of galaxy structure and trace the formation of the Hubble sequence with cosmic time.